7 Full-Scale WECs

In this chapter, some of the concepts that have reached the full-scale stage are described in detail. Other examples could be given, but the analysis was limited to four main technologies: OWC (Oscillating Water Column), AWS (Archimedes Wave Swing), Pelamis and Wave Dragon, which are presented in sections 7.1 to 7.4, respectively. Each illustrates one particular power conversion mechanism that was addressed in Chapter 6, namely air turbines, direct drive (linear generators) and hydraulics. A subsection regarding overtopping theory is also presented, as it was not addressed in the previous chapter and is linked with one of the technologies (Wave Dragon). Section 7.5 gives an account of the operational experience gathered by the several technology developers. Such detail provides valuable lessons to those interested in the field and also to a wide engineering audience. To conclude, section 7.6 gives a brief update on test centres, pilot zones, a review on the most relevant EU funded projects and a case study related to one of the technologies.

7.1 Oscillating Water Column

7.1.1 LIMPET

Tom Heath

Wavegen
Inverness
Scotland, UK

Since the inception of the UK Wave Energy Programme in 1974 the combination of an Oscillating Water Column (OWC) collector and a Wells turbine has been promoted as a reliable and cost effective combination for converting wave energy into useful power.

An OWC is formed by a chamber which is filled with air above the water line. Driven by wave action the water level inside the chamber rises and falls, alternately pressurising and rarefying the air within the chamber. As the water level inside the chamber rises pressurised air escapes from the chamber through a turbine-generator

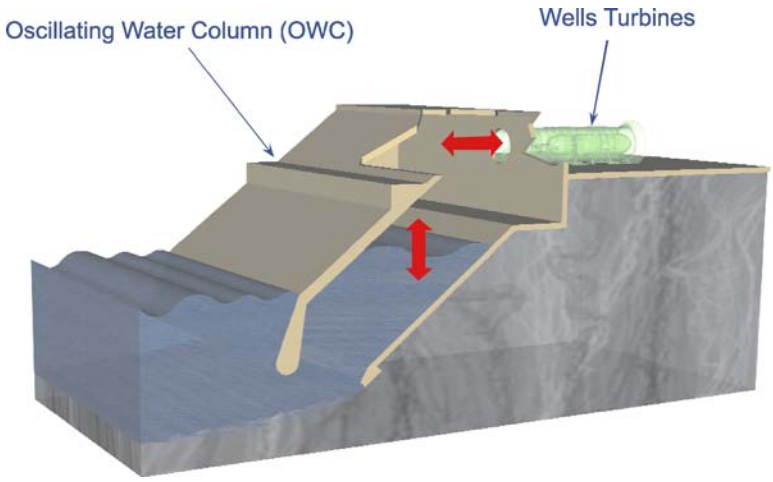

Fig. 7.1. Schematics of the LIMPET OWC

unit producing electrical power. As the water level in the chamber falls air is drawn back into the chamber through the turbine-generator assembly to continue power production. Wells turbines are self rectifying so that the direction of turbine rotation remains constant throughout the power cycle.

The technology has found commercial application in navigation buoys and numerous demonstration plants have been built across the globe in India, China, Norway, Japan, Portugal and in the UK, including Wavegen's LIMPET plant on Islay (N.E.: LIMPET is an acronym for Land Installed Marine Power Energy Transmitter). OWC breakwater units are under construction at Mutriku in Northern Spain and in Portugal at Porto. OWC's are not uniquely fitted with Wells turbines; a minority of developers favour impulse turbines whilst some systems with valve ducted flow feeding unidirectional turbines have also been proposed (see section 6.1). At present however the simplicity and flexibility of the Wells system make it the most attractive conversion option for OWC systems. The great virtues of the Wells turbine are its simplicity and effectiveness. The simplicity can we judged from Fig. 7.2 which shows, with the outer duct removed, the final stage of assembly of one of the pair of $250\,kW$ turbine rotor units originally fitted to the LIMPET plant. The seven blades of the $2.6\,m$ diameter unit are of a symmetrical airfoil section. The blades are bolted via a containment ring (which carries the centrifugal loads) to a plate which in turn fits directly on to the shaft of the generator (which is hidden under a cylindrical cover). The baseline configuration of the LIMPET plant used two of these assemblies, back to back, so that the combination formed a contra-rotating biplane turbine. Dependent upon the particular plant requirements other configurations may be used. For example an individual turbine-generator may be run as a monoplane turbine (with or without stator vanes) whilst a through shaft generator may be fitted with a turbine at either end to form a co-rotating bi-plane unit.

Fig. 7.2. Wells turbine used in the LIMPET plant

The principle of operation of the Wells turbine may be described with reference to Fig. 7.3. The plane of the rotating turbine is perpendicular to the air flow in the turbine duct. The forward motion of the blade combined with the perpendicular air flow means that relative to the blade there is an angle of attack of the air relative to the plane of the turbine blades. This angle of attack may vary

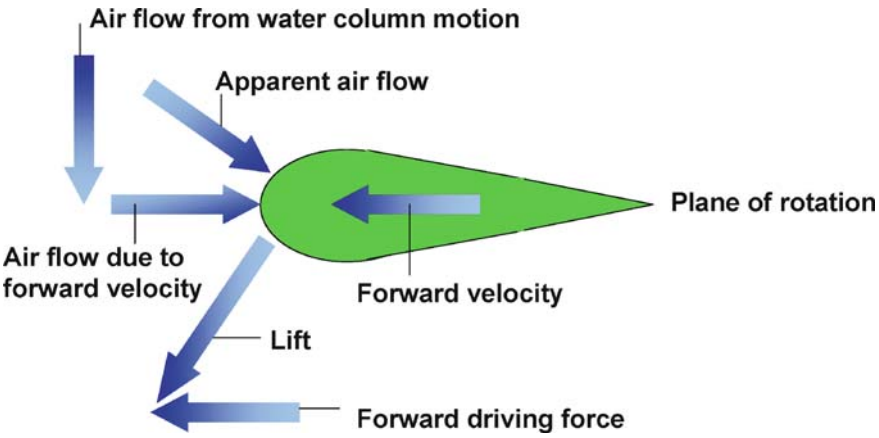

Fig. 7.3. Principle of operation of the Wells turbine

between zero (when the turbine is rotating but there is no airflow in the duct) to 90° (when there is airflow in the duct but the turbine is stationary). All airfoils generate lift at 90° to the angle of attack and, as is seen from Fig. 7.3, this lift has a component in the same direction as the rotation of the turbine. The great virtue of the Wells turbine is the fact that, irrespective of the direction in which the air is flowing, the turbine is driven in the same direction. In this regard the system is described as self-rectifying.

In practice there are drag forces on the turbine blades as well as lift and by comparison with some turbine forms the drag, by virtue of the large blade area, can be relatively high. This means that at small angles of attack (typically $< 2°$) the component of lift in the direction of rotation is insufficient to overcome the drag force and the turbine will not drive. The same thing happens at high angles of attack (typically $> 14°$) when the blade stalls and again the turbine will not drive. The blades are most effective at an angle of attack of around 7°.

Rather than describe the condition of the air flow on the turbine in terms of the angle of attack (θ) it is more usual to use a non-dimensional flow coefficient (Φ) which is defined as the tangent of the angle of attack at the blade tip. Thus $\Phi = \tan(\theta) = \frac{V_x}{V_t} = \frac{V_x}{r\omega}$, where V_x is the axial flow velocity, V_t the turbine tip speed, r the turbine radius and ω the rotational speed.

The detailed performance of the turbine changes with the form of the airfoil and the size of the turbine and peak efficiencies approaching 90 % are possible but the efficiency curve shown in Fig. 7.4 may be taken as representative for discussion purposes.

The peak efficiency shown is 75.5 %. As the water level in the OWC rises and falls in response to wave action the flow through the turbine will vary and hence the flow coefficient also changes. This means that the flow coefficient is constantly tracking up and down the efficiency curve with the effect that the whole cycle efficiency will be lower that the peak.

An estimate of the whole cycle efficiency can be made by noting that the instantaneous input pneumatic power is

$$P = cQ^2 , \tag{7.1}$$

where Q is the instantaneous flow and $c = \frac{P}{Q}$ is the turbine damping (or pressure drop per unit flow), where P is the instantaneous pressure. Similarly the instantaneous power converted by the turbine is $P_t = \eta(\Phi)cQ^2$ and integrating over a cycle the average efficiency is given by

$$\eta_{av} = \frac{\sum cQ^2}{\sum c\eta(\Phi)Q^2} = \frac{\sum Q^2}{\sum \eta(\Phi)Q^2} . \tag{7.2}$$

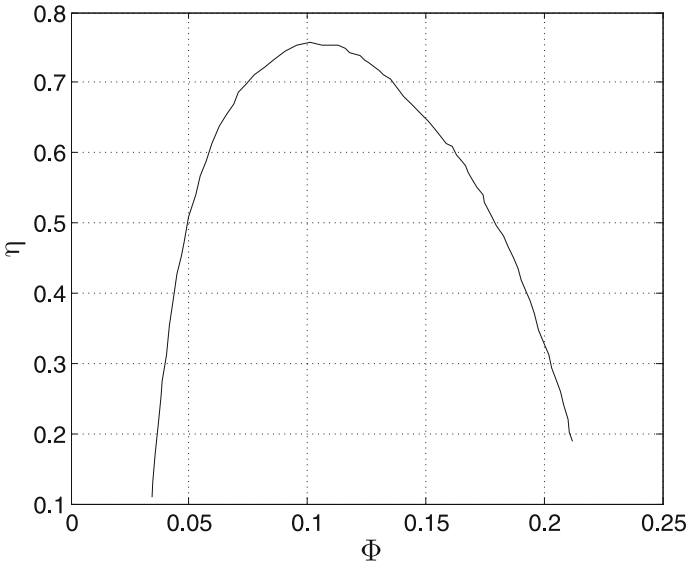

Fig. 7.4. Representative turbine efficiency curve

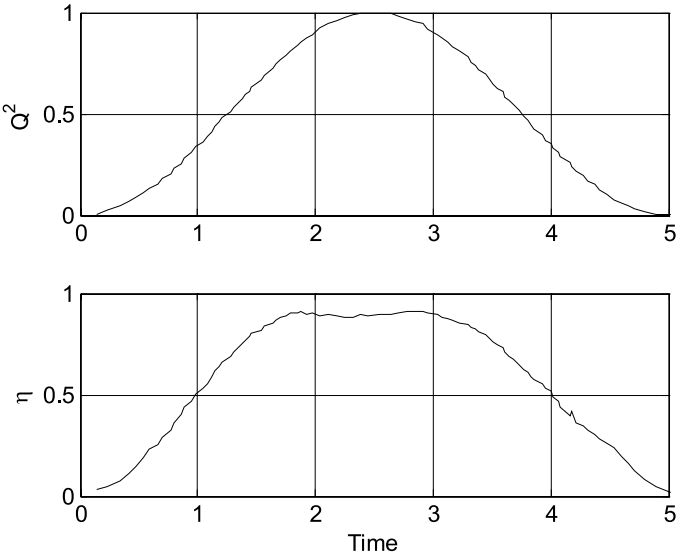

Fig. 7.5. Profiles of pneumatic power and instantaneous efficiency

If a sinusoidal flow profile is assumed and the turbine tip speed is optimised in relation to the assumed flow velocities then it is possible to develop the profiles of pneumatic power and instantaneous efficiency shown in Fig. 7.5. It is seen when there is significant pneumatic power the efficiency is close to the maximum and conversely when the efficiency is low there is little or no pneumatic power. For the example shown the average efficiency is 72 % which is surprisingly close to the peak of 75.5 %. This demonstrates that, in principle, the simple Wells turbine can deliver good conversion efficiencies even under random flow conditions.

The turbine-generator system does not work in isolation of the OWC capture chamber and the characteristics of the turbine and the influences of the power take-off damping and the motion of the water surface in the column are critical in determining the effectiveness of the primary power capture of the OWC.

As previously described in Chapter 6, the behaviour of the pneumatic power capture as a function of turbine damping for the LIMPET OWC was tested on a tank model for four different sea states. It became clear that there is an optimum damping which increases with the power in the sea. A turbine which over or under-damps the water column by a factor of two will cause the pneumatic power capture to fall by approximately 15 %. The turbine design must therefore take full account of the influence of the interrelationship between primary power capture and turbine characteristics and it must also take account of the wide range of incident wave energies which will be encountered in a typical year. The power in the sea is not uniformly distributed. Figure 7.6 shows the distribution of pneumatic powers measured on the LIMPET plant between November 2001 and March 2003. It is seen that there are a large number of occurrences of low power and a small number of high power, or storm, events.

This is a typical power distribution with the skew increasing with the distance from the equator. In this data set approximately 70 % of occurrences are below the annual average pneumatic power of 112 *kW*. In designing the turbo-generation equipment a compromise must be found between the ability of the generating plant to extract the maximum power from storm events and the additional parasitic losses of larger plant generating at part load.

For the turbine to work most effectively it must simultaneously operate at the ideal flow coefficient whilst at the same time producing the right damping to maximise pneumatic power capture. To complicate the situation it must do this in all sea states. Fortunately the Wells turbine has the right characteristics to achieve this. Section 6.1 focus such characteristics in detail but a summary is presented here, along with an application exercise to the LIMPET case.

It can be shown that the damping of a Wells turbine (c) is proportional to turbine speed (ω) so that $c = k\omega$. Also: the axial flow velocity is $V_x = \frac{Q}{A}$ or $Q = V_x A$. Combining these relationships with Eq. (7. 1) gives:

$$P_n = cQ^2 = k\omega\left(V_x A\right)^2 . \tag{7.3}$$

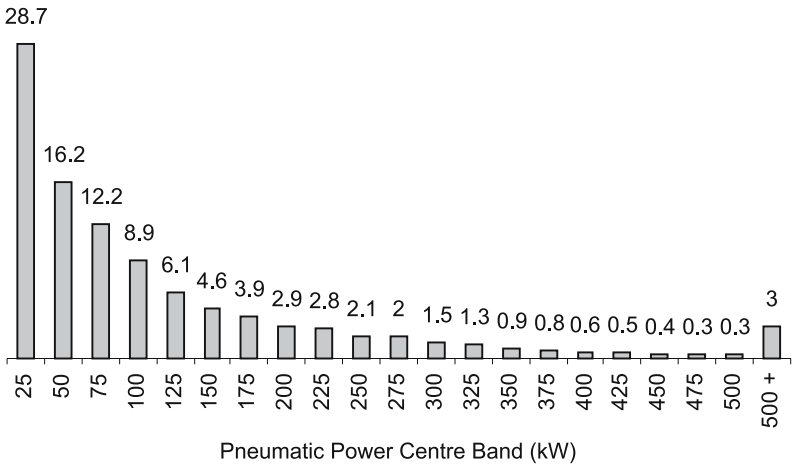

Fig. 7.6. Distribution of pneumatic power in percentage of applicability (Nov. 2001–Mar. 2003)

But if the objective is to maintain the flow coefficient in order to achieve peak turbine performance then $\frac{V_x}{V_t} = \Phi_{opt}$ or $V_x = \Phi_{opt} V_t = \Phi_{opt} r\omega$ (where r is the turbine tip radius). Substituting this in Eq. (7.3) gives:

$$P_n = k\omega\left(\Phi_{opt} r\omega A\right)^2 = k^* \omega^3, \tag{7.4}$$

where $k^* = k\Phi_{opt}{}^2 r^2 A^2$.

This means that for optimum turbine efficiency the turbine speed must vary in proportion to $\sqrt[3]{P_n}$. If the optimum damping measured for the LIMPET collector is compared to a plot of damping against $22P_n^{1/3}$ it can be concluded that there is a reasonable fit between the two, confirming that the Wells turbine has the required characteristics for good generation under a wide range of sea conditions. It is interesting that with inverter drive systems it is wholly practicable to vary the working speed of the turbine by a factor of 4 or more so that the optimum flow coefficient can be maintained for input powers varying over a $64:1$ range whilst keeping the collector damping close to ideal. This offers an excellent turn down ratio enabling generation from both the frequently occurring low sea states and the more intensive storm events.

Table 7.1 Optimum damping for different collectors (off resonance)

Type of Collector	Optimal Turbine Damping -15 *kW/m* input power ($N.s/m^5$)	Area (m^2)
4 m square breakwater section	600	16
7 m diameter Monopile	251	38.5
LIMPET	57	168

Theoretically it can be shown that in general terms the optimal damping of an OWC collector varies inversely with the water plane area. Table 7.1 shows values for optimum damping measured by Wavegen on three different collectors of widely different designs (but working off resonance). The data from Table 7.1 leads to a theoretical relationship of Optimal Turbine Damping $(N.s/m^5) = 9609 \times \text{Area}^{-1}$ (m^{-2}).

Changing the input power will change the gradient of the line and OWC systems operating near resonance will not follow the same trend but an initial estimate of the optimum damping requirement can be based on the water plane area of the OWC.

Whilst the foregoing describes features of interest in OWC technology it makes no attempt to discuss the fine detail of the influence of detailed collector form or turbine design on the overall system performance. The technology is continuing to evolve and the overall performance improving with both experience and understanding.

The majority of practical experience with OWC systems has been obtained from shoreline systems where land access is possible but a number of floating OWC systems are also under development and will become more prevalent as the technology develops.

7.1.2 Pico – European Pilot Plant

António Sarmento, Frank Neumann, Ana Brito e Melo

Wave Energy Centre
Lisbon
Portugal

Until now only shoreline or nearshore bottom standing OWC plants have been developed, except the KAIMEI and Mighty Whale floating prototypes developed in Japan in the late eighties (JAMSTEC, 1998), a project without further continuation, and in Ireland with the OE Buoy project (a floating BBDB concept – Backwards Bend Duct Buoy): a 1 : 4 scale model underwent sea tests in the Galway Bay test site in January 2007. One of the pilot plants built so far has been the

shoreline Pico plant in the Azores (Falcão, 2000). This is a 400 kW rated plant, equipped with a 2.3 m diameter Wells turbine coupled to an asynchronous generator. The turbine includes two fixed guide-vane stators, one at each side of the rotor. The generated electrical power is rectified and modulated with power electronics equipment (a hyper-synchronous cascade) before being fed into the electrical grid. The plant is also equipped with a pressure relief valve in parallel to the turbine as shown in Fig. 7.7. It also shows the sluice-gate isolation valve between the air chamber and the air duct and the fast reacting valve. The former is intended to be used whenever the plant is disconnected for a long time, whereas the latter is intended to be used to avoid turbine over-speed if in energetic seas an electrical grid fault occurs.

The monitoring equipment of the plant includes sensors to measure the:

- Rotational speed;
- Air pressure and water free-surface elevation in the air chamber;
- Static pressure both at the inner and outer covers of the air duct immediately upstream and downstream to the stators;
- Dynamic pressure at three radius averaged along three circumferential angles at the sections where the static pressure is measured;
- Vibrations and oil temperature at the turbo-generator bearings;
- Temperature, voltage and current at each of the three electrical circuit phases;
- Lubrication flow;
- Total, active and reactive power delivered to the grid;
- Cumulative active energy produced.

The plant was built with support from the European Commission through two Joule projects and a national funded project by EDP (Electricidade de Portugal) and EDA (Electricidade dos Açores), respectively the national and local utilities. The scientific responsibility of the European projects was of IST, Technical University of Lisbon, in particular of Prof. António Falcão. IST was also responsible for the conception and basic engineering of the plant and turbine aerodynamic design. Profabril was responsible for the civil engineering design and Marques Lda for the erection of the plant. The electrical, power electronic and monitoring equipment was supplied by EFACEC (Portugal) and ART (Scotland) supplied the mechanical equipment.

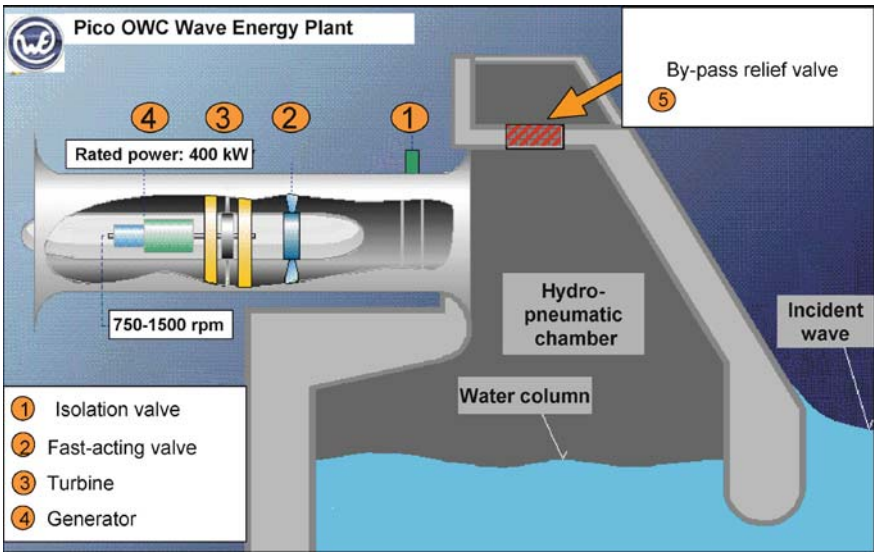

Fig. 7.7. Schematics of the Pico plant

Fig. 7.8. Back view of the Pico Plant

7.2 Archimedes Wave Swing (AWS)

Miguel Prado

Teamwork Technology BV
Zijdewind
The Netherlands

Among the main full-scale concepts, the Archimedes Wave Swing (AWS) is a unique wave energy converter because it is completely submerged. This is extremely relevant for its design as it makes the system less vulnerable to storms. Also, it is not visible, thus the public acceptance of a AWS wave farm is not as problematic as, for example, a wind farm. It can be consider to be of the point-absorber type (characteristic length, in this case the diameter, small when compared with the wavelength), and, as in the case of Pelamis (for example), it is envisaged to be deployed in arrays of devices unit rated in a few *MW*. This contribution aims to provide the historical background of the AWS and details regarding its design, and it is based in two previous publications: Prado et al. (2006)[1] and Cruz and Sarmento (2007)[2].

The AWS consists of an air filled chamber fixed to the seabed and open at the top (the silo), closed by another cylinder (the floater). An air lock is created between the two cylinders and so water can not flood the silo. The floater can move up (or down), due to the pressure increase (decrease) linked with the incoming wave crest (trough) directly above the device. By adding a power take-off (PTO) system this oscillation can be converted into electrical power. In the case of the AWS, the PTO is a permanent-magnet linear generator (see 'Generator Design' for more details). By tuning the system frequency to the mean wave frequency, the stroke of the linear motion can be made larger than the wave height. In Fig. 7.9 the device is moored to the seabed. For simplicity, the 2 *MW* pilot plant that was built as a full-scale demonstration project was attached to a pontoon (Fig. 7.10). A brief description of the evolution of the concept is therefore justified.

7.2.1 History

The inspiration for the AWS emerged in 1994 in a novel company called Teamwork Technology B.V, and one year later a $1:20$ model was tested in regular waves in a partnership that involved the Netherlands Energy Research Foundation/Energy research Centre of the Netherlands (ECN) and WL Delft Hydraulics.

[1] Reprinted from the Journal of Power and Energy, Volume 220, 2006, Pages 855–868, with permission from the Institution of Mechanical Engineers (IMechE).
[2] Reprinted from Ocean Engineering, Volume 34, Issues 5-6, 2007, Pages 763–775, with permission from Elsevier.

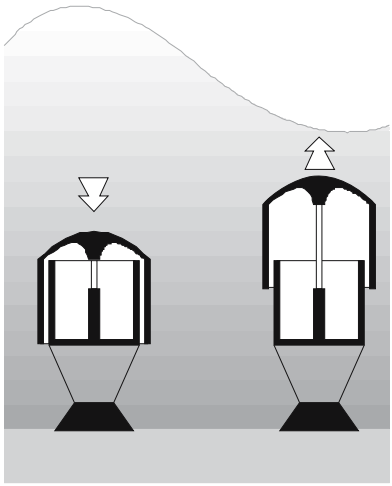

Fig. 7.9. Schematics of the AWS concept (Sarmento et al., 1998)

Fig. 7.10. The AWS at the Leixões harbour in 2004

Portugal was selected in 1995 as the location for the full scale-testing, with the north area being considered suitable not only from the energy resource point of view but also due to the proximity between the shore and the national electricity grid. The existence of several harbours and shipyards, which could be useful manly for maintenance purposes, was also seen as a vital aspect.

In the following years the target 2 *MW* prototype was assessed on the basis of overall system performance. This work was conducted by ECN, Instituto Superior Técnico (IST), WL Delft Hydraulics, Teamwork Technology and some industrial partners. A new set of 1 : 20 scale model tests were performed in the beginning of 1997, with irregular waves. By analysing the performance of the system and simulating it computationally, specifications for the regulation and transport of the electricity were made. By mid 1997 AWS B.V. was founded, joining NUON, ECN, Delft Hydraulics, Teamwork Technology and a private investor. Again a year later experimental tests, now on a 1 : 50 scale model, performed at the Hydraulics and Maritime Research Centre (HMRC) in Cork, Ireland, led to small changes on specific components like the power take-off (PTO) solution and confirmed the 2 *MW* rated capacity as the one to aim for the prototype to be installed offshore Portugal.

Fig. 7.11. Model tests (WL Delft Hydraulics)

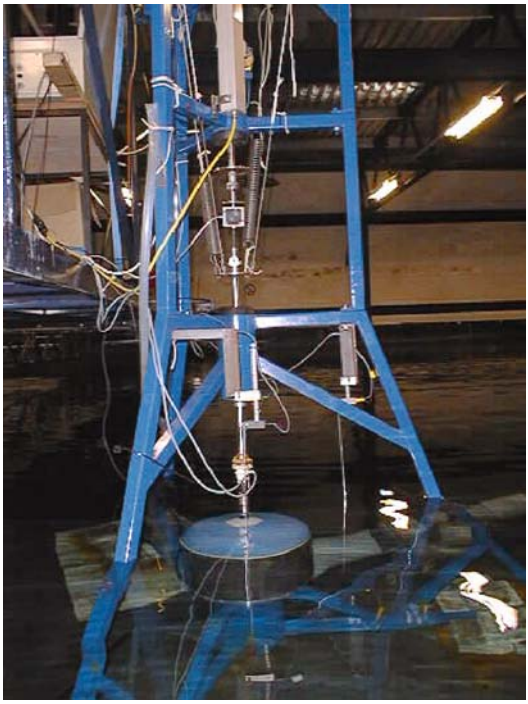

Fig. 7.12. Model tests (HMRC Cork)

7.2.2 Design of the Full-scale Pilot Plant

By early 1999 the AWS design was ready, and components were ordered from several partners. The pilot plant was then assembled in Romania, with two main additions to the original concept: a pontoon used as support for the submergence operation and a vertical guidance structure to assist the floater's motion (see Fig. 7.10). Both these features are not present in the plans for future devices, and were intended to add additional control to operations with the prototype. In November 2001 the AWS was towed to the test site and the first submergence attempt was made offshore the Portuguese coast. Stability issues emerged and the operation was suspended. The AWS was towed back to the harbour of Leixões (near Porto). A second attempt one year later was also unsuccessful but the experience gathered proved valuable when the pilot plant was finally submerged in 2004 (for more details on the submergence operation see Prado and Gardner, 2005b). The pilot plant was then tested in a variety of sea states and operation conditions with the help of the several codes developed, including a time domain simulation of the whole system, by the team at the substation located at Aguçadoura beach, and by the team members at the support boat near the plant.

Table 7.2 Characteristic dimensions of the AWS pilot plant

Description	Length (*m*)	Diameter (*m*)	Height (*m*)	Width (*m*)	Weight (*ton*)
Floater	–	9.5	21	–	400
Pontoon	48	–	5.5	28	1200
Guidance Structure	–	–	33.5	–	120

Figure 7.10 shows the pilot plant while docked in May 2004 at Leixões. Both the guidance structure for the floater and the pontoon (with the four corner towers that would be filled with water during the submergence operation) are clear in the photo. Table 7.2 synthesises the main dimensions and weights of the AWS' components. For a detailed description see Prado et al. (2005a) and Rademakers et al. (1998).

The maximum peak power is 2 *MW*. The rated stroke is 7 *m* and the rated velocity is 2.*2 m/s*. A braking system had to be included in the device to damp the motion in case of generator's limitation or failure. This system consists on two cylinders sliding into each other, forcing the water trapped inside to flow through an orifice. By changing the area of the orifice the braking force can be adjusted to the desired level. During the tests, the area of the orifice was always kept at the minimum (water brakes were closed) and therefore the damping was quite high. The moving part of the device has a mass of around 400 *ton*, and the total mass of the device, including the pontoon, is approximately 7000 *ton* (from which around 5000 *ton* are just due to the sand ballast tanks). Most of the volume is reserved for the ballasting tanks necessary for the submerge/emerge operation. The air volume of the device at mid position is approximately 3000 m^3 and can be changed by pumping in/out water. The total volume of water that can be pumped is approx. 1500 m^3 and permits to tune the natural period of the device in the range of 7–13 *s*.

7.2.3 Linear Generator Design

To finalise the basic description of the AWS technology, some generic considerations about the design of the power take-off system are made. When designing the PTO for the AWS, the key driving forces were identified as the following:

- Maximum stroke: 7 *m*;
- Maximum speed: 2.2 *m/s*;
- Maximum force: 1 *MN*;

- Robustness;
- Maintenance as low as possible;
- Efficiency;
- Cost;

During the design process, the following choices were made in order to meet the requirements as good as possible.

1. Probably, a generator system consisting of a gearbox that converts the linear floater motion into rotating motion and a standard rotating generator would be a cheap and rather efficient solution. However, it appears to be extremely difficult to build one that is robust and maintenance-free. Therefore, a linear generator is used.
2. It is nearly impossible and extremely expensive to make the generator large enough to take all possible forces generated by waves. Therefore, the AWS also has water dampers that can absorb very high forces. This implies that the generator can be designed as a compromise between energy yield and cost.
3. The linear generator that converts the mechanical energy into electrical energy is a permanent-magnet (PM) generator because it has a rather high force density and efficiency at low speeds.
4. The magnets are on the translator that moves up and down, so that there is no electrical contact between the moving part (the translator) and the stator, which is important because such an electrical contact suffers from wear.
5. The generator is flat. Possibly, round generator constructions fit better in the construction of the AWS. However, for a single generator for a pilot plant, it was much cheaper to remain close to existing production technology and build a flat generator.
6. The number of slots per pole per phase is one. Increasing this number would lead to large pole pitches, resulting in thicker yokes and a higher risk of demagnetization. Decreasing the number of slots per pole per phase (using fractional pitch windings) would lead to additional eddy-current losses due to additional space harmonics.
7. The magnets are skewed to reduce cogging.
8. The translator with the magnets is only a few meters longer than the stator in order to reduce cost. This means that in the central position, the magnets of the translator are completely overlapping the stator so that maximum forces can be made, but in the extreme positions, the magnets only partly overlap the stator.
9. To balance the attractive forces between stator and translator, the generator is double sided, as depicted in Fig. 7.13.
10. For cooling the stator of the generator, a water cooling system was implemented.

11. The power electronic converter for the grid connection is placed on shore so that possible problems with the power electronics and the control could be easily solved. A 6 *km* long cable connects the generator terminals to the converter on shore.
12. A current source inverter on the shore is used for the utility grid connection. A voltage source inverter would have advantages of better control characteristics, better power factor, better generator efficiency and higher forces and energy yield (Leijon et al., 2005). However, it appeared to be easier and cheaper to use a readily available current source inverter.
13. Coatings are used to protect the generator against the aggressive environment.

Figure 7.13 depicts a cross section of the generator. When the translator with the magnets moves up and down, voltages are induced in the coils in the stator slots. Figure 7.14 shows a photograph of a part of the stator.

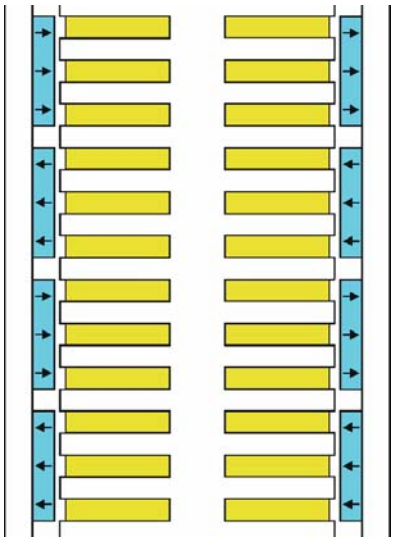

Fig. 7.13. Section of four pole pitches of the linear PM generator. The middle part is the stator with stator iron and coils in the stator slots in between. The left and right parts are the translators with the magnets with arrows indicating the magnetisation direction

Fig. 7.14. Photograph of a stator in the AWS

7.3 Pelamis

Richard Yemm

Pelamis Wave Power Ltd
Edinburgh
Scotland, UK

The Pelamis wave energy converter (WEC) is a semi-submerged, articulated structure composed of cylindrical sections linked by hinged joints and is held on station by a compliant mooring system that allows the machine to weathervane to align itself head-on to incoming waves (it takes its 'reference' from spanning successive wave crests). As waves travel down the length of the machine they cause the structure to articulate around the joints. The induced motion of these joints is resisted by hydraulic rams that pump high-pressure oil through hydraulic motors via smoothing accumulators. The hydraulic motors drive electrical generators to produce electricity. Power from all the joints is fed down a single umbilical cable to a junction on the seabed. A number of devices can be connected together and linked to shore through a single seabed cable. Some key features should be highlighted:

1. A Pelamis wave farm can be installed in a range of offshore water depths and sea bed conditions to allow site developers flexibility in selecting installation sites.

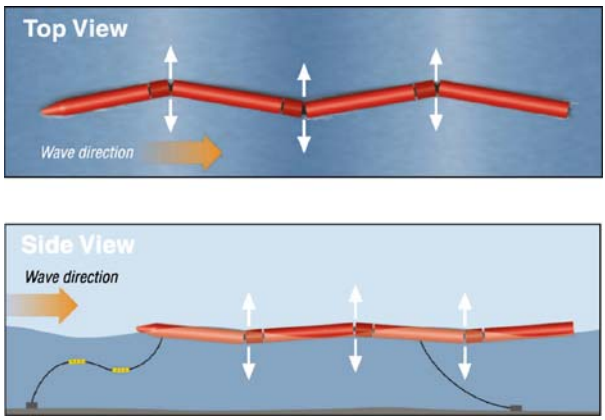

Fig. 7.15. Schematics of the Pelamis WEC (top and side views)

2. The Pelamis is constructed, assembled and commissioned off-site in safe conditions on land or in sheltered dock facilities, therefore requiring an absolute minimum of installation work required on-site. This avoids more expensive extended offshore construction activities, which are subject to longer weather delays.
3. The Pelamis has a rapid attachment / detachment electrical and moorings connection, which also allows the machine to be quickly retrieved and taken offsite to a safe quayside facility for any maintenance requirements, thus avoiding costly offshore operations with specialist equipment and vessels.

In this section details regarding the development of the Pelamis concept and a thorough description of the power take-off system are given. Some generic considerations regarding the hydrodynamics of the Pelamis are also presented.

7.3.1 Development Programme

Since its inception in 1998 it has been the sole objective of Pelamis Wave Power Ltd (PWP) to develop the Pelamis technology. At present, over 70 members of staff work daily from different locations to ensure that the Pelamis concept will become the market leader in the near future. It is fair to say that the Pelamis is one of the most studied WECs in history. Such claim is based on the several test rounds that were conducted at different wave tanks with several scale models, and the numerical modelling programme that was (is) followed in parallel. Table 7.3 presents the most significant test rounds, mentioning both the scale and the location of the tests. The experimental modelling programme is vital for validation of the numerical simulations, particularly when envisaging

Table 7.3. Detail of the experimental test round conducted to date

Model	*Test Objective*	*Location*	*Date*
80th Scale	Survivability	University of Edinburgh wide tank	May 1998
35th Scale	Numerical model validation	University of Edinburgh wide tank	July 1998
35th Scale	Alternative configurations	University of Edinburgh wide tank	July 1998
20th Scale	Survivability	London City University 55 *m* wave flume	Sept 1999
20th Scale	Numerical model validation	Glasgow University 77 *m* wave tank	Aug 2000
20th Scale	Power capture and mooring specification	Trondheim Ocean Wave Basin, Norway	Oct 2000
33rd Scale	Power capture	University of Edinburgh wide tank	Jan 2001
33rd Scale	Power capture	University of Edinburgh wide tank	Aug 2001
7th Scale	Digital control systems	Firth of Forth	Oct 2001
33rd Scale	Mooring response	Glasgow University 77 *m* wave tank	Mar 2002
50th Scale	Survivability	Glasgow University 77 *m* wave tank	Aug 2002
20th Scale	Control and survivability	Ecole Centrale de Nantes wide tank	Oct 2002
20th Scale	Control systems	Ecole Centrale de Nantes wide tank	Mar 2003
7th Scale	Mooring response and development	Ecole Centrale de Nantes wide tank	Apr 2003
20th Scale	Control and survivability	Ecole Centrale de Nantes wide tank	Mar 2005
21st Scale	Control and survivability	Ecole Centrale de Nantes wide tank	Feb 2007
21st Scale	Alternative configurations; Numerical model validation	Ecole Centrale de Nantes wide tank	Apr 2007

the next generation(s) of Pelamis machines. The role of numerical and experimental modelling in the development of the Pelamis WEC was addressed earlier in this book in section 5.4.

Among other significant milestones, the commissioning of a full-scale test rig for testing the power conversion module was pivotal for the development of the Pelamis. The test rig provided the final benchmark towards a full-scale prototype, by validating all steps of the power conversion chain. Two sets of actuation rams were mounted outside the module to simulate the wave action and drive the internal systems. Cycle testing of the power conversion module has provided confirmation of the suitability of each of the components and the reliability of the power conversion and electrical systems prior to the first offshore testing of the prototype.

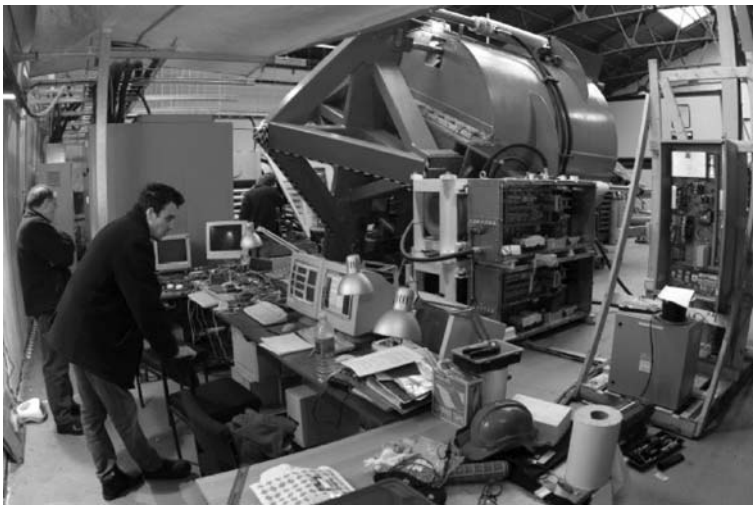

Fig. 7.16. Full-scale test rig (view from control station)

The natural step forward was fulfilled with the construction of the first full-scale Pelamis wave energy converter, which can be seen as both a pre-production prototype as well as a technology demonstrator. It uses 100 % 'available technology' as all system components are available 'off the shelf'. As with the full-scale test rig, the UK Department of Trade and Industry (DTI) have contributed to the funding of this demonstration machine. Verification of the design was performed by WS Atkins to ensure that it complies with offshore codes and standards (DNV). The machine was constructed entirely of steel using conservative safety factors. Steel has been chosen to simplify structural analysis, design and instrumentation and to ensure that modification and repair are straightforward. To reduce capital costs, the possibility of post-tensioned concrete tube elements is being investigated for subsequent devices.

The modular power-pack is housed in a second fully sealed compartment behind the ram bay so that in the event of seal failure only the hydraulic rams are immersed. Access to all system components is via a hatch in the top of the power conversion module. Maximum individual component weight is less than 3 tonnes to allow replacement using light lifting equipment.

The wave-induced motion of each joint is resisted by sets of hydraulic rams configured as pumps. These pump hydraulic fluid into smoothing accumulators which then drain at a constant rate through a hydraulic motor coupled to an electrical generator. The accumulators are sized to allow continuous, smooth output across wave groups. Output smoothness from the complete device will be comparable with that of a conventional thermal generator set. An oil-to-water heat exchanger is included to dump excess power in large seas and provide the necessary thermal load in the event of loss of the grid. Overall power conversion efficiency ranges from around 70 % at low power levels to over 80 % at full capacity.

Each of the three generator sets are linked by a common 690 *V*, 3 phase 'bus' running the length of the device. A single transformer is used to step-up the voltage to an appropriate level for transmission to shore, *HV* power is fed to the sea bed by a single flexible umbilical cable, then to shore via a conventional sub-sea cable.

Following construction the prototype machine underwent a comprehensive series sea trials in the North Sea (Fig. 7.17). After its success the device was towed to Orkney where it began a test programme at the European Marine Energy Test Centre (EMEC) in August 2004 (Fig. 7.18). When on site the machine's performance in supplying electricity into the grid is monitored and independently verified (see section 7.5.4). The Electric Power Research Institute (EPRI) presented a study in late 2004 which, in light of the success of this test round, concluded that the Pelamis technology was the only one available for immediate deployment.

Since the first sea trials and installation the prototype has been removed from site several times for both inspection and maintenance. The machine underwent a major refit at in 2006, when it was towed to a dry dock in Leith (Edinburgh) for a thorough check-up. This opportunity also allowed significant engineering improvements that tried to emulate the next stage: the P1A project.

Fig. 7.17. The Pelamis WEC full-scale prototype (150 *m* long, 3.5 *m* in diameter)

Fig. 7.18. The Pelamis WEC installed at the European Marine Energy Centre (Orkney)

Fig. 7.19. One of the P1A machines being assembled in Portugal

The P1A iteration of Pelamis machines corresponds to the first three machines that were ordered by a Portuguese consortium lead by Enersis in 2005. The three machines were towed to the Port of Peniche in 2006, for final assembly and commissioning (Fig. 7.19). The machines are to be installed in the north of Portugal, 5 *km* offshore Póvoa de Varzim, in what will become the first offshore wave energy farm. A letter of intent was already signed for a much larger project at the same location, involving a total of 30 Pelamis machines. The Enersis project is in the wake of the success of PWP's development programme, particularly the testing of the full-scale prototype. Such success was also recognised by the Scottish Executive, which recently (2007) announced that it would provide financial support to a Pelamis wave farm (four machines) at EMEC, in a project lead by Scottish Power.

7.3.2 Power Take-off

The power take-off system within the Pelamis is housed in Power Conversion Modules (PCM's) – as shown in Fig. 7.20 (previously presented in Chapter 6). There is a PCM positioned between each long tube section of the machine. There are four long tube sections in a Pelamis machine and three PCM's. The power take-off system uses hydraulic rams to resist the bending moments experienced

about hinged joints at either ends of the PCM ($1\times$Heave Joint and $1\times$Sway Joint). The bending moments are a result of the machine flexing under variable buoyancy forces from the local wave condition. The bending forces drive the hydraulic rams in extension and compression generating a high pressure flow of hydraulic fluid. This fluid is stored in pressure accumulators where it can be released under the control of a high pressure valve to flow across a variable displacement hydraulic motor which is coupled directly to a three-phase asynchronous generator with a rated output of $125\,kW$. Control of the high pressure fluid flow from the accumulator to the motor-generator set allows impulses from the absorbed wave energy to be smoothed within the accumulator so that the continuous out-flow of fluid at a constant pressure provides a smooth electrical output from the generator.

Once the fluid has passed through the hydraulic motor it is fed back into the low pressure hydraulic circuit where it is stored and recycled back into the high pressure circuit. For environmental reasons PWP only uses biodegradable hydraulic fluid so that in the unlikely event of a leak of fluid into the marine environment it will break down within days. Figure 7.21 shows a simple drawing of a single hydraulic circuit from the PCM (also previously presented in Chapter 6).

Within each PCM there are two separate hydraulic circuits similar to the one shown above. These circuits can be operated in combination or in the event of a component failure, or in an effort to increase system efficiencies, the circuits can be operated in isolation of each other. Each circuit contains one hydraulic ram resisting the heave bending moment and one hydraulic ram resisting the sway bending moment- this provides control on both axes in the event of a component failure within one of the circuits. Pelamis also has the ability to "dump" all absorbed power in response to grid constraints or cable connection failure; this is achieved through heat exchangers. As each of the hydraulic circuits has the capacity to generate $125\,kW$, each PCM therefore has the capacity to generate $250\,kW$. The three PCM's within one Pelamis machine give a rated capacity of $750\,kW$. The generated electricity is transported from the three PCM's down the length of the machine to the nose via medium voltage cabling where it then passes through a step-up transformer ($11\,kV$ in the prototype system) before being connected to the static sub-sea cable through a flexible umbilical electrical inter-connector.

The Pelamis benefits from a number of inherent characteristics and technological principles that gives it a unique and optimised balance of power absorption and survivability characteristics. To understand these it is essential to grasp the underlying principles behind the resource – wind driven water waves. Chapter 4 is fully dedicated to the wave energy resource, but particular aspects of its influence on the hydrodynamics of the Pelamis are detailed in section 7.3.3.

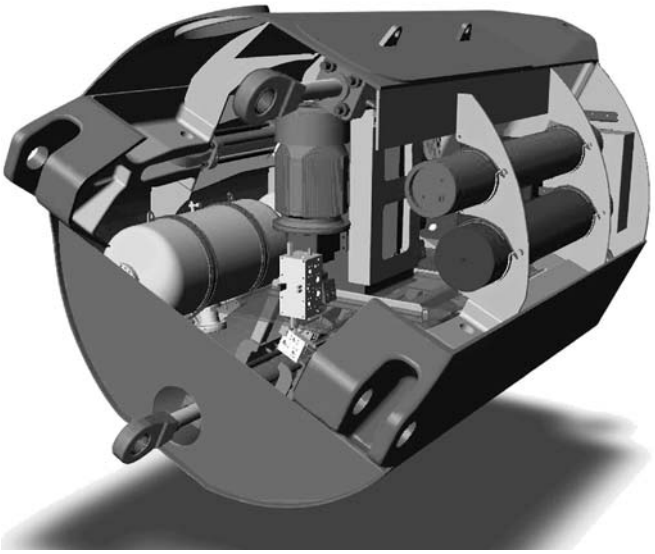

Fig. 7.20. Detail of the Pelamis Power Conversion Module

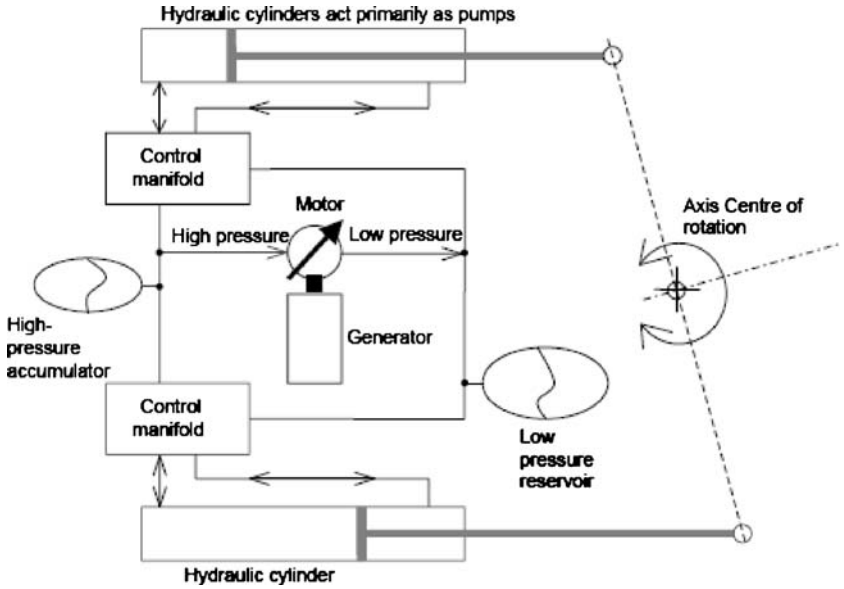

Fig. 7.21. Simplified schematic of the Pelamis PTO (Henderson, 2006)

7.3.3 Pelamis Hydrodynamics – Harnessing and Hiding

The primary driver

The ability of a wave energy converter to absorb power is directly related to its 'water-plane area' (for pressure activated systems, like Oscillating Water Columns or the Archimedes Wave Swing, this corresponds to the pressure-plane area). Generally speaking, the greater the water-plane area, the larger the forces that will be induced, and the larger the power capture potential. This concept is similar to that of the swept area of a wind turbine, or the swept volume of the pistons in a car engine. However, a large water-plane area would normally mean a very large volume. Volume equals weight, and weight is a good indicator of costs. Pelamis gets round this by creating a large water-plane area to volume ratio by distributing its volume thinly along its length. For reference - a spherical buoy of the same water plane area would be $20\,m$ in diameter, and have thirteen times the volume

A source of reaction

One of Newton's laws of motion states that every force or action must have an 'equal and opposite reaction'. This fundamental principle must be obeyed by all physical systems including wave energy converters. In order to absorb power, the source of reaction must be able to provide solid reaction against the large wave induced loads. Providing an effective source of reaction is therefore a key design challenge for WECs. Offshore structures and wave energy converters have included a number of sources of reaction:

- Rigid coupling to the sea bed, either through self weight, direct fixture, or via a rigid mooring system is the most obvious and common choice of reaction reference. This requires either enormous mass or major insitu civil construction including extensive piling or rock anchors. As the system is essentially fixed in place, there is little or no scope for limiting hydrostatic or hydrodynamic loads in extreme conditions.
- Internal reaction mass. Here the relative acceleration of the WEC body and a coupled mass (either a solid lump or a constrained volume of water) is used. The problem with this system is that at the wave periods of interest the mass must be very large compared to the WEC body mass to provide sufficient reaction. Even with large masses there is significant 'lost motion' associated with 'dragging' the weight around with you, reducing the efficiency of the system. There is no scope for force limiting as wave height becomes larger.
- External reaction plate or body. Here a large mass is created using a large submerged plate, oriented at 90 degrees to the direction of motion, to push and pull against the surrounding water like a bi-directional parachute. Again, as inertial forces are weak relative to buoyancy forces at the wave periods of interest, the plate must be very large compared to the WEC body and waterplane area to provide even modestly effective reaction. Extreme loading on this type of system is typically even worse than for the case of an internal reaction mass.

All of the above systems require a separate reaction system to be supplied, often significantly larger or more massive than the WEC body itself. This separate system has to be strong enough to take extreme loads that may be an order of magnitude higher than typical operational forces. The direct and inescapable impact of this is significantly increased cost per unit power.

The Pelamis introduces the concept of 'self-reference' whereby the buoyancy forces applied by the waves are reacted against by buoyancy forces elsewhere on the machine. The length of the machine is chosen to be comparable to the maximum wavelength of interest, so that the system acts as a bridge between successive wave crests that pass by. The relative motion of the machine body to the water surfaces induces strong bending-moments along the machine while maintaining an overall vertical equilibrium with the wave. It is these bending-moments that drive the joints to absorb power. All forces are internal to the machine, no external source of reaction is required, and all components in the system both directly absorb energy from the wave and provide a source of reaction for the rest of the machine. Such direct link between power absorption and source of reaction make the Pelamis concept unique.

Tuning-up

Waves provide a cyclic or harmonic force input. It has long been understood that absorbing the energy from such an input is maximised by 'tuning' the natural frequency of the system to the frequency of the input force – very much like pushing a swing in time with its motion. This ideal match between the force applied and the response of the system at its natural frequency is known as 'resonance'.

Physics dictates that the frequency at which a mechanical system will naturally oscillate when pushed is a simple function of both its stiffness and its mass. The stiffer and lighter a system, the higher its natural frequency, and vice-versa. To be an efficient absorber, a WEC must therefore be given a stiffness and mass carefully chosen to provide a natural period matched to that of the incoming waves.

Most modern WEC concepts attempt to take advantage of this principle by carefully choosing their stiffness (buoyancy) to couple with their mass (weight) to produce a natural oscillation, or bobbing, period that matches the waves where most power is found. Some can, to some degree, 'tune' themselves to the incoming waves by varying their stiffness or mass. However, most WECs have this condition 'hard-wired' into their design - they are resonant, or near-resonant, whether the waves are small or large. In the latter case loads and motions become extreme at exactly the time when the WEC should to be reducing its response to survive.

The Pelamis achieves resonance in a creative way: the cross section of the machine is chosen to give a natural period far shorter than the waves of interest – typically, the Pelamis structure would 'bob' up and down once every 2 or 3 s, which is three or four times quicker for the most commonly encountered waves. This is because the system is hydrostatically too stiff for its own weight. It is as if

we have artificially shortened the ropes on our swing to make it impossible to push quickly enough. To achieve resonance we must then find a way of either increasing the mass or reducing the stiffness. The former is not possible without incurring a large cost penalty. However, the geometry of the Pelamis joints is designed to dramatically reduce the stiffness of the system when desired through the following patented mechanism.

Each Pelamis power conversion module allows motion about two independent axes; these axes are arranged at 90° to each other. However the axes are not horizontal and vertical – they are, instead, biased 25–30° away from this to give an orthogonal pair of inclined axes of motion. The axis that allows motion in a more vertical direction is known as the heave axis, the axis that allows motion in a more sideways direction is known as the sway axis. Together these axes allow motion in any direction, like a universal joint on a car transmission shaft.

The challenging part comes with controlling the restraint applied to each axis depending on the waves encountered. If equal or similar restraint is applied to both joints the machine will respond as a simple articulated raft. All motions will be vertical as if the system only had simple horizontal hinges along its length. If, however, a much larger restraint is applied about the heave axis than the sway axis a very different response is stimulated. The joints will preferentially respond about the sway mode, giving an amplified sideways 'snaking' response along an inclined path. This response is analogous to the traditional child's toy snake that when held by the tail weaves its body and head vigorously back and forth under the action of very small motions of the tail. However, the twist in the tail for Pelamis is that the inclined axis of motion has a dramatically lower hydrostatic stiffness than the vertical mode, corresponding to what is need to achieve resonant response at the wave periods of interest. The key is that this cross-coupled, resonant response is only a result of a deliberate control application – the default mode is equal joint restraint and a safe, non-resonant response.

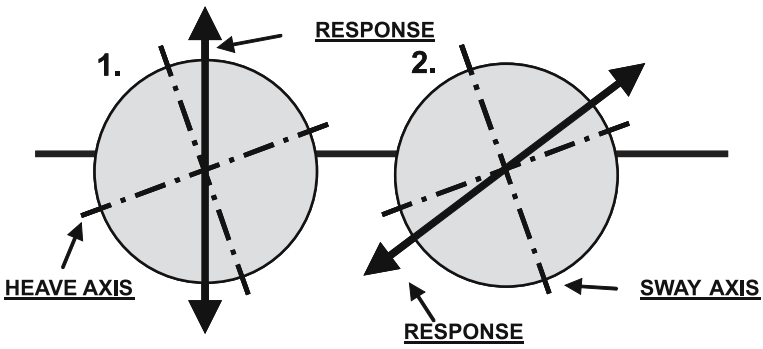

Fig. 7.22. Schematics of the Pelamis response under non-resonant (1) and resonant (2) conditions

Focusing your efforts

Engineers and mathematicians are always looking for ways to simplify the analysis of complex systems. In the case of wave energy, a very powerful analysis technique is to look at the waves a WEC can generate in still water if it was driven through a given motion cycle. That is to think of the machine as a wave-maker rather than a wave-absorber. It is an incontestable fact that a good wave-absorber must be capable of being a good wave-maker (Falnes, 2002). Some of these radiated waves can be used to cancel out the incident wave stream through destructive interference thereby absorbing power. This abstract technique allows the fundamental power capture capability of different WEC types to be studied more easily.

Another mathematical definition created to assess a wave energy converters performance is its 'capture-width' (see Chapter 3). This is the width of wave front absorbed, defined as the power output from the machine divided by the incident wave power level per metre of wave front width.

WEC's currently under development are, almost exclusively, of the heaving buoy 'point-absorber' type. Water is displaced by the vertical motion of a buoy on the surface, or by expansion/contraction of a submerged or semi-submerged volume. This action generates a symmetrical, circular set of waves propagating equally in all directions – similar to dropping a stone into a pond. Because of this, only a proportion of these radiated waves can cancel out the incident waves we are trying to absorb. Even so the theoretical limit of wave absorption capture-width turns out to be the wavelength divide by 2π, which for typical waves works out to be 15–25 m, irrespective of the frontal width of the machine. The maximum power of the machine is limited by the volume of the unit as this determines the maximum size of wave that can be radiated, and therefore absorbed.

Pelamis' radiation-pattern is fundamentally different. Imagine the Pelamis as a long line of dynamically linked, small heaving buoys, spaced along a line in the direction of propagation of the wave; hence the description of *line absorber*, mentioned previously in Chapter 3. When bobbed up and down, each of these produces a circular pattern of waves as before. However, if the relative phase of their motion is chosen carefully, these individual waves will reinforce in one chosen direction, while cancelling each other out in all other directions. This produces a focused wave pattern like a torch beam rather than the diffuse light from a lantern. The phenomenon is exactly the same as used by modern 'phased-array' radars to scan the radar beam without moving the antenna. The phasing of these motions can be actively controlled to maximise power capture in small seas, or minimise response under survival conditions. An example of the interaction of the directional radiation pattern with a regular wave field is shown in Fig. 7.23.

This inherent, and unique, hydrodynamic property of Pelamis means that the theoretical capture width of the system rises up to half a wavelength, three times higher than a simple heaving point absorber system. It follows directly that, for a given volume, the Pelamis is capable of absorbing up to three times as much power as the same volume configured as a heaving buoy.

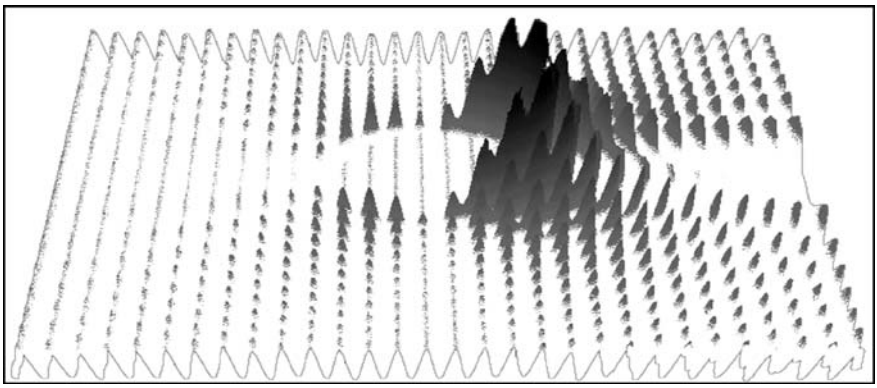

Fig. 7.23. Interaction of the directional radiation pattern with a regular wave field

Put more practically – on a good wave energy site, with an average annual incident power of 50 *kW/m* a WEC will be designed to reach rated power at an incident power level of approximately 50–60 *kW/m* to make most effective use of its power take-off system and electrical tie-back to shore. This inherently limits the economic rated power of any heave only buoy, irrespective of size, form or mode of operation, to approximately 1 *MW*. The corresponding ultimate limit for Pelamis is three times this, 3 *MW*.

This kind of conceptual advantage is analogous of the kind of advantage enjoyed by modern wind turbines, which use lift to drive the rotor, over old forms that used drag. Another analogy is the example of the torch versus the unfocussed bulb. The torch makes very efficient use of the bulb and batteries energy and power, compared to the omni directional lantern.

7.3.4 Shedding the Load

Power capture effectiveness is only one desirable characteristic of a WEC. Another is limiting loads and motions once rated power has been reached as the wave height increases. Figure 7.24 is a typical 'probability-of-exceedance' plot for wave height at a typical site.

For most of the year ($>90\,\%$) wave heights are less than $\sim 4\,m$. It is in these conditions that the system must generate as much power, as efficiently, as possible. For the remainder of the year during storms (less than 10 % of the time), wave heights increase to much higher levels, greater than 15 *m* in the worst storms. It is critically important that the fundamental hydrodynamics of the system limit the power that has to be absorbed by the onboard power take-off systems once the rated power sea state has been reached. Without this characteristic the power-take-off system would have to be rated for a much higher level with the dual penalty of higher capital cost, and significantly reduced efficiency at the normal operating power levels.

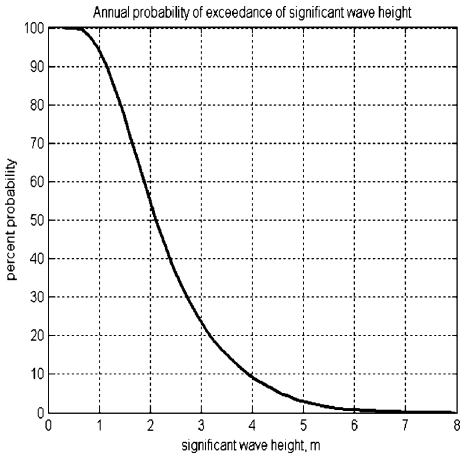

Fig. 7.24. Typical annual probability of exceedance plot (significant wave height)

Pelamis achieves this characteristic on account of its finite local volume down the length of the machine. As the wave height and steepness increases, the tubes locally fully submerge under, and emerge from wave crests, limiting the buoyancy and weight forces that generate bending moments in the machine. This process, known as hydrostatic-clipping, means that as wave height rises further the bending moments and joint angles (and therefore absorbed power) limit close to the chosen rated power level. This effect is analogous to the self-limiting characteristics of stall-regulated wind turbines whose blades stall above the rated power wind speed, limiting power capture without the need for complex control.

The effect described above also gives rise to desirable survivability characteristics that are at the heart of the Pelamis concept. Limiting the primary hydrostatic driving forces is an essential first step. However, most extreme loads in the marine environment arise from hydrodynamic effects – drag loads and inertia (or slamming) loads.

Drag loads arise from the turbulence created by the high speed flow of a fluid past a solid obstruction, in our case the body of the WEC machine. Loads rise with the square of velocity with the result that they are almost insignificant in small seas but rise rapidly to dominate loading in very large waves. For example, drag loads in 15 m high winter storm waves will be over 200 times those on a gentle 1 m summer swell. It is essential that the form of the machine is as 'slippery' and low drag as possible to minimise these loads, just as a racing car must be as streamlined as possible to increase speed.

Slamming loads can be even more destructive. These arise when a fast moving volume of fluid hits a solid body whose shape prevents its easy 'escape'. The most painful analogy is 'belly-flopping' off the top diving board at the swimming pool. The pressure spike that leads to red skin and a red face can crush or tear marine structures. The worst slamming loads occur on structures that have large flat pan-

els that stop the fluid flow rapidly. Non-slamming forms are small, rounded or pointed, thereby allowing easy diversion of the flow rather than deceleration.

Research shows that load spikes induced in the vessel structure by the bow slamming are an order of magnitude higher than the basic hydrostatically induced bending loads (Cook, 1998). If these loads cannot be minimised or eradicated, the structure will have to be designed to withstand them, with an associated increase in material and cost.

A survivable WEC concept must be near invisible to hydrodynamic loading to prevent loads rising uncontrollably in storm seas. Pelamis tries to achieve this by presenting the 'slipperiest' form and minimal cross sectional area to the oncoming waves, and by buoyancy so that the machine can dive cleanly through the crest – similar to a surfer swimming out against breaking seas.

7.3.5 Implementation – Technology Transfer

Hydraulics

Wave loading is characterised by high forces and low velocities, continuously changing with time. An appropriate technology is required to effectively harness this and extract the energy. High pressure hydraulics are universally specified where similar characteristics are encountered or required in engineering. Everyday examples of this include:

1. Heavy lifting or pulling equipment
2. Metal presses and rolling machines
3. Extrusion machines
4. Excavators
5. Large traction vehicles

In addition, the lumpy, unsteady nature of energy input to a WEC means that its power take-off system has to cater for high instantaneous input power levels, and provide a significant amount of short-term energy storage to deliver a steady output power. Smooth output will be essential allow a large number of machines to work together and supply to the land electricity grid. Hydraulic accumulators are a cost effective technology currently available that offer the required balance of energy storage and high instantaneous power capability.

Optimising capture of wave energy also requires reliable, accurate control of forces and motions. Hydraulic systems can be highly effective for this due to the absence of significant control delay, the rigid coupling between the load and structure, the absence of inertia, and the very high instantaneous powers available. Hydraulics are used extensively for accurately controlled, high load, safety critical applications throughout engineering such as:

1. Aircraft control surface actuators
2. Power steering on road vehicles
3. Ship steering and stabilizer systems
4. Robot arms and industrial manipulators

This combination of proven high force, high power, and accurate control makes hydraulics one of the best-fit technologies for wave energy (if not the best).

Available technology – no prototypes-within-prototypes

The central rule of avoiding prototypes-within-prototypes has been learnt the hard way over and over again in the world of engineering. All WEC concepts are complex assemblies of structure and systems and many early designs fell foul of breaching this maxim. PWP set out to build the first prototype machine and all early production machines from 100 % available technology. All of the machine elements are proven components with a service track record. Wherever possible, subassemblies of components, such as the motor-generator sets, are tested under operational conditions prior to deployment in Pelamis.

Capable and flexible control system

The importance of control to successful wave energy extraction has already been described. However, it is worth re-iterating that the ultimate ability of a WEC to absorb energy and generate smooth power across a wide range of conditions, whilst surviving extreme conditions, depends on the effectiveness of the control system. The flexibility and capability of the Pelamis power take-off and control system means that as better control methods are developed, they may be implemented on existing hardware (potentially hundreds of machines) with a remote software upgrade at little cost. Operation and monitoring must be automated to allow many machines to run without human intervention. This functionality has already been developed as part of the prototype programme.

Redundancy and robustness

All components crucial to the safe operation of Pelamis have a level of redundancy within each power module to avoid safe operation being compromised due to a single component failure. For example, multiple transducers, of negligible cost relative to the entire machine, are installed and can be switched between automatically if one fails. The entire hydraulic circuit of each power module may be split in half to avoid a fault on one side, such as a leak, from affecting the other (analogous to dual circuit brakes in a car, or redundant controls in an aircraft). All communications are dual routed and any failures are handled by distributed intelligence and ultimately a mechanical failsafe system of joint restraint that can operate without electrical power for indefinite periods. The benefit of this approach lies not just with the safety of the machine, but also with the reduced requirements for intervention and maintenance. The Pelamis power take-off and control system has been designed from the outset not to be vulnerable to single-point failures. It can continue to operate after a number of individual components have failed.

Deployment, operations and maintenance

Major cost is associated with the installation and retrieval of offshore systems. It is essential that the mooring system of a WEC is designed to minimise time spent on-site, minimise equipment costs (size and classification of vessel required), and maximise the range of conditions under which operations can take place. The Pelamis mooring system requires no sub-sea work or divers, all connections are made at the surface, and it can be installed using a single vessel.

In addition, PWP is committed to the policy of off-site maintenance. As long as the system can be removed and reinstalled quickly and safely in a wide range of conditions it is much more cost effective to take the machine to the equipment, rather than the equipment to the machine. A simple example of this is a 200 tonne crane on wheels costs less than £1000 per day, an equivalent waterborne unit costs upwards of twenty time this. The Pelamis mooring and connection system minimises the amount of work on-site, and maximises the range of operable conditions.

Volume production

At every stage of the design process, the engineers at PWP consider the implications of their design on mass production. Every aspect of the machine lends itself to volume manufacturing, notably the modular nature of the tubes and power modules, and the identical subassemblies within those modules. Effort is ongoing to reduce material costs and use innovative methods of production to make a more effective machine for less money.

7.4 Wave Dragon

James Tedd[1], Erik Friis-Madsen[1], Jens Peter Kofoed[1], Wilfried Knapp[2]

[1]Wave Dragon ApS, Copehagen Denmark
[2]Technical University of Munich, Munich, Germany

Wave Dragon is one of the foremost technologies within the field of wave power. Unlike most other devices is does not oscillate with the waves; it gathers the wave energy passively by utilising the overtopping principle. The front face of the device is a curved ramp, oncoming waves surge up it, as if it were a beach. Behind the crest of this ramp lies a reservoir which gathers the water “overtopping” the ramp which now has higher potential energy than the surrounding water. The effect of Wave Dragon is amplified by long reflector wings. Mounted to the reservoir, they channel the waves towards the ramp. The energy is extracted as the water drains back to the sea through low head hydro turbines within the reservoir.

Fig. 7.25. The Wave Dragon prototype in Northern Denmark. The reservoir and ramp are situated in the middle, with the reflectors concentrating the waves towards the ramp

The Wave Dragon is designed as a floating offshore device to be placed in water depths above 20 *m*. These areas are where the greatest wave energy is, and also where it is easiest to gain the permission to deploy. Over three years of sea testing have been conducted on a prototype in Northern Denmark.

This section will introduce the technology and the history of the Wave Dragon. A short introduction to overtopping theory is presented. The rationale behind the design is considered in detail for the wave reflecting wings, the low head hydro turbines and the control strategies of the Wave Dragon.

7.4.1 A Floating Overtopping Device

The Wave Dragon is built on the concept: use proven technologies when going offshore. It consists of three main elements:

- Two patented wave reflectors focusing the waves towards the ramp, linked to the main structure. These wave reflectors have the verified effect of increasing the wave height substantially and thereby increasing energy capture.
- The main structure consisting of a patented double curved ramp and a water storage reservoir built in concrete. This is very comparable to concrete boats, many of which were built during the first world war and are still floating to this day.
- A set of low head propeller turbines for converting the hydraulic head in the reservoir into electricity. These are similar to turbines which have been used in low head river hydro plants for generations.

The challenge is to put these sub-systems together to work in this novel method and survive in the extreme environment present in offshore conditions.

Wave Dragon is by far the largest envisaged wave energy converter today. Each unit will have a rated power of 4–11 *MW* or more depending on how energetic the wave climate is at the deployment site.

This will be a device with a displacement of approximately 30,000 tonnes and dimensions as shown in Fig. 7.26. This size brings many advantages. The device will respond minimally to waves, reducing fatigue problems. Also as it is

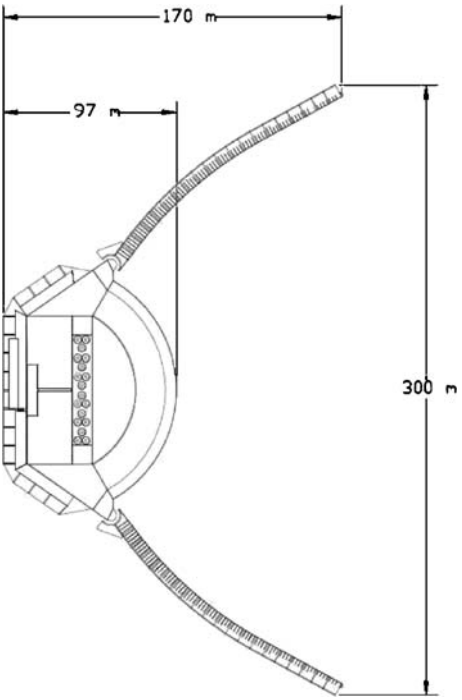

Fig. 7.26. Top view of the 7 *MW* Wave Dragon

large and stable it will be possible to work on board the device, which will dramatically reduce maintenance costs and downtime. As an overtopping device there are also many advantages to robustness of the design, in particular there are no end-stop problems as in larger seas the waves will wash over the platform harmlessly.

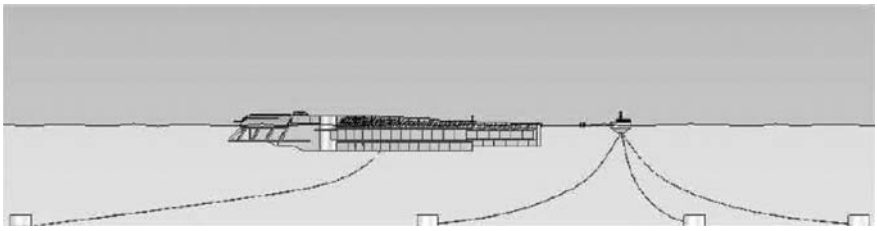

Fig. 7.27. This figure shows the CALM mooring system envisaged to be used on the demonstrator unit

The front mooring of the device will be a Catenary Anchored Leg Mooring (CALM) buoy, with a single rear mooring to restrain the device to a given rotation about the front mooring. The choice of anchor will depend on the sea bed. For the demonstrator unit concrete buckets filled with ballast rocks will be used as gravity anchors.

7.4.2 History of the Wave Dragon

The inventor, Erik Friis-Madsen, initiated the development of the Wave Dragon in 1986. In the early years he developed the principle of the Wave Dragon, and in 1994 an application for patent was submitted. Both Danish and European patents for the Wave Dragon have been obtained since then.

During the period 1995–1999 a number of studies of structural layout, overtopping of a fixed model, reflector efficiency, financial aspects, geometry, optimal choice of turbine configuration, and movements of the Wave Dragon were carried out. The findings are described fully in the report EMU et al. (2000) and Kofoed et al. (2000). Using the findings of these studies, the Wave Dragon design was slightly modified and the first test programme formulated.

The first test programme, financed by the Danish Wave Energy Program, consisted of thorough laboratory investigations of movements of the floating structure, mooring forces, forces in the reflectors, overtopping/amount of captured energy and survival in extreme wave conditions. These tests were carried out at the Hydraulics and Coastal Engineering Laboratory, Aalborg University, 1998–1999, using a floating 1 : 50 scale model of the Wave Dragon built by the Danish Maritime Institute, see Fig. 7.28.

As a continuation of the work performed under the Danish Wave Energy Program and on the basis of the research feasibility study, from 2000 to 2002 the EU granted funding for the project “Low-pressure Turbine and Control Equipment for Wave Energy Converters” under the Non-Nuclear Energy RTD Program. The total budget for this project was 1 *M€* of which the EU funds contributed 50 %.

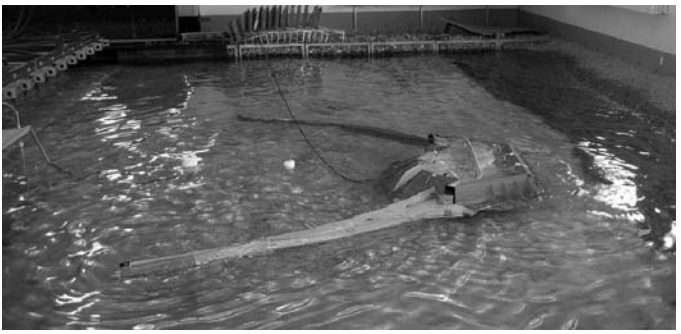

Fig. 7.28. Testing of 1 : 50 scale Wave Dragon in Aalborg University wave basin

The objective of this project was to optimise the hydraulic performance, structural design, design of configuration, control and regulation of the turbines and design of electrical components and connection to grid. The laboratory model was modified, and tested at Aalborg University and at the facilities in University College Cork-HMRC (Ireland). The modifications showed significant improvements to energy capture and hydraulic behaviour. In parallel the configuration and regulation of the turbines was designed by the following companies: Ossberger Turbinenfabrik (Germany) / Kössler GmbH (Austria), Hälleryd Turbiner AB (Sweden) and Veteran Kraft (Sweden) together with turbine tests and computer simulations conducted at the Technical University Munich (Germany). The structure was designed by the inventor Erik Friis-Madsen and adjusted to shipbuilding standards by Armstrong Technology (UK). Electrical components and connection to the grid was designed by Balslev (Denmark), Belt Electric (Denmark) and Elsamprojekt / Eltra (Denmark).

After these successful tests, the next stage for Wave Dragon was to build, deploy and operate a field prototype. Funding from the Danish Energy Authority and European Commission led to deployment of this prototype in April 2003 in The Nissum Bredning (Broads), an inland sea, connected to the Danish North Sea (see section 7.6 for complete details). Testing has been ongoing since then on the many aspects of the device, from control systems and hydraulic performance to behaviour in extreme sea states (during a 100 year storm) to effects on bird life to subsea acoustic behaviour and more. As the world's first grid-connected floating WEC this Wave Dragon has been providing power to the grid of Northern Denmark consistently. Section 7.5 gives the full details of this deployment, including results and operational experiences learnt. Progress was reported in the conference papers of Sørensen et al. (2003, 2005).

The current focus for the Wave Dragon technology is to build and deploy a multi *MW* unit. A European Commission project was begun in May 2006 to implement the design for this commercial size. Off the coast of Pembrokeshire in South West Wales much work is ongoing to gain the relevant permissions to deploy a unit there. This is mainly focused on the Environmental Impact Assessment (EIA), studying the flora, fauna, geology, shipping and other aspects.

After the first successful deployment of a Wave Dragon unit there are several projects in the pipeline to construct farms of Wave Dragons in a variety of countries.

7.4.3 Overtopping Theory

The theory for modelling overtopping devices varies greatly from the traditional linear systems approach used by most other WECs. A linear systems approach may be used with overtopping devices. This considers the water oscillating up and down the ramp as the excited body, and the crest of the ramp as a highly non-linear power take-off system. However due to the non-linearities it is too computationally demanding to model usefully. Therefore a more physical approach is taken. The time series of the overtopping flow is modelled, thus relying heavily upon empirical data.

Figure 7.29 shows the schematic of flows for the Wave Dragon. Depending on the current wave state (H_S, T_p) and the crest freeboard R_c (height of the ramp crest above mean water level, MWL) of the device, water will overtop into the reservoir ($Q_{overtopping}$). The power gathered by the reservoir is a product of this overtopping flow, the crest freeboard and gravity. If the reservoir is over filled when a large volume is deposited in the basin there will be loss from it (Q_{spill}). To minimise this, the reservoir level h must be kept below its maximum level (h_R). The useful hydraulic power converted by the turbines is the product of turbine flow ($Q_{turbine}$), the head across them, water density and gravity.

Within the field of coastal engineering there is a considerable body of work looking at the overtopping rates on rubble-mound breakwaters, sea walls and dykes. The studies of Van der Meer and Janssen (1994) provided the basis of the theory on the average expected overtopping rate. Gerloni et al. (1995) investigated the time distribution of the flow. However this work was focused on structures designed to minimise the rate of overtopping, counter to the aims of the Wave Dragon. Kofoed (2002) performed laboratory tests on many permutations of ramp angles, profiles, crest freeboard levels in a variety of sea states, all with heavy overtopping rates. These studies showed the Wave Dragon's patented double curved ramp to be highly efficient at converting incident wave power.

When comparing results between different scales of model testing it is very useful to use Non-Dimensional figures to describe the variables. Results from the model scale can then simply be used for any size of device. In coastal engineering the average flow $\overline{Q}$ is converted into non dimensional form by dividing by the breadth of the device b, gravity g and the significant wave height H_S:

$$Q_{ND} = \frac{\overline{Q}}{b\sqrt{gH_S^3}}. \tag{7.5}$$

In the case of the floating Wave Dragon it has been seen that there is a dependency on the wave period. The dominant physical explanation for this is the effect of energy passing beneath the draft of the structure. Figure 7.30 shows a typical distribution of wave energy in the water column, with the left side showing the portion influenced by the ramp of Wave Dragon and therefore available to be exploited.

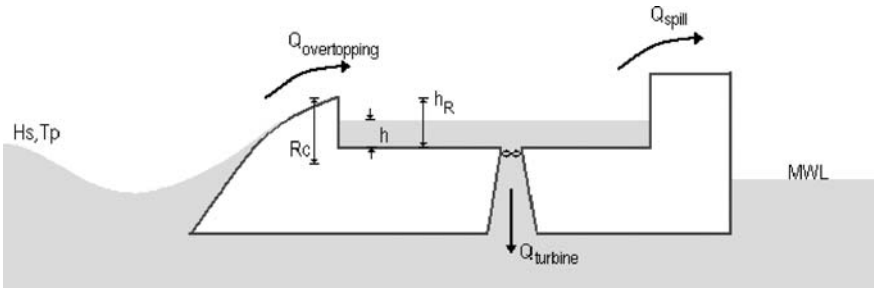

Fig. 7.29. Schematic of flows on the Wave Dragon

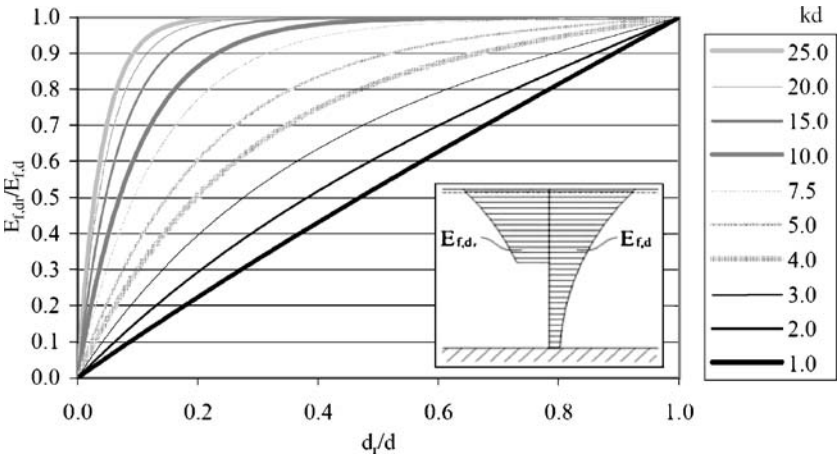

Fig. 7.30. Vertical distribution of energy in water column (Kofoed, 2002)

Shorter period waves have their energy concentrated in the upper part of the water column so Wave Dragon will absorb proportionately more energy from these. For Wave Dragon the following non-dimensional form has been used to include this period effect:

$$Q_N = \frac{1}{\lambda_{d_r}} \frac{\overline{Q}}{b\sqrt{gH_S^3}}. \tag{7.6}$$

This uses the coefficient λ_{d_r}, the ratio of energy between free surface and device draft ($E_{f,dr}$) to incident wave energy ($E_{f,d}$). This is based on linear wave theory and defined as following equation:

$$\lambda_{d_r} = 1 - \frac{\sinh(2k_p d(1-\frac{d_r}{d})) + 2k_p d(1-\frac{d_r}{d})}{\sinh(2k_p d) + 2k_p d}, \tag{7.7}$$

where k_p is the wave number at peak period, d is the water depth and d_r is the draft of the device.

To analyse the overtopping flow performance the Non-Dimensional overtopping rate is compared to the relative crest freeboard R, as shown in Eq. (7.8). This allows scale test results to be scaled to a full sized device:

$$R = \frac{R_c}{H_S}. \tag{7.8}$$

Time variation of the overtopping flow is also very important for modelling the power produced by the Wave Dragon. To make the model overtopping events are

assumed to be random and independent, with a Weibull distribution. This has been confirmed by comparisons with data from a prototype Wave Dragon (section 7.5).

With this good understanding of the overtopping flows a simulation programme was designed and has been extensively used to optimise and model the Wave Dragon behaviour. This programme provides as an input a randomly generated time history of waves overtopping the ramp according to a mean rate and a specified distribution. This allows modification of many attributes (such as: reservoir depth and area, crest freeboard height, turbine number and type and turbine operational strategy) in order to pick the configuration which will produce the most electricity for each sea condition present at a location.

7.4.4 Wave Reflector Wings

One of the most distinctive aspects of the Wave Dragon are the long slender wings mounted to the front corners of the reservoir platform. These are designed to reflect the oncoming waves towards the ramp. A wider section of wave is available to be exploited with only a moderate increase in capital cost. The overtopping volume in a wave is very dependent on the wave height, therefore by providing only a moderate increase in height, much more energy can overtop the ramp.

In order to choose the correct lengths, angles, and position of these wings Kramer and Frigaard (2002) did extensive computer modelling of many combinations of these. The computer modelling used a 3D boundary element method. The meshing requirement is reduced to the structure's boundary surface, so as a result it provides a fast, efficient and accurate frequency domain solution for linear wave structure interaction problems. The method modelled the wings in isolation. The energy flux through the central gap (where the ramp and reservoir would be) gave

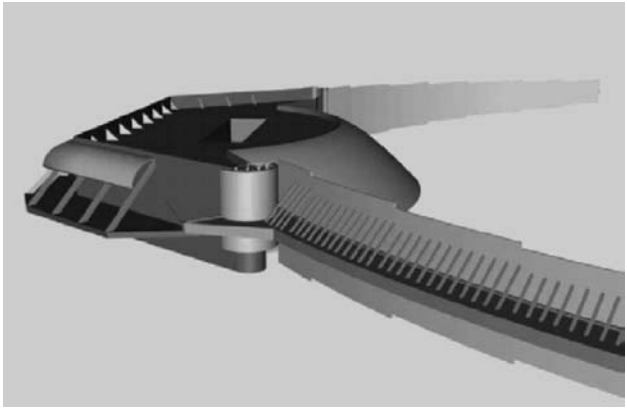

Fig. 7.31. Computer image of Wave Dragon. This shows the double curved ramp facing waves approaching from the right. The reservoir is behind and would have the turbines placed roughly in the centre. The slender wave reflectors are shown, with a flat side facing the waves, and stiffeners on their rear side

a performance coefficient for each setup. A smaller selection of sea-states and configurations was tested in a similar manner in a wave basin. Here again the wings were fixed, the platform removed and wave probes measured the waves passing through the central gap. A very good correlation was found between the two methods.

Reflectors which are floating and have finite draft will reflect higher frequency waves better than lower frequency. Typically these waves are also the smaller waves. Therefore increasing their input is very advantageous, improving the bandwidth of the device. The results show an increase in energy approaching the ramp of 85 % in these smaller operational wave states. When averaged over the sea states expected within the Danish part of the North Sea during one year, this translates to an increase in power of around 40 %.

Secondary bonuses of the presence of the wave reflector wings include: better weather-vaning performance to face the waves, lower peak mooring forces, and improved horizontal stability of the main platform.

As the aft and rear mooring attachment points are separated further, the yaw of the platform is more stable. Therefore the device will not turn away from the predominant wave direction, and will also realign itself faster as when the wave direction changes.

The peak mooring force is decreased as there is an internalisation of the wave loading forces within the structure. As the length of the device is comparable to the length of the waves, at some instants the wave force will push the platform, while pulling the wings or vice versa. Therefore the net peak force on the mooring links will be lower. This does however demand careful consideration for the design of this joint to resist these forces. Initial work and prototype work has concentrated on strain gauges mounted in the shoulder. Corona and Kofoed (2006) were able to show this internalisation of forces in practice by analysing the frequency spectrum of the strains close to the joint. Two force peaks were evident, one corresponding to wave frequencies and a secondary lower frequency peak at the slow surge frequency of the device.

Lastly the reflectors wings act as stabilisers to the device. As they float under their own buoyancy they counteract any list of the platform. This is important as the more horizontal the platform is kept the less water is spilt and so the more efficient the device operation.

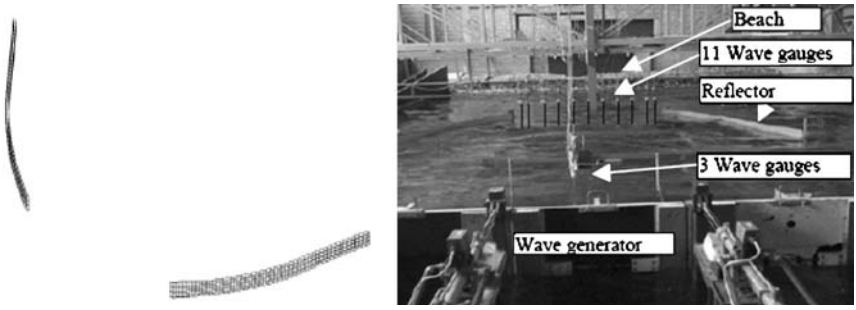

Fig. 7.32. Computer mesh of the reflector wings and laboratory set up

7.4.5 Low Head Turbines and Power Train

Water turbines which are suitable for this purpose have been used in low head river water power plants for many decades and have been developed to a high level of efficiency and reliability. In France the 240 MW La Rance tidal power station has used such turbines in a salt water environment since 1967. Thus, in contrast to most of the other WEC principles, a proven and mature technology can be used for the production of electrical energy.

Turbine operating conditions in a WEC are quite different from the ones in a normal hydro power plant. In the Wave Dragon, the turbine head range is typically between 1.0 and 4.0 m, which is on the lower bounds of existing water turbine experience. While there are only slow and relatively small variations of flow and head in a river hydro power plant, the strong stochastic variations of the wave overtopping call for a radically different mode of operation in the Wave Dragon. The head, being a function of the significant wave height, is varying in a range as large as 1 : 4, and it has been shown by Knapp (2005) that the discharge has to be regulated within time intervals as short as ten seconds in order to achieve a good efficiency of the energy exploitation.

From a river hydro power installation which is properly maintained, a service life of 40–80 years can be expected. On an unmanned offshore device, the environmental conditions are much rougher, and routine maintenance work is much more difficult to perform. Special criteria for the choice and construction of water turbines for the Wave Dragon have to be followed; it is advisable to aim for constructional simplicity rather than maximum peak efficiency.

Figure 7.33 shows the application ranges of the known turbine types in a graph of head H vs. rotational speed n_q. The specific speed n_q is a turbine parameter characterising the relative speed of a turbine, thus giving an indication of the turbines power density. Evidently, all turbine types except the Pelton and the cross flow type are to be found in a relatively narrow band running diagonally across the graph. Transgressing the left or lower border means that the turbine will run too slowly, thus being unnecessarily large and expensive. The right or upper border is defined by technological limits, namely material strength and the danger of cavitation erosion. The Pelton and the cross-flow turbine do not quite follow these rules, as they have a runner which is running in air and is only partially loaded with a free jet of water. Thus, they have a lower specific speed and lower power density. Despite its simplicity and robustness, the cross flow turbine is not very suitable for wave power applications:

- Its operating principle entails a ‘lost head’ in the order of one runner diameter. This leads to a very low efficiency at very low heads.
- Due to the typically very narrow blade passages this turbine cannot cope very well with debris like seaweed and fishing net parts.
- Due to its low specific speed, the turbine itself is rather bulky, and it needs a gearbox to drive the generator.

This type of turbine has thus not been further evaluated.

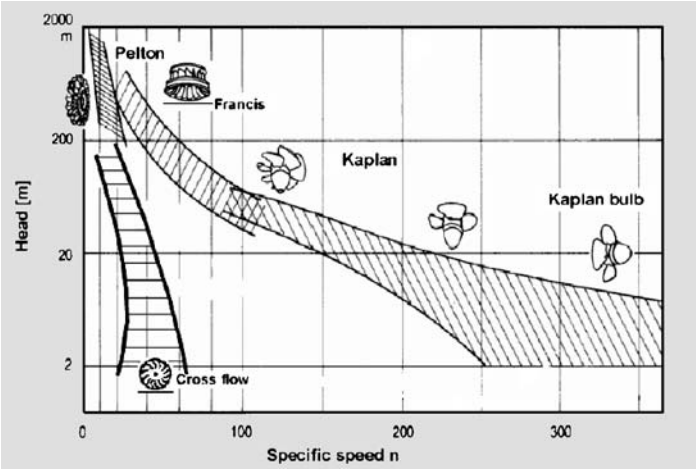

Fig. 7.33. Head range of the common turbine types (Voith and Ossberger characteristics; see Knapp et al., 2000)

The Kaplan type is the only turbine suitable for the head range in question. The shape of a turbine's guide vanes and runner blades is designed to give an optimal energy conversion in its design point, which is defined by optimum values of head and flow (H_{opt} and Q_{opt}) at a given speed. For every other operating point, there will be a discrepancy between the flow angles and the blade angles, decreasing the efficiency of the turbine. Whenever a turbine is required to operate in a relatively wide head and flow range it is important that the efficiency curve is flat and widely spread. This criterion is best fulfilled by the double regulated Kaplan type.

In this type of turbine, both the guide vanes and the runner blades are adjustable, thus making the turbine very adaptable to varying operating conditions. This is only achieved by a relatively complex construction which implies an oil-filled runner hub with a number of critical bearings and oil seals and a great number of joints and bearings in the guide vane operating mechanism. There is an immediate reflection in higher manufacturing costs, but also in a higher demand for maintenance, especially when the turbine is operated in an aggressive environment i.e. saltwater with possible silt contents. For these reasons single regulated variants of the Kaplan turbine have been conceived, namely the Propeller type with fixed runner blades, the Semi-Kaplan type with fixed guide vanes and the unregulated on/off turbine with fixed runner blades and fixed guide vanes. These turbines are simpler in construction, but they have a narrower efficiency curve, see Fig. 7.34.

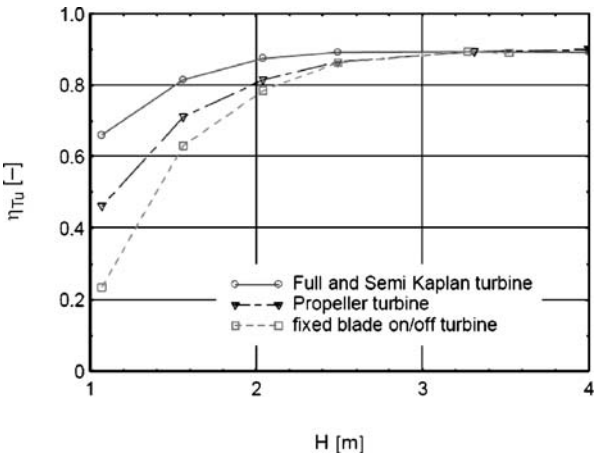

Fig. 7.34. Efficiency vs. Head for variants of the Kaplan turbine

With a projected plant of a larger size, it should be considered to use a number of smaller turbines instead of a single larger turbine. This has the following advantages:

- By stopping a number of turbines at lower flow rates, the flow rate can be regulated over a wider range without sacrificing efficiency, see Fig. 7.35.
- Single units can be taken out of service for maintenance without stopping production.
- Capacity demanded for hoisting and transport equipment to perform repair and maintenance work is greatly reduced.
- The smaller turbines have shorter draft tubes, and are thus easier to accommodate in the whole device.
- The smaller turbines have a higher speed, which reduces the cost of the generator.

Depending on the location of a production Wave Dragon it is envisaged that there will be between 16 and 24 turbines mounted.

In normal hydro power stations, the turbines are operated at constant speed, as they are coupled directly to generators feeding into a fixed frequency grid. However, if the generator is connected to a frequency converter, the turbine can be operated in a relatively wide speed range. This is very advantageous in situations where a large variation in turbine head occurs. By adapting the speed to the actual turbine head, the efficiency of the turbine can be kept almost constant, see Fig. 7.36.

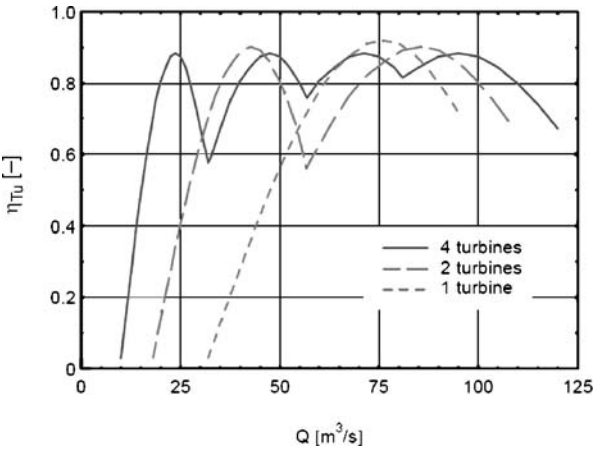

Fig. 7.35. Turbine efficiency vs. flow rate for a single and a multiple turbine configuration

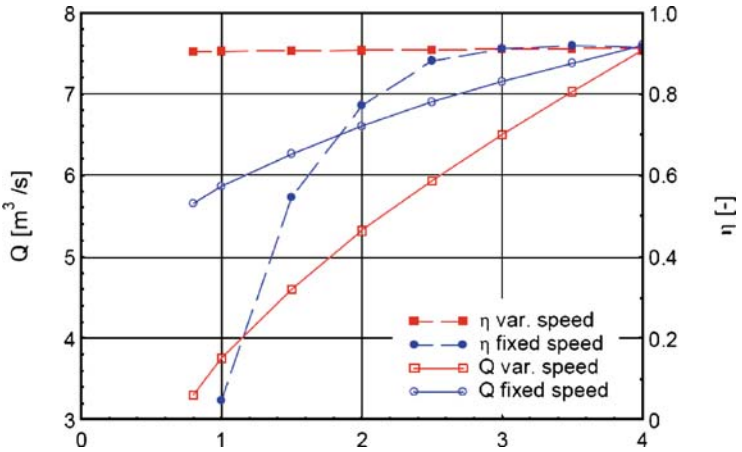

Fig. 7.36. Turbine efficiency and flow rate vs. head for fixed and variable speed drive

In the development of the Wave Dragon, different turbine regulation strategies have been evaluated by means of simulation software. Maximum overall plant efficiency was obtained when the turbine flow was reduced along with the emptying of the reservoir. The variable speed turbines adapt well to this, naturally reducing flow at the lower head. Therefore by using enough variable speed on/off turbines a good efficiency can be delivered, with smooth power delivery and a high load factor.

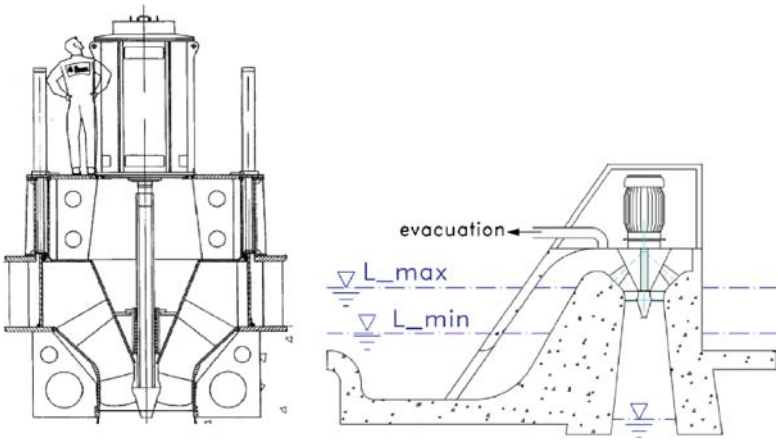

Fig. 7.37. A full scale Wave Dragon cylinder gate turbine and a Siphon on/off turbine

Two alternative methods for interrupting the flow have been analysed, the first one using a large mechanically operated cylinder gate, the second one using a siphon principle, see Fig. 7.37. The siphon type has no gate, it is stopped by simply admitting air into the top of the inlet duct; the turbine is started again by partly evacuating the air until the flow starts again and takes the rest of the air along with it. The cylinder gate type has the advantage of shorter start-up time and slightly better efficiency. If suitably designed it has been found that it has low maintenance requirements.

7.4.6 Control

Improved control algorithms are very valuable, as for no extra capital cost or maintenance cost they can improve the performance of a device, effectively free extra energy capture. Therefore this is an area which currently is a major focus of research work. On the basic level, as with several other WECs, Wave Dragon has two control loops. A slow acting control loop is used to tune the device to the current sea state. A much faster acting control strategy is used to extract the maximum energy from wave to wave.

The long period control's main aim is to regulate the floating height of the Wave Dragon to the optimal level for the sea state. This aims to maximise the power flowing over the ramp. A lower floating level will have more flow but at a lower head, and a higher floating level will have lower flow but a higher head – the optimum must be found. The time scale of the seas state's increase is of the order of a few hours, therefore the platform can also change its buoyancy at a similar rate. The input to this control strategy is the current, or future sea state which can be measured directly in the region of the Wave Dragon, or predicted based on weather forecasts.

The method for controlling the floating level of the platform is by blowing air into, or venting air from, open compartments beneath the reservoir. Due to the free surface of the reservoir this can be compared to balancing a tray full of water. The layout of these compartments and the detailed strategy for filling them is crucial to maintain stability. For example if there is a large central compartment filled with air, and low buoyancy at the edges the device will be quite unstable. In general the more stable the platform is, the closer to full the reservoir can be, and so the more power will be generated.

The fast acting control is to maintain a suitable water level within the reservoir. If the water level is too high, then large waves will not be able to be accommodated in the reservoir so there will be considerable spill from it. However if the water level is lower the head across the turbines is also low so less power can be produced from the same water overtopping the ramp. Again an optimal level must be found.

The reservoir level is controlled by the turbines. They are controlled on and off in a cascade fashion using the cylinder gates as explained earlier. At a minimum reservoir set point, the first turbines cut-in. As waves fill the reservoir, the remaining turbines progressively start. At a maximum level all turbines are operational. The input for this can either come from pressure transducers within the reservoir itself giving the level, or from direct measurements of the power generated by the generators, from which the head can be inferred. An area of development here is in the use of predictive algorithms, to control the turbines dependant on the expected overtopping in the next few waves. By lowering the reservoir level when some large waves are expected, spill would be minimised. Also by maintaining a higher reservoir level when smaller waves are expected, less water would be discharged at a lower head. Initial studies have shown that this small work alone could increase performance by 5 to 10 % (see Tedd et al, 2005).

7.4.7 Summary

Wave Dragon is a large floating overtopping type WEC. Its natural broad-banded behaviour and the use of established components make it one of the leaders in the wave energy field. It is a challenge to operate in the uncompromising environment where wave energy is greatest. Progress has been made in implementing existing technologies in this new manner. More development continues to improve the Wave Dragon device.

7.5 Operational Experience

Section 7.5 is effectively a compilation of contributions from technology developers (the same that were responsible for sections 7.1 to 7.4) which aim to gather the operational experience that has been acquired so far. The lessons that are presented are extremely relevant for the wave energy industry, and also interesting to

a wider engineering community, particularly at a time when the deployment of the first large scale wave energy farms is being envisaged. For the first time the experiences from several of the key technology developers are presented in the same publication, a fact that greatly enhances the appeal of this section.

7.5.1 Oscillating Water Column - LIMPET

Tom Heath

Wavegen
Inverness
Scotland, UK

The most extensively studied and reported OWC plant in operation is Wavegen's LIMPET plant on the Scottish island of Islay. The grid connected plant has been in operation since November 2000 and serves both as a generator and research unit. The original configuration of the turbo-generation equipment gave an installed capacity of $500\,kW$ but this was reduced to $250\,kW$ after it became clear that the pneumatic power capture of the plant had been overestimated at the design stage. The LIMPET project was coordinated by the Queens University of Belfast supported by the EU under the JOULE III programme. Wavegen are now owners and operators of the plant.

Fig. 7.38. LIMPET OWC operating on Islay since 2000

Collector Form and Construction

The LIMPET OWC is inclined at an angle of 40° to the horizontal (Fig. 7.39). The column inclination affords and easy entry for water in surge and also facilitates tuning to longer periods.

The structure was designed to withstand either a frontal wave pressure of 6 *bar* across the full 21 *m* width of the device or a peak internal pressure of 1 *bar*. This necessitated internal supports for the roof dividing the water column into three equal chambers each 6 *m* wide.

To avoid the uncertainties associated with rock quality at the site a rear wall was added to the structure so that the internal pressure forces were totally contained within the collector structure. In this way the requirement for anchoring the structure to the site rock was minimised. With the exception of the lower section of the roof structure the collector was built primarily entirely of in-situ cast reinforced concrete. The lower section of the roof was formed from beams pre-cast at site which provided a firm foundation for an in-situ capping without the need for complex scaffolding. The major problem faced when building the collector was the need to protect the construction site from wave activity during the construction phase. This was achieved by excavation a hole behind the cliff edge and building in the lee of the protective bund (Fig. 7.40).

In times of storm waves overtopped the bund and in bad weather conditions it was necessary to cease working at the base of the structure. The degree of protection was however sufficient to limit lost time to 25 % during the summer months when construction activity had been planned. In general terms the construction team was able to use 10 day weather forecasts to predict weather down time and could plan accordingly.

On completion of the excavation the construction commenced with the casting of the rear wall. This was followed by the erection of the side walls and finally the roof of structure to leave the structure complete but isolated from the sea by the wave wall (Fig. 7.41). The final stage of the construction was then to remove the

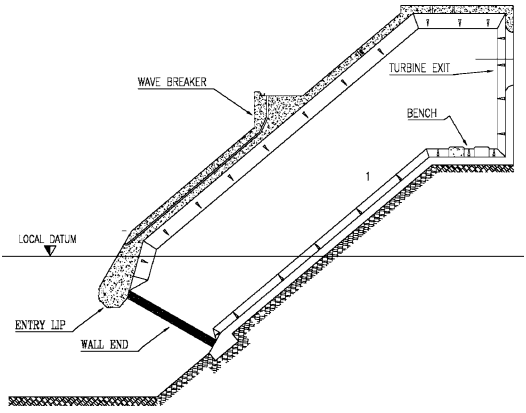

Fig. 7.39. Schematic of the LIMPET plant (side view)

Fig. 7.40. Details of the construction of the LIMPET plant

wave wall. This was achieved by using explosives. A series of four rows of holes were drilled along the length of the wall and the rows blasted sequentially, with millisecond separation, with the row to seaward being the first to be fired. The result of the sequential firing was to throw the blasted rock towards the sea and away from the structure.

Prior to the blast the excavation had been pumped full of water with the objective of creating a differential head to apply an outward force to the final pillar of rock to be fired. The rock was overcharged in relation to a normal quarrying operation in order to ensure that the shattered rock was in small enough pieces to be

Fig. 7.41. Completion of the structural work

Fig. 7.42. Rock removal operations

removed by a long reach excavator (Fig. 7.42). Prior to blasting the wave wall valves had been fitted to the two outlets on the landward side of the collector to facilitate the fitment of power take-off systems. The turbo-generation equipment, which had previously been assembled and tested by Wavegen was transferred to the LIMPET site and connected to the collector. Figure 7.43 shows the turbo generation system connected to the outlet at the centre of the collector back wall. A second outlet, which is available for testing alternative power take-off systems, is also visible. After installation the turbo generation equipment was enclosed in a simple building to give protection against the worst vestiges of the weather.

As well as generating to the grid via the main plant a second outlet is available on the collector chamber which facilitates the continuing development of

Fig. 7.43. Turbo-generation system

the turbine-generator system. These developments have centred on a 750 *mm* diameter unit rated at 18.5 *kW* (Fig. 7.44). The focus of the development is on ensuring the long term reliability of the system whilst maintaining or improving performance. It is only when the high availability of the generation system necessary to justify economic power production have been demonstrated that, other than for research purposes, turbines will be installed on the floating systems now under consideration.

Figures 7.45 and 7.46 show typical site measured curves for non dimensional turbine torque and non-dimensional pressure drop measured on the LIMPET plant. These curves combine to give an overall conversion efficiency from pneumatic to electrical power of approximately 50 %.

The non-dimensional parameters are defined as follows:

- Non-dimensional Torque $T^* = \dfrac{T}{\rho\omega^2 r^5}$ where T is torque, ρ air density, ω angular speed and r turbine radius.
- Non-dimensional pressure $P^* = \dfrac{P}{\rho\omega^2 r^2}$ where P is the pressure drop across the turbine.

The immediate prospects for OWC technology appear excellent with OWC breakwaters under construction in Portugal and Spain for commissioning in 2008 and a number of other schemes worldwide in the pipeline. Once the baseline technology has been firmly established there will be opportunities for significant step increases in performance by, for example, introducing advanced turbine technologies such as the variable pitch Wells units under development at Wavegen. There is every indication therefore that OWC technology, which is perhaps the longest established concept for extracting power from the waves, will continue at the forefront of wave energy development and make a major contribution to the harnessing of ocean energies.

Fig. 7.44. 18.5 *kW* turbine-generator system

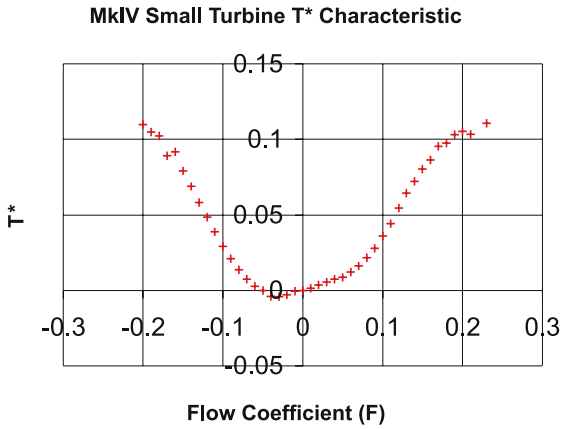

Fig. 7.45. Non-dimensional torque vs. flow coefficient

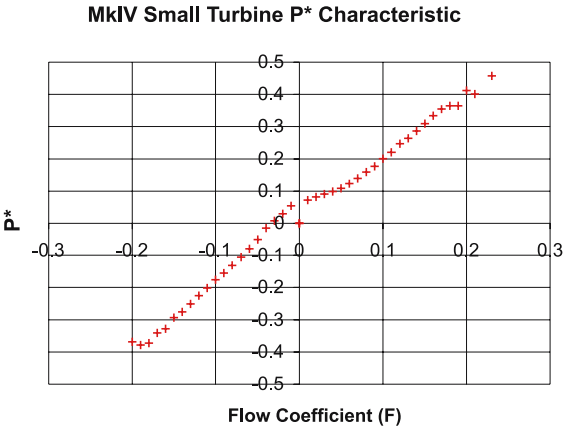

Fig. 7.46. Non-dimensional pressure drop vs. flow coefficient

7.5.2 Oscillating Water Column – Pico Plant

António Sarmento, Frank Neumann, Ana Brito e Melo

Wave Energy Centre
Lisbon
Portugal

The Pico plant was built from 1995 to 1999 under sometimes difficult conditions. These resulted from a number of reasons: Pico is a small island (15000 inhabitants) with limited infra-structures and qualified man-power about two thousands kilometres away from Lisbon; no direct flights were available at the time and the access to the island could be difficult in the winter due to rough weather and in the summer because of shortage of available seats in the flights due to tourism; a storm destroyed the breakwater protecting the in situ construction of the plant in the early phase of the plant erection and a second storm destroyed a small part of the machine room and was responsible for flooding the room with the electrical equipment a few weeks before the completion of the plant. The main lesson learned with the erection of Pico plant is that in situ construction must be avoided whenever possible and that the plant should be as much accessible as possible.

The initial tests in the Pico plant started in 1999. Since the beginning a number of problems with the mechanical equipment were found: vibrations in the guide-vanes of the stator due to very fragile guide-vanes; vibrations on the turbo-generator support structure (due to a resonance frequency excited by the turbine rotation); fatigue in the housing of the sluice-gate isolation valve produced by pressure fluctuations propagated from the air chamber (about 3.000.000 cycles per year); significant loss of oil in the turbine lubricating circuit. Due to the limited technical support available at Pico and the difficulty in accessing the plant in waves higher than $3\,m$, the planning of the actions to repair these faults and problems was difficult. On top of these the cost of all the repairs/actions also created problems. These problems affected and delayed the testing programme of the plant, which in reality had a negligible amount of operational hours in these early days. Problems of different nature also occurred related to leakage of rain water and sea water under big waves to the machine room through the cover of the opening at the machine room ceiling used to install or remove the turbo-generator unit. Along the years this was responsible for the damage of some of the auxiliary electrical, electronics and monitoring equipment and for the need of significant repairs of some auxiliary mechanical components, namely the pneumatic actuators of the sluice-gate and blade valves.

As a result of the described conditions at the plant, the Wave Energy Centre submitted and coordinated a project financed by the Portuguese DEMTEC/PRIME program to refurbish the plant and proceed with the plant testing (Neumann et al., 2006). The co-funding of the project was provided by EDP, EDA, EFACEC, IST, Irmãos Cavaco and INETI. This project is now briefly described and the main results from several months of plant testing are described.

The first phase of the project consisted in the refurbishment of the plant: this included the removal and renovation of the auxiliary electrical, power electronics and control equipment by EFACEC and its installation in two containers outside the plant, about 100 *m* away. The electrical transformers were also placed in one of these containers, and so new electrical connections were established between the plant and the containers and between these and the electrical grid. This phase also included the cleaning and repair of the pneumatic actuators of the two valves mentioned earlier, the repair of the turbine lubrication system, the reinforcement of the turbo-generator support structure, the connection between the housing of the sluice-gate valve and the outside atmosphere by an air duct in order to maintain approximately atmospheric pressure in the housing and thus reduce the fatigue problems, the proper isolation of the machine room opening at the ceiling and the installation of a slow relief-valve (supplied by Kymaner, Portugal) to allow the air chamber to escape directly to the atmosphere in very rough seas.

The second phase of the project consisted in the testing of the plant with the equipment as indicated above. The third phase of the project was intended to allow the testing of new blades with optimised profiles for this application and a fast-reacting relief-valve to be operated in a wave-to-wave basis. However due to problems encountered during phase two, and the additional costs involved, phase three shifted from the original program to the testing of the plant with the original turbine blades and no fast-reacting relief valve, but now without the guide vanes stator on the atmospheric side as will be explained later. The problems mentioned above were basically two: i) one of the blades of the stator on the atmospheric side of the turbo-generator broke due to fatigue and destroyed this stator, affecting the turbine ring and the other stator – these components were repaired and new and stronger stators (with blades), supplied by Kymaner, were built and installed in October 2006; ii) one of the ball-bearings of the turbine broke due to deficient assembly after inspection (new bearings were installed after this occurrence).

The experience gained with roughly 56 tests of 20 minutes duration along five months in two years can be summarised as follows (see also Figures 7.47 to 7.49):

- Fatigue on the mechanical components is a critical issue that needs to be properly addressed at the design stage.
- The vibrations on the support structure could not be completely removed and so the turbine could not operate above 1100 *rpm* – note that maximum turbine rotational speed is 1500 *rpm* and that the power increases with the cube of the rotational speed.
- As a result of the previous limitation the power levels at the turbine shaft are significantly less than what could be attained: 1,172 *kWh* of pneumatic energy (average power of 62.8 *kW*) were available to the turbine, of which 617 *kWh* were delivered to the grid (average of 33.1 *kW*), this representing an average efficiency from pneumatic to electric energy delivered to the grid of 52.6%.

- The analysis of the three test periods (October-November 2005; October 2006 without guide vane in the atmospheric side of the turbine; November 2006 with the new set of guide vanes) shows that:

1. The wave conditions were less energetic in 2006, leading to significantly smaller pneumatic energy available to the turbine;
2. The turbine average efficiency is about the same in the two first sets of tests, respectively 58.6 % and 57.5 % and a bit lower in the third set (49 %) – these values are computed from the data in Figures 7.47 to 7.49.

- The inertia of the turbine allows smoothing the electrical power output as can be seen in Fig. 7.50 for a particular test. Other tests show similar results.
- Due to the limited water depth in front of the plant (about 8 m) in many cases the wave propagates in very shallow waters as a second order wave: shorter and more intense crests than troughs. This originates much higher upward velocities (and outward flows) than downwards velocities (and inwards flows) as seen in Fig. 7.51.
- Large outward flows mentioned in the previous point produces turbine blade stall with decrease of energy production and an increase of fatigue (typically in the stator on the atmospheric side) and noise generation.
- The very careful design of the air ducts originated very uniform flow velocities in the turbine entrance, in particular for outward flows (see Fig. 7.52). They are also responsible for the very good turbine average efficiency mentioned above and for the excellent agreement with the numerical estimations (see Figures 7.53 and 7.54).
- In energetic seas, when the relief-valve in the top of the air chamber (see Fig. 7.7) is open, an air jet is produced from the atmosphere into the chamber during the downward motion of the internal water free-surface. The air jet impinges directly in the free-surface pulverising the water. The resulting water droplets are subsequently transported through the turbine by the outward air flow thus reducing the turbine rotational speed and shaft power and eroding the turbine blades.
- The tested control laws produce a very stable and efficient operation of the power take-off equipment.

The efficiency of the first two sets of data (Figures 7.47 and 7.48) is very close, which is surprising as we would expect to have much higher efficiencies when the plant operates with the stator on the atmospheric side (Fig. 7.47). The efficiency of the third set of data (Fig. 7.49) is unexpectedly smaller than the ones for the two previous sets of data and seems to indicate that the new stator is less efficient than the original one. This is very surprising since they were built with the same aerodynamic design. Also surprisingly is to notice that the efficiency is smaller than the one measured without stator (data of October 2006). Research is ongoing to provide further clarification.

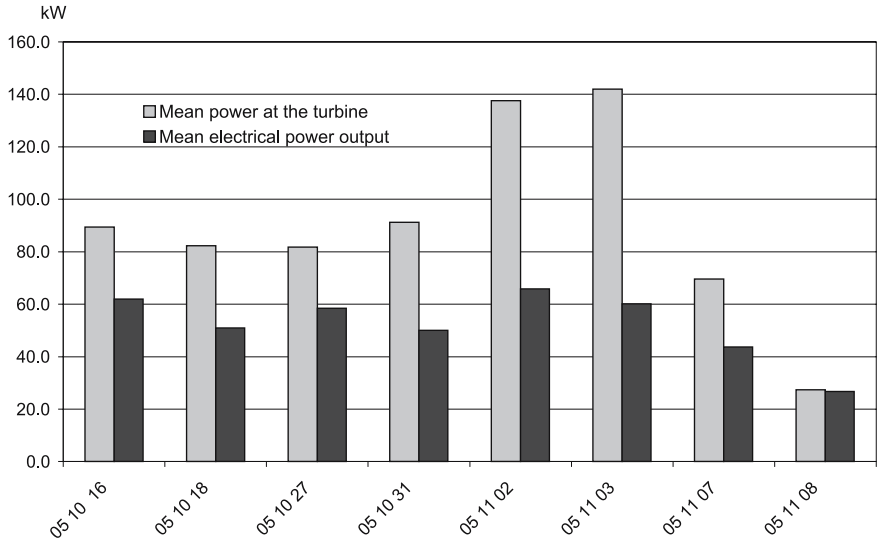

Fig. 7.47. Mean pneumatic and electrical power delivered to the grid in sea tests conducted in October and November 2005 (original stators)

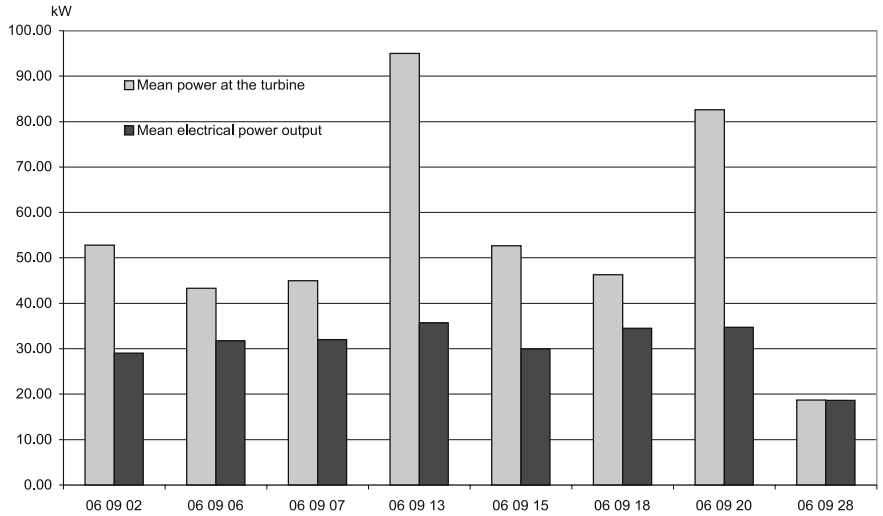

Fig. 7.48. Mean pneumatic and electrical power delivered to the grid in sea tests conducted in September 2006 (with no guide vane in the atmospheric side)

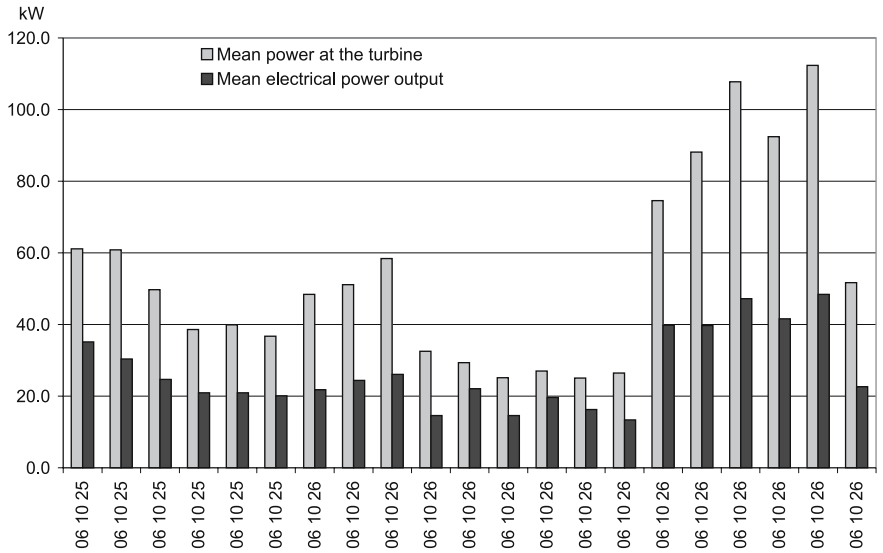

Fig. 7.49. Mean pneumatic and electrical power delivered to the grid in sea tests conducted in November 2006 (new set of guide vanes)

It is also strange that in two of the tests (051108 and 060928) the electrical and pneumatic energy are almost the same, resulting in turbine and generator efficiencies close to 100 %. This results from having the Pitot tubes that measure the dynamic pressure upstream the turbine blocked with dust, thus measuring dynamic pressures (and air flows) smaller than the real ones. As the pneumatic power is the product of the air flow and the static pressure drop in the turbine, smaller estimates of the real pneumatic power result in higher turbo-generator efficiencies.

Figure 7.50 shows that with the relief-valve closed the pneumatic power available at the air chamber is almost equal to the one available to the turbine, meaning that aerodynamic losses are very small. It is also seen that the electrical power delivered to the grid is much more stable as a result of the control strategy and the turbine inertia.

Figure 7.51 shows for a particular, but representative test, that positive (outwards) flows are significantly larger than negative flows due to wave shoaling produced by the reduced water depth close to the plant site (about $8\,m$). It also shows that, as expected, the pressure drop and flow rate are in phase.

Figure 7.52 shows the dynamic pressure measured at both sides of the turbine for three radii: inner, mean and outer radius. The uniformity of the measurements is outstanding and shows a very uniform velocity profile, in particular if it is noted that the differences in the dynamic pressure are the double of those in the velocity. Uniform velocity profiles are critical for good turbine efficiency as otherwise stall can be anticipated.

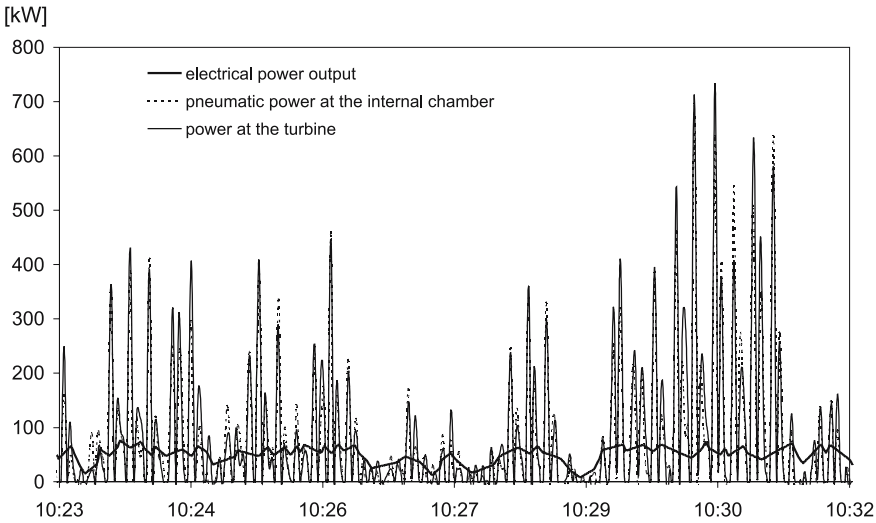

Fig. 7.50. Sample of time-series of pneumatic power in the air chamber, pneumatic power available to the turbine and electrical power delivered to the grid

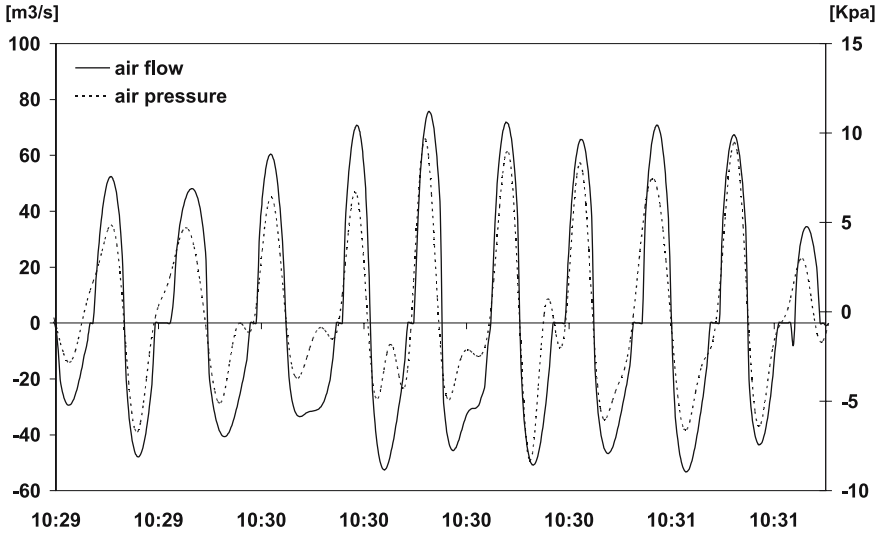

Fig. 7.51. Sample of time-series of flow and pressure drop trough the turbine

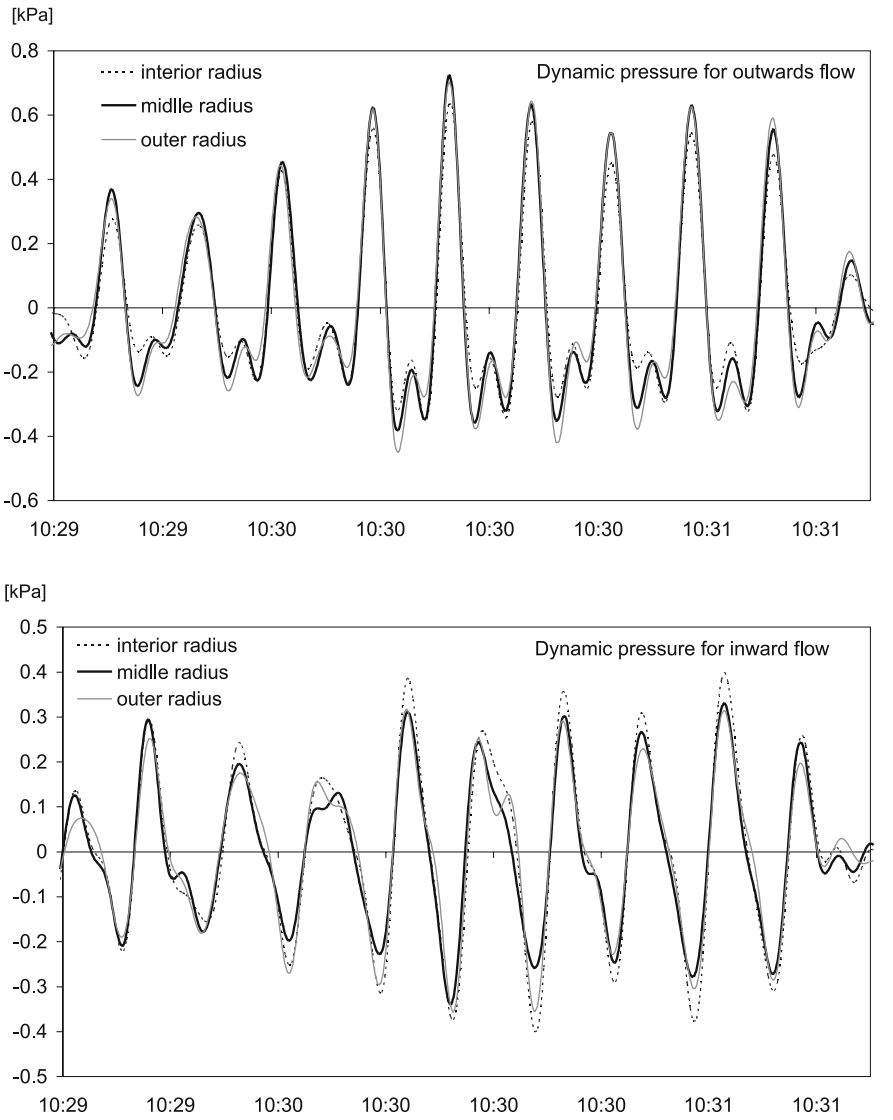

Fig. 7.52. Sample of time-series of dynamic pressure measured upstream (top) and downstream (bottom) the turbine. Only positive dynamic pressures are relevant

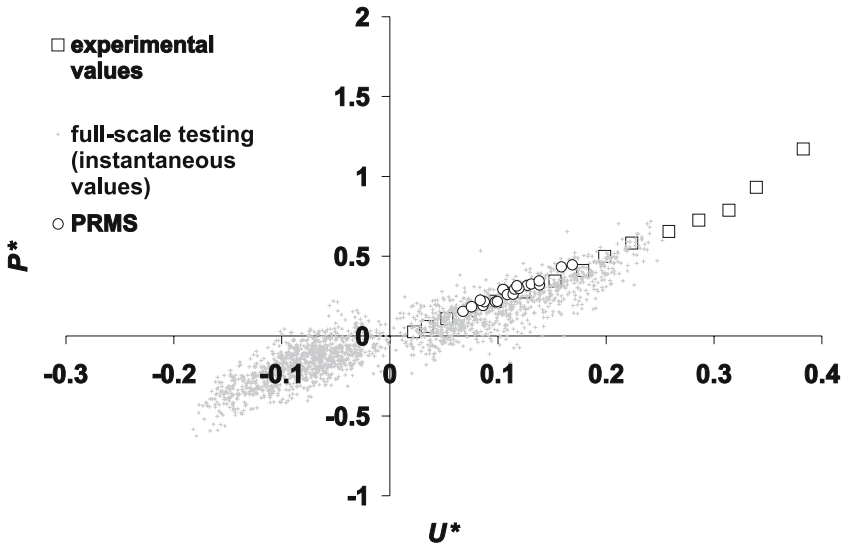

Fig. 7.53. Comparison of dimensionless flow rate versus pressure drop on the turbine

Figure 7.53 shows the comparison between the experimental curve measured in a steady flow wind tunnel (Gato and Falcão, 1990), the instantaneous and the *rms* values measured at the full-scale plant. The spread of the instantaneous values is expected due to measurement uncertainties. The root mean square values coincide extremely well with the experimental ones, showing that, as expected, the turbine flow is quasi-steady.

Finally Fig. 7.54 shows comparisons between numerical results and measured data relating the average power delivered to the electrical grid and root mean square values of the air pressure in the pneumatic chamber. A very good agreement is seen to occur indicating the good quality of the numerical model used to design the aerodynamics of the turbine. Again it is noted that the agreement is only possible because of the very uniform flow velocity approaching the turbine.

The results and conclusions presented here could only be possible with the contribution from a very large number of people and institutions, both in relation to the construction of the plant and its reimbursement and test. Prof. António Falcão was already mentioned as the scientific responsible for the two European JOULE projects that allowed the construction of Pico plant. Prof. Luís Gato, also from IST, was the responsible for the aerodynamic design of the turbine, guide vanes and air ducts. The technical contributions from Consulmar, Kymaner, EFACEC, Irmãos Cavaco, INETI, IST and EDA were also fundamental and must be acknowledged.

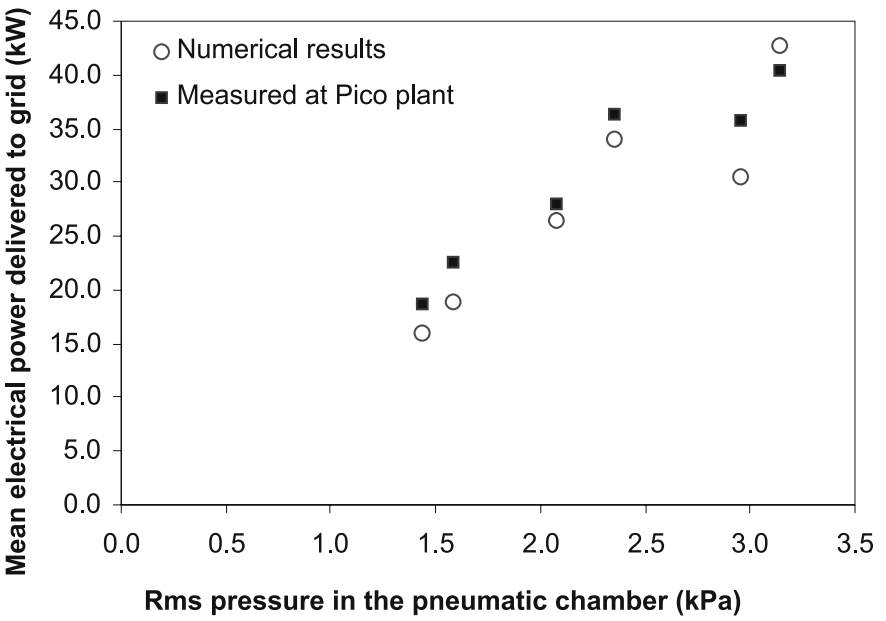

Fig. 7.54. Comparison of numerical estimations of turbine power delivery and measured values at Pico plant

7.5.3 Archimedes Wave Swing (AWS)

Miguel Prado

Teamwork Technology BV
Zijdewind
The Netherlands

The 2 *MW* pilot plant of the Dutch Archimedes Wave Swing (AWS I) was successfully submerged 5 *km* offshore Póvoa de Varzim (Northern Portugal) in May 2004, and decommissioned after testing approximately six months later. Despite resulting in a short operational phase, the AWS is thus among the first devices with operational record in significant dimensions, having tested components and proven the technology at full-scale.

Results of the AWS dynamic analysis process were presented and correlated with the theoretically expected results in Prado et al. (2005a). A short summary of the main milestones that were reached is presented in this section, but firstly some considerations regarding the submergence operation are given.

Submerging the AWS pilot plant

The controlled submergence of an offshore device requires a detailed stability study in order to predict and avoid problems that may occur during operation (like general instability, resonance effects, etc).

To guarantee a robust design of the submergence operation of AWS, a theoretical analysis of AWS dynamics was developed for all the steps of the operation. A quasi-linear model in the frequency domain was developed for the six degrees of freedom of the device (surge, sway, heave, roll, pitch and yaw) based on linear wave theory. Non-linearties due to drag damping forces were included in the model by equivalent linearisation. Critical aspects like natural periods and dynamic response to wave excitation can be evaluated for each degree of freedom.

One of the main problems of submerging a device in a controlled way is related to the fact that the dynamic behaviour of the device is not constant during all the operation and changes with the submergence depth. This results mainly from changes in the inertia and buoyancy of the device, inflicted by the ballasting procedure and the changing underwater geometry. Critical points of the operation could be identified with the described calculation methodology, which were confirmed later during operation.

The theoretical analysis used for evaluate AWS dynamics proved to be a vital tool in the design process of the submergence operation, leading to its success after two previous failed attempts. As described in 7.2, the first AWS full-scale prototype was composed by a generator (central cylinder) installed on top of a pontoon (see Fig. 7.55). The pontoon itself is not necessary for wave energy

Fig. 7.55. View of AWS at the harbour of Viana do Castelo, Portugal

conversion and it was only built with the purpose of facilitating the submergence operation during the test phase. In future versions the pontoon will be suppressed.

The pontoon is composed by several tanks that are ballasted during the submergence operation (Fig. 7.56):

- Four ballast tanks (BT), with a total capacity of 2200 m^3.
- Four Air & Water tanks (AW), with a total capacity of 1000 m^3.
- Four towers (T), with a total capacity of 150 m^3.

The total mass of the device at an unballasted state is 7200 *ton*, from which 5500 *ton* are due to the sand tanks (SD). The purpose of the sand tanks is to decrease the gravity centre of the device in order to increase its stability.

Taking into account that the total ballast capacity of the pontoon is 4700 m^3, at 100% ballasted state the device mass will be 11900 *ton*.

The submergence operation can be described in the following eight steps:

1. Starting point, no ballast, depth 5.25 *m*;
2. Deck underwater, ballast 340 m^3, depth 5.5 *m*, fill AW tanks;
3. AW tanks full, ballast 750 m^3, depth 7.5 *m*, fill BT tanks;
4. Towers underwater, ballast 1870 m^3, depth 17.5 *m*, fill BT tanks;
5. Ballast tanks full, ballast 2980 m^3, depth 21 *m*, fill towers;
6. Lift floater by pumping air inside, ballast 3260 m^3, depth 25 *m*, fill towers;
7. Floater underwater, install buoys, ballast 4070 m^3, depth 31.5 *m*, fill towers;
8. Device at seabed, ballast 4150 m^3, depth 43 *m*.

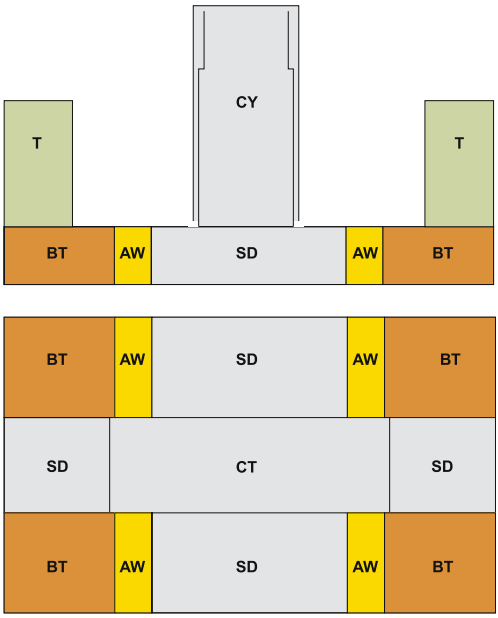

Fig. 7.56. Sketch of the inner arrangement of AWS's tanks

During the submergence operation, the device dynamics changed with submergence depth. It is therefore very important to analyse for each step the dynamic behaviour of the device.

The submergence operation took place between the 16th and the 18th of May 2004, 6 *km* offshore Póvoa de Varzim in Northern Portugal. The maximum recorded sea state during that period of time was $H_s = 1.6\,m$ with T_z between 7 and 9 *s*. Figure 7.57 shows the different steps of the operation. More details can be found in Prado et al. (2005b).

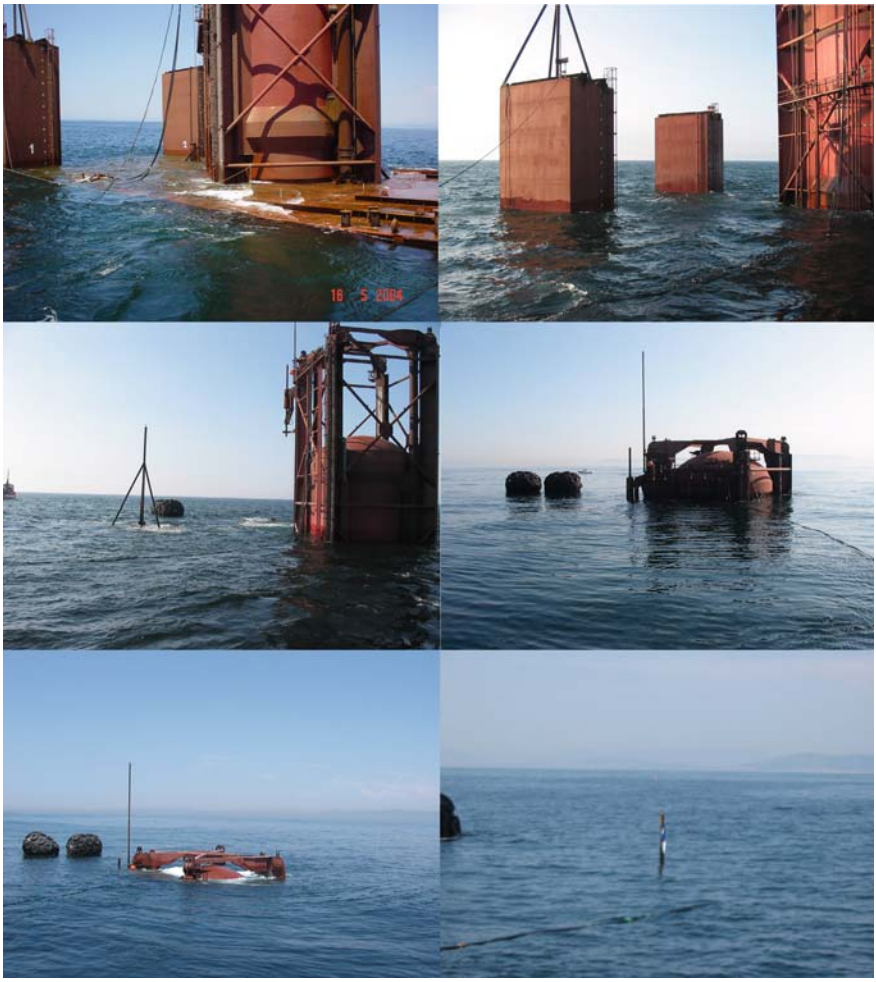

Fig. 7.57. Several stages of the submergence operation: deck submersion (top left), towers half submerged (top right), towers submerged (mid left), floater lifted to upper position (mid right), floater submersion (bottom left), pilot plant installed (bottom right)

Testing of the AWS pilot plant: results

Results from the testing round are valuable in order to validate the numerical simulation and to gather experience in a true operational environment. A $15\,min$ set of data is particularly interesting for detailed analysis. The measurements presented were performed on the 3rd of October of 2004, around $14:30$. At that time, the following conditions were observed:

1. Sea

- Significant wave height: $H_s \approx 2.3m$;
- Wave periods: $T_P \approx 11.7s$, $T_e \approx 10.5s$;
- Tide level: $\eta_T \approx 1.43m$.

2. AWS

- Water volume inside AWS: $V_W \approx 1180m^3$;
- Average air pressure inside AWS: $\overline{p}_a \approx 32.3mwc$;
- Water brakes closed (hence additional damping affecting the motion).

3. Landstation

- Converter input resistance: $R_{AC} = 2.75\Omega$.

The following signals were measured (see Fig. 7.58):

- Water pressure on top of the AWS, to identify the waves;
- Air pressure inside AWS, to identify the air spring and the motion of the device;
- Electrical power at the converter, to quantify the energy output.

By visual inspection of the peak values in Fig. 7.58 it is possible to see that a correlation between the three signals exists. However it is necessary to quantify this correlation in order to use the numerical models which describe the dynamics of the machine (more details in Prado et al., 2005a).

One way of evaluating the consistency and correlation of the measured signals is by calculating a common signal. The electrical power produced by the generator P_{GEN} was calculated from the measured signals. The generated power can be related to the converter power P_{CONV} by

$$P_{GEN} = \frac{R_{AC} + R_{GC}}{R_{AC}} P_{CONV}\,, \tag{7.9}$$

where $R_{GC} \approx 1\Omega$ is the resistance of the generator plus the power cable and $R_{AC} = 2.75\Omega$ is the input resistance of the converter.

The velocity of the device for small displacement is related to time derivative of the air pressure

$$\dot{x} = -\frac{S_f}{k_a}\dot{p}_a\,, \tag{7.10}$$

with S_f being the surface area of the floater and k_a the air spring coefficient.

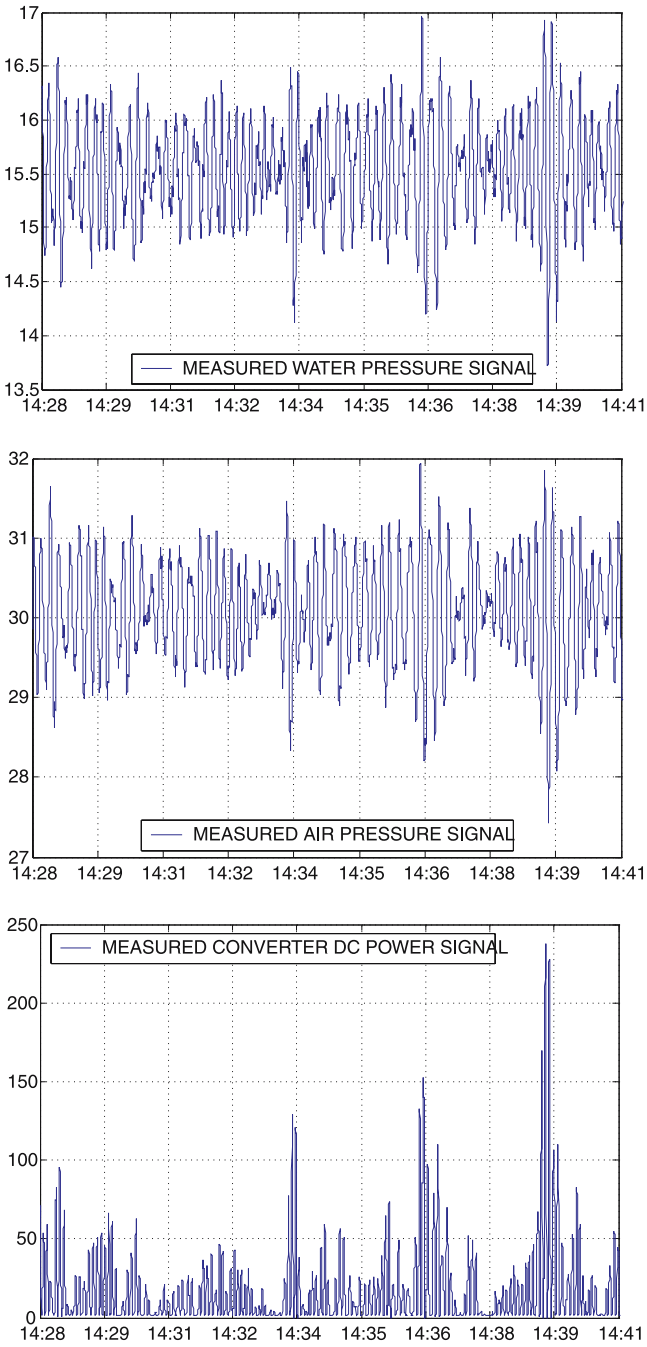

Fig. 7.58. Measured signals (3rd of October 2004)

The velocity is also related to the water pressure through the time domain model:

$$(m_f + m_{add\infty})\ddot{x} + \beta_L \dot{x} + \beta_{NL}\dot{x}|\dot{x}| + kx = F_{WAVE}\,, \tag{7.11}$$

where m_f is the mass of the floater (including all moving parts of the device), $m_{add\infty}$ is the added mass at infinite frequency, β_L is a linear damping coefficient due to the generator and the radiation force, β_{NL} is a nonlinear damping coefficient due to the drag forces and the water brakes, k is the total spring coefficient (air + nitrogen + hydrostatic) and F_{WAVE} is the wave exciting force.

The generator power may be computed using either air or water pressure velocity estimate by

$$P_{GEN} = \beta_{GEN}\dot{x}^2\,, \tag{7.12}$$

where β_{GEN} is the mechanical damping due to the generator:

$$\beta_{GEN}(R_{AC}) = \left.\frac{\partial F_{GEN}(\dot{x}, x, R_{AC})}{\partial \dot{x}}\right|_{\dot{x}=x=0} \approx \frac{1.83\times10^6 (N.s.m^{-1}.\Omega)}{R_{GC} + R_{AC}}\,. \tag{7.13}$$

The estimated generator powers from the measured signals are shown in Fig. 7.59. The signals are quite similar, especially the generator powers estimated from the converter and the air pressure. The generator power estimated from the water pressure signal differs considerably with regard to the peak values. It is however interesting to see that the average powers derived from all three signals are very similar. To better evaluate the correlation between the estimated signals, a *XY* plot of the different estimates can be made (Fig. 7.60).

From Fig. 7.60 it can be seen that the estimated generator power from the converter and air pressure correlate quite well. However the estimated generator power from the water pressure deviates on average from the estimated generator power from the converter for higher values. For lower values the fit on average is reasonably good, although the dispersion is considerably higher than in the case of the estimated power from the air pressure. This difference in the correlation was expected since the relation between water pressure and electrical power is more complex the one between the air pressure and the electrical power.

To better evaluate the effect that the water brakes and the settings of the device have on its performance, the motion and the generator power were computed from the model for different scenarios. Figure 7.61 illustrates the scenario observed during the testing day and Fig. 7.62 shows what would happen for the same day if the water brakes were open and the device was optimally tuned. A very significant difference in performance by releasing the brakes and tuning the device with the optimal settings can be observed. The motion and the average generator power both increase by approximately a factor of eight.

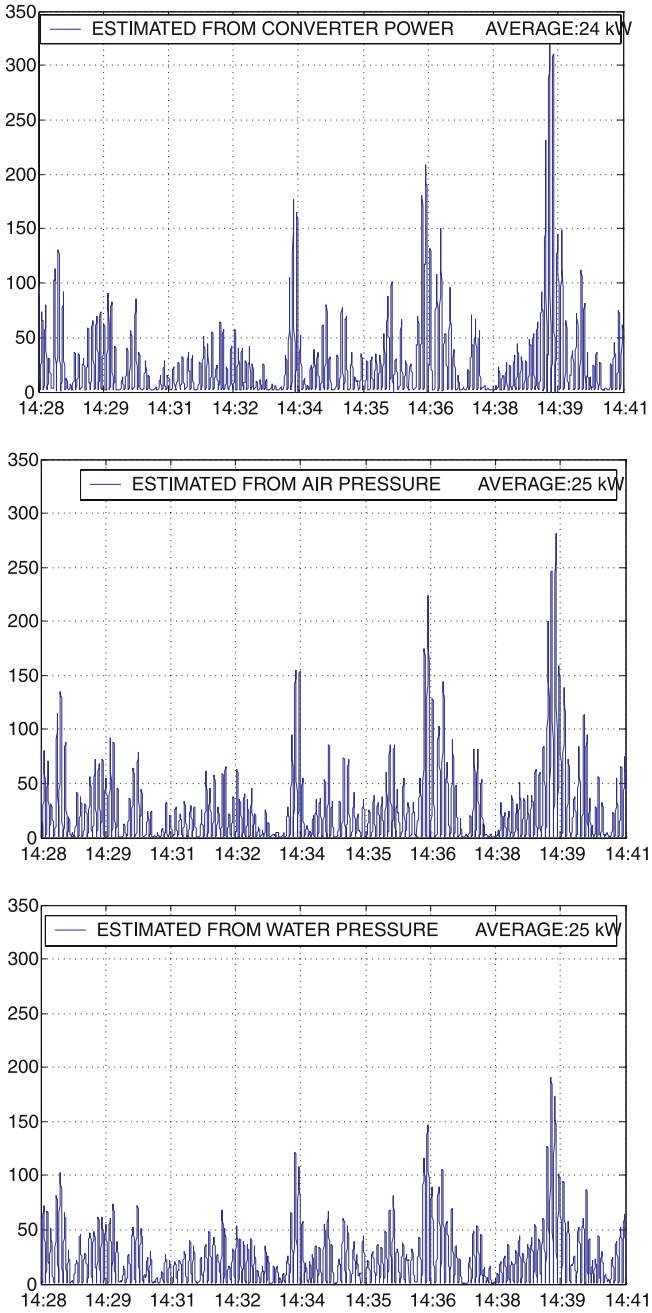

Fig. 7.59. Estimated generator powers

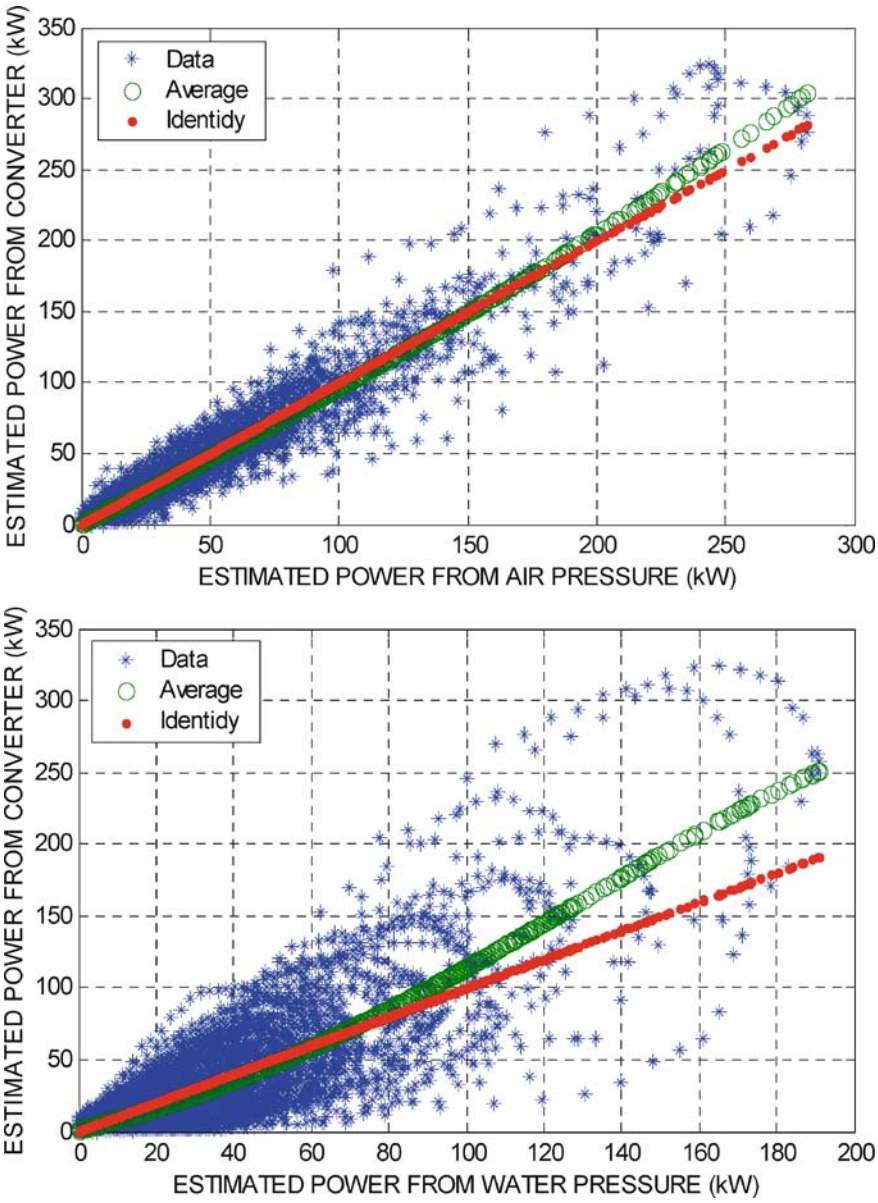

Fig. 7.60. Correlation between the different estimated generator powers

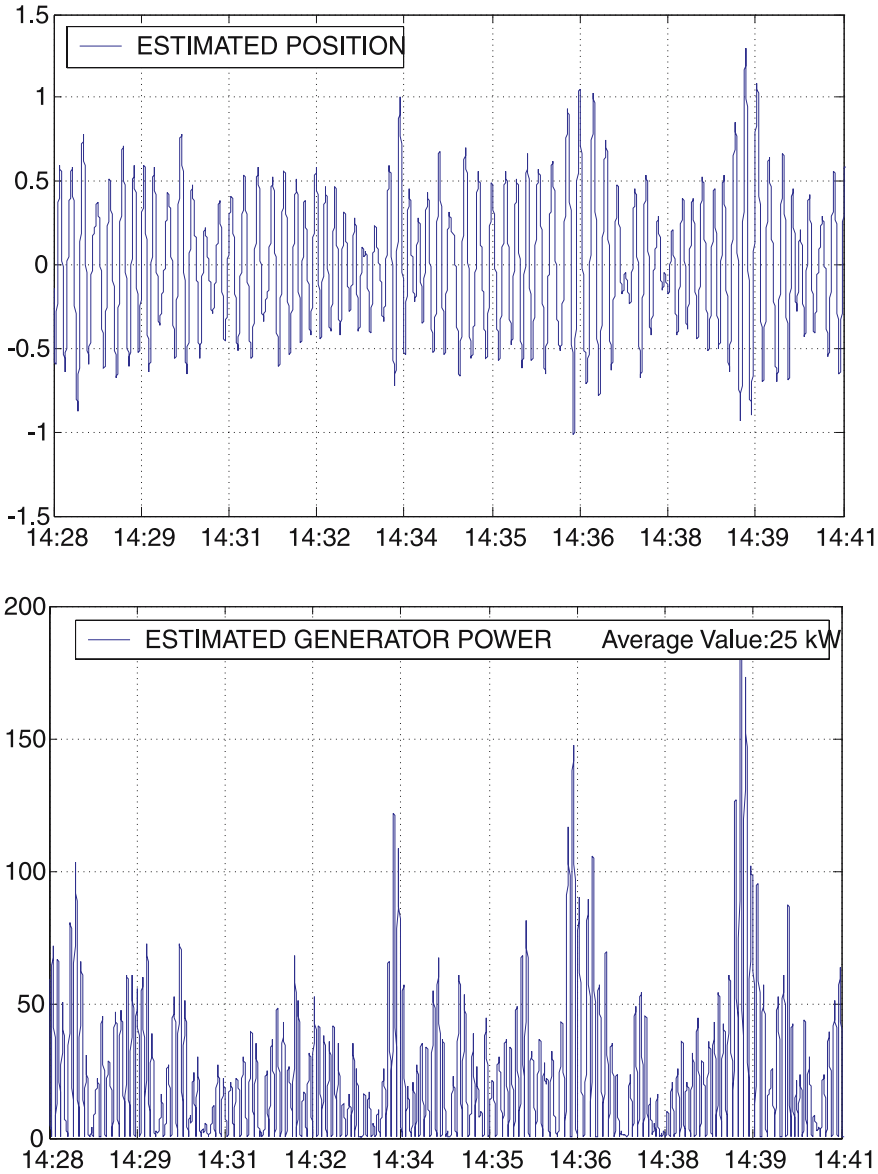

Fig. 7.61. Estimated motion and generator power for the test day

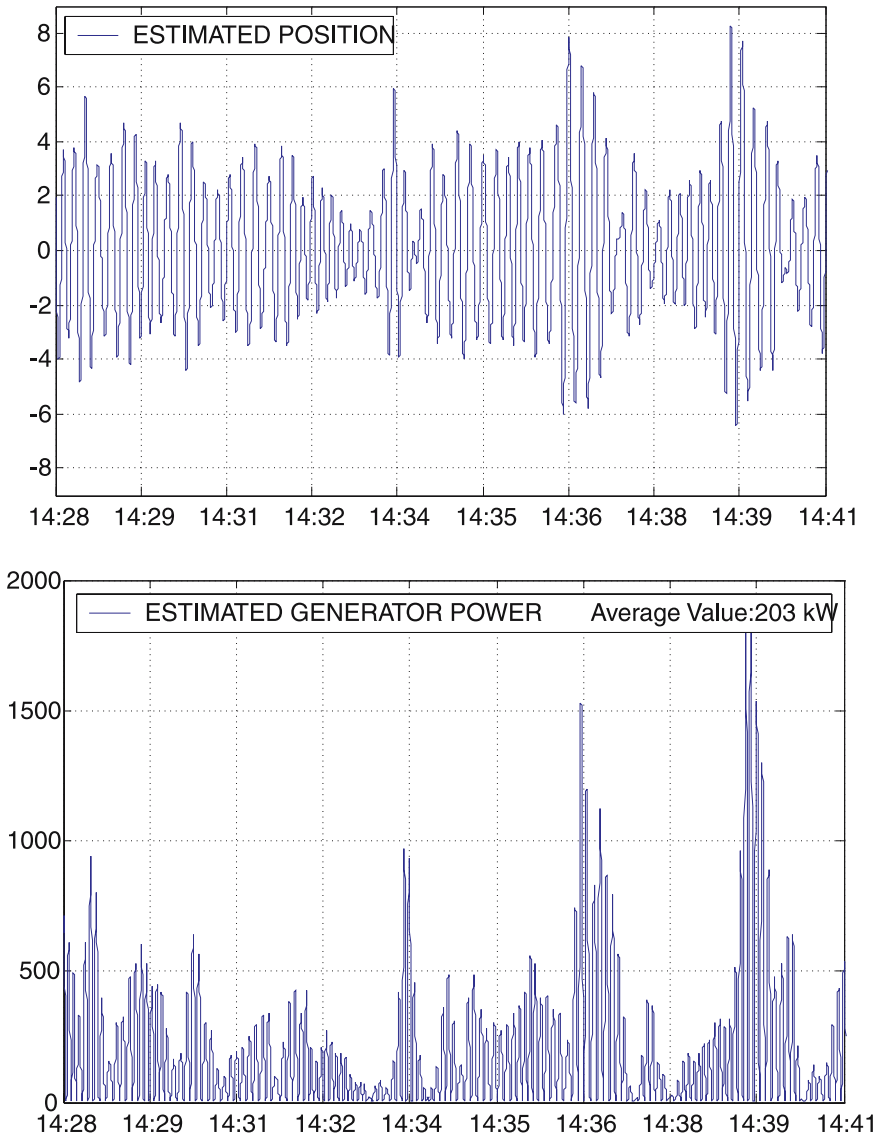

Fig. 7.62. Estimated motion and generator power for the test day, with water brakes open and optimal settings

The effect of the settings of the device can be better appreciated by envisaging the maximum position and average generator power versus the natural period and the setpoint resistance of the converter. There is a drastic effect caused by the action of the water brakes, resulting in excessive damping and thus reduction of the power output. Note that the water brakes were used at this stage given the nature of the tests. Correct tuning of the settings reveals a big impact on the performance. Average power levels of 200 kW can be obtained for the same sea state. It should be noticed however that for this kind of power, the expected maximum stroke should be around 16 m, which is higher than the stroke of 9 m available. For a maximum 9 m stroke, average power levels of 150 kW are estimated. In practice using a dynamic adjustment of the converter resistance, it is s possible to reach average power levels higher than 150 kW.

In summary, the experience with the pilot plant results shows that a simple 2nd order mass-spring system fits reasonably well to the measured data, which leads to the conclusion that the main structure of the AWS dynamics is relatively simple. Average power outputs can be estimated with high accuracy but peak values are underestimated by the model. A higher-order non-linear model should be used to get better fits to the measured data. Since water brakes were always closed, other forms of damping like drag and radiation could not be identified. From the model it could be seen the significant impact that the water brakes have on the overall performance of the device. By opening the water brakes and correctly adjusting the settings of the device, the average power level could reach levels in the range 150–200 kW. All the lessons learned in Portugal, both in the submersion and when in operation, are expected to be vital when developing the next generations of AWS machines.

7.5.4 Pelamis

João Cruz, Ross Henderson, Richard Yemm*

Pelamis Wave Power Ltd
Edinburgh
Scotland, UK
** Now at Garrad Hassan and Partners Ltd, Bristol, England, UK*

As previously mentioned in 7.3, Pelamis Wave Power's (PWP) development programme reached a significant milestone in August 2004, when the first full-scale prototype (FSP) was installed at the European Marine Energy Centre (EMEC), in Orkney, and the first electricity generated from an offshore wave energy converted was delivered to the UK grid. The ongoing FSP programme provides operational knowledge which is pivotal for the first offshore wave farms, such as the Agucadoura wave farm in Portugal (three Pelamis machines at a first stage). This short contribution aims to briefly describe the production and assembly knowledge, the

O&M procedures and operational experience that PWP has gathered over the past years. Representative data from a recent round of tests at EMEC is also presented.

Production and Assembly

A production programme was initiated in 2005, following the first commercial order for three Pelamis machines to be installed in Portugal. The new P1A Pelamis machines have a few design improvements with regard to the full-scale prototype, including a rapid mooring connection system.

In June 2005 the first construction contracts were issued with the majority of the fabrication contracts being awarded to Scottish manufacturers. The main tube fabrication was given to Camcal, for completion at the Arnish manufacturing site on the Isle of Lewis. The Stonehaven based company, Ross Deeptech, secured the order for the fabrication of the nine power conversion modules. After completion of the first module, it was transported to the PWP site in Methil, Fife. Based in the ex-Kvaerner yard, now the Fife Energy Park, the PWP production team have established an assembly facility. Drawing upon the local skills base, twelve members of the production team were given the task of populating the power conversion modules with their internal components (Fig. 7.63). Further orders will allow PWP to develop their assembly facilities and work has already been initiated with the objective of reducing costs for the next generation of Pelamis machines.

Fig. 7.63. Seven of the nine power conversion modules of the P1A machines lined up at the Fife Energy Park during initial assembly

The power modules, tubes and all remaining components for the first three P1A machines were transported to Portugal for final assembly by PWP staff (Figures 7.64 and 7.65). The assembly of the machines at the quayside of the Peniche shipyard uses a new 'habitat' system, a localised floating 'dry dock', tested in accordance with DNV standards and certifications. It allows maximum flexibility for operations whilst ensuring work is carried out in a safe and dry environment.

Fig. 7.64. Arrival of the P1A machines at the Peniche (Portugal) for final assembly

Fig. 7.65. Detail of the power conversion modules at the Peniche shipyard (Portugal)

Once assembled, the three machines will undergo commissioning and sea trials prior to installation of the wave farm, which will take place 5 *km* off the Portuguese coast, near Póvoa de Varzim. The project will have a rated capacity of 2.25 *MW*.

O&M

Suitable maintenance strategies are vital to ensure the long term reliability of any technology, in particular for wave energy converters. The design for reliability and the initial maintenance schedules must be cautious because systems failures can be aggravated and there may be no suitable weather window immediately available to retrieve the machines in the event of any given failure.

The Pelamis is designed to be resistant to single point failures through a combination of inherent robustness and redundancy where required. It is cost effective to avoid loss in generation or integrity through the inclusion of redundant systems. It is also cost effective to avoid any on-site maintenance and make use of the ability to connect and disconnect quickly and cheaply across a wide range of conditions. The Pelamis mooring system has been repeatedly demonstrated on the refitted prototype machine allowing connection in under two hours and removal in around 15 minutes in seas of $H_s > 2\,m$. Further enhancements will allow even faster operations over a greater range of conditions.

PWP acknowledged the importance of inspections and maintenance from the start of its operational programme. The offsite maintenance policy means that if and when necessary the Pelamis can be removed from site and docked at the quayside; for the FSP this was in Lyness (Orkney). All electrical systems are kept alive while the machine stays in a default control mode, thus allowing continuous monitoring of all systems. The easy access to the prototype ensures that if any modification to a given component needs to be made then it can be done promptly and in conformity with strict health & safety policies. In order to maximise the knowledge of issues like fatigue and to proceed with technological updates, inspections and the opportunity for refits also need to be programmed. Figure 7.66 shows the refit of the FSP which took place in mid 2006 at one of the dry docks in the Port of Leith (Edinburgh). Along with the introduction of engineering innovations such as the quick moorings connection system (note that two years had passed since the launch of the full-scale prototype) inspections were carried out on major structural elements such as the main bearings and attachment points, and other systems such as hydraulic rams, accumulators, cable transits, and bellows seals.

After this operation, the full-scale prototype was ready for a new set of sea trials (which took place in early 2007) and for a further installation round at EMEC. Results from one of the installation periods are presented in the following subsection.

Full-Scale Prototype – Results

The full-scale prototype Pelamis has been in Orkney since 2004. Following a set of sea trials in the North Sea (see Fig. 7.17) the first installation took place in

Fig. 7.66. The full-scale Pelamis prototype while being refitted in Leith (Edinburgh), 2006

August 2004 (Fig. 7.18). As previously described the machine then underwent a major refit operation in Leith (Edinburgh) in 2006. New systems where installed to reflect the design enhancements of the P1A machines due to be installed in Portugal and to test other novel components.

The success of this refit operation lead to a new round of sea trials which were conducted by early 2007 in the North Sea. Subsequently the Pelamis FSP was towed up to Orkney for a further installation round at EMEC, which spanned between April and July.

In analogy to other subsections of this chapter, a significant 30 minute window was selected for detailed examination (the period between 14 : 00 and 14 : 30 on 08/07/2007). During that half-hour the sea state was characterised by $H_{m0} = 2.8\,m$ and $T_{-10} = 6.7\,s$.m. The average absorbed power over the half hour was 147 kW, while the average generated power was 95 kW, resulting in a 30 minute average wave-to-wire conversion efficiency of 65%, as expected for the FSP. The peak (instantaneous) values for absorbed and generated power over that period were 842.2 kW and 201.2 kW, respectively. The *rms* equivalents were 182 kW and 101.9 kW. The performance assessment software developed by PWP allows a thorough check of selected variables. For example, plots of averaged time series can be produced with an arbitrary buffer size (Fig. 7.68 shows the results for a 10 minute window, now for an hour period stating at 14 : 00). In this hour the corresponding levels of wave power dropped from 28 kW/m to 19 kW/m at 14 : 30, keeping this lower bound roughly for 20–25 minutes until 15 : 00. The efficiency however remained well above 60 % throughout the entire one hour period. It is interesting to zoom in the absorbed and generated power time series: Fig. 7.69 shows a three minute window of the instantaneous values of both. The effect of the sea state is clear in the absorbed power plot, while the hydraulic power take-off system allows the generated power to be much

smoother with respect to time. In fact, this plot would present a flat line if the control settings were not so conservative (as previously mentioned), even in a sea state such as this one, where the effects of different wave groups were particularly clear. All power measurements are independently verified by EMEC. Testing of the FSP has followed a cautious approach with steady implementation of the most robust control strategies with conservative settings relative to design constraints. Power absorption can be significantly higher with bolder control settings and future designs include constraints adjusted to take full advantage of potential absorption.

All machine data can be included in automatically generated summary reports, which also include the relevant wave statistics and the characterisation of the frequency and of the directional spectrum. Figure 7.70 shows the corresponding frequency spectrum for this half hour, where the continuous curve represents the Pierson-Moskowitz (PM) spectrum with the same H_{m0} and T_{-10}. Early Pelamis simulation work assumed a model PM spectrum but more recent models allow the use of buoy data directly. Thus the state of the art simulations include non-linear hydrodynamics, accurate modelling of the control and hydraulic PTO, moorings system, and wave excitation generated from buoy measurements in real seas. When such methodology is used, the outputs of the numerical simulation are typically within 10% of both the absorbed and generated power. This is a reassuring example of numerical models extending from the recreating tank tests and hypothetical situations into the real world with good agreement with a full-scale machine operating in real seas.

Another significant milestone achieved during the 2007 FSP operations is demonstration of rapid installation / removal times using small work boats in conditions up to $2\,m$ H_s. This proves that future Pelamis wave farms can be serviced cost effectively. Greater advances in Pelamis operations technology are currently underway to further streamline the installation and removal of machines and extend the range of conditions available for intervention.

Fig. 7.67. The Pelamis full-scale prototype installed at EMEC (June 2007)

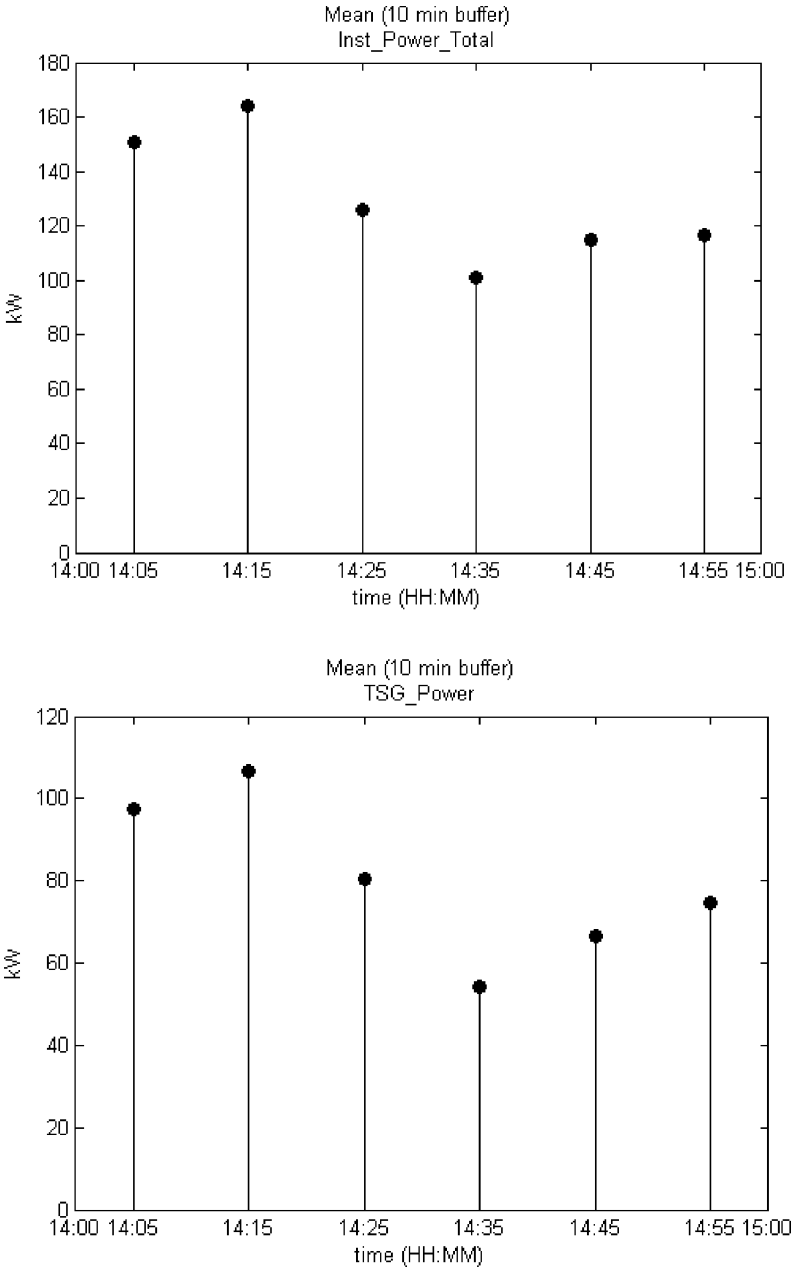

Fig. 7.68. 10 minute averaged absorbed (top) and generated power (bottom) – 08/07/2007

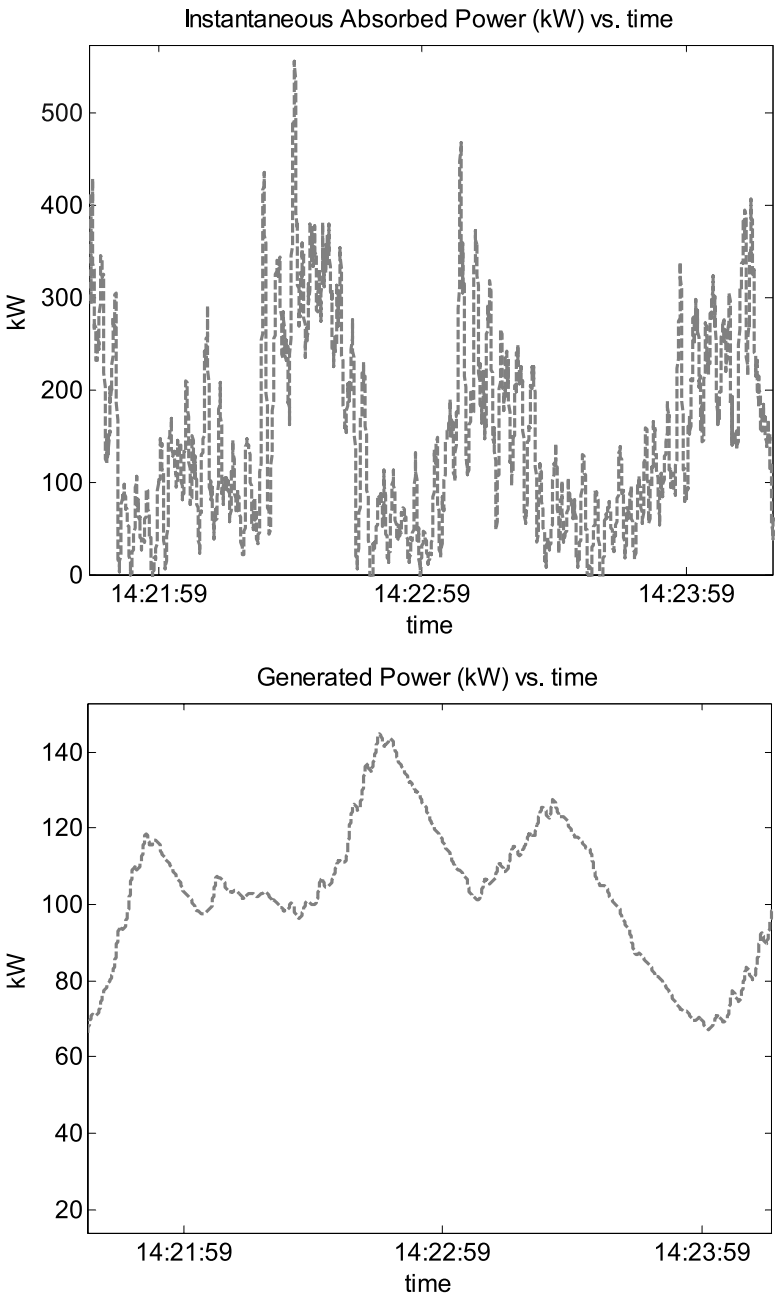

Fig. 7.69. Time series of absorbed and generated powers – 08/07/2007 14 : 21–14 : 24

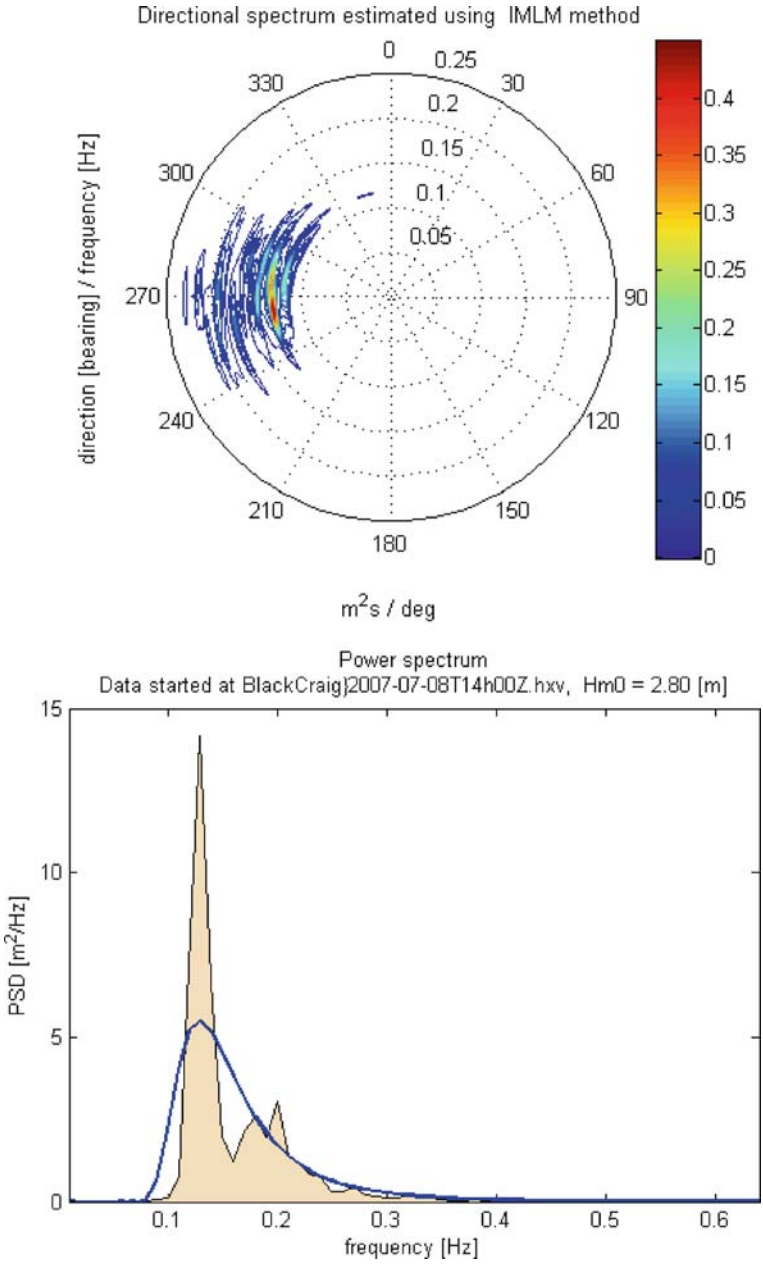

Fig. 7.70. Directional (top) and frequency spectrum (bottom) – 08/07/2007 14 : 00–1430

Control

Control of Pelamis is achieved by means of a bespoke real time system with a custom graphical user interface (GUI). Every output in the machine can be controlled in real time with respect to every input. This allows immensely powerful control algorithms to be implemented and provides the flexibility to improve the power absorption capability of existing machines through the upgrade of control algorithms. The potential for performance improvements through control upgrades is immense and the associated costs marginal.

While advances in the user interface are being made as the technology progresses towards less user intervention and greater autonomy. The FSP interface allows low level control of every aspect of the machine and continuous monitoring of all systems. Figure 7.71 shows the main screen of the FSP GUI. The left hand side represents the machines dynamic response and the right hand side represents the power generation systems. Each side is further split into three parts, each corresponding to one of the power conversion modules. Such flexibility and independence allows the PWP control team to safely implement new control algorithms which can maximise the generated power without compromising the survivability of the machine.

Fig. 7.71. Snapshot of the Pelamis control graphical user interface (GUI)

All changes to the control system in service are carried out as part of a robust development and testing programme. A key element in this is the testing of all software changes on a purpose built test-bench which includes all the control hardware of the real machine along with emulation hardware to provide real electronic signals to the various devices and model the physical systems of the real machine. Thus the software can be bench tested for errors in the context of the real hardware with real representative signals. This bench test approach also allows any issues that appear on the real machine to be recreated and examined safely.

Summary

This subsection has provided a short account of the operational experience that PWP has gathered from its full-scale demonstration programme in Orkney. The direct results of the lessons are now being applied in new designs and in other projects, like the Aguçadoura wave farm in Portugal. The flexibility and power of the control system is likely to provide dramatic improvements in performance in the newer generations of machines. PWP's numerical simulation package has been demonstrated its ability to model detailed full scale machines in real seas. The monitoring and post-processing packages are also a continuous reassurance of the quality of the methodology and these are now undergoing integration into the control and analysis suite for the new farm interface.

7.5.5 Wave Dragon

James Tedd, Jens Peter Kofoed, Erik Friis-Madsen, Lars Christensen

Wave Dragon ApS
Copenhagen
Denmark

Introduction

Wave Dragon have deployed and run a successful prototype wave energy power plant in Northern Denmark for over 3½ years. The device is located in an inland sea and so is scaled appropriately, while maintaining all automatic control and power take-off system and grid connection which will be seen in larger open sea power plants. This section will introduce the device and the Europe-wide consortium who built it. The operational experience gained from running the device will be shared by considering a selection of the subsystems on board. The power production results will be presented showing how the prototype has shown Wave Dragon to achieve an efficiency of 18 %, close to the long term goal.

A scale prototype in a 1 : 4.5 scale sea

Nissum Bredning, a sheltered sea connected to the Danish North Sea, was chosen as the site to deploy the first Wave Dragon prototype (see Figures 7.72 and 7.73). By deploying in a less energetic site many of the components and subsystems could be tested and developed at a reasonable cost. Also the expense of a site visit was greatly reduced. The available wave energy in the site makes it suitable for a 1 : 4.5 scale machine (relative to the North Sea). Therefore the original concrete construction drawings were scaled down and the construction material replaced with steel, allowing small changes to the structure to be made on board.

The main aspects to be tested at this site were those which can not be successfully modelled in the laboratory, like the low head hydro turbines controlled by variable speed Permanent Magnet Generators, and the hydraulic response of the platform with its open buoyancy compartments. In addition, control strategies for optimal power production and buoyancy regulation have been focused. Operating in the harsh offshore environment has taught many additional lessons.

The device itself has been very highly instrumented with over 100 sensors. These include: pressure sensors to measure the incoming waves, floating height and water in the reservoir; strain gauges and force transducers to measure the

Fig. 7.72. The platform at the dockside in 2003 before being launched. On the right the open air compartments used for buoyancy regulation can be seen

Fig. 7.73. Wave Dragon in Nissum Bredning. Wave Dragon was deployed at two sites in the sea, initially at the Northern site, and then later at the more energetic southern site

forces in the structure; a wind station; accelerometers and inclinometers to view the positions of the device; electrical sensors within the power take-off system and many more. Amongst the most used of these have been the five web-cameras mounted on board, allowing 24 hour visual checks of the situation on the platform.

Wave Dragon consortium

An early decision by the Wave Dragon team was to have the majority of work performed by experts in the field. This philosophy has led to a very dynamic company structure with a small core element, and a broad selection of trusted partner companies with years of experience in their own field. This structure is favoured by many public funding bodies, and allowed the Wave Dragon project to qualify for support from the European Commissions R&D targeted funds. The partner companies provided match funding for their own work and were rewarded with an option of a share in the Wave Dragon core company. With the modern age of telecommunications there was no problem with the wide spread of work across the European continent. The partner companies involved and their respective roles are:

Wave Dragon ApS is the development company for the wave energy converter technology.

Löwenmark Consulting Engineers FRI – A small Danish company which is home to the inventor of Wave Dragon Erik Friis-Madsen. This company has worked closely with all the engineering companies in the project to ensure the best possible design for the device. Most work is now performed by the Wave Dragon company.

SPOK ApS – This small Danish company provided the project management for the consortium and developed the Wave Dragon corporate side and initiated further projects. In addition to this work they had the responsibilities for the environmental surveys and Life Cycle Analysis work conducted for the prototype. Most work is now performed by the Wave Dragon company.

Balslev A/S – As a larger Danish electrical and control engineering company they have worked on the active control of the Wave Dragon. This has involved implementing the control strategies into the Programmable Logic Controller (PLC) and development of the System Control and Data Acquisition (SCADA) user interface for the operation of the Wave Dragon.

ESBI Engineering Ltd – This large Irish consultancy (once part of the Electricity supply board of Ireland) have had responsibility for the design and monitoring of the grid connection of the Wave Dragon.

NIRAS AS – As a larger structural engineering consultancy based in Denmark this company has had a broad brief of responsibilities. The core of their work was to define the design criteria for the device and perform some detailed design. In addition they worked with Finite Element Modelling of the internal forces within the structure and prediction of waves from the wind states.

Promecon A/S – A subsidiary of MT Højgaard this company is one of the largest steel constructors in Scandinavia. They constructed the main structure in Steel and were responsible for the successful deployment of the device.

Kössler Ges.m.b.H. – This Austrian company has decades of experience in construction of hydro turbines. As a partner in the consortium they brought this experience into play when constructing the turbines used on board the device.

Aalborg University – As the local university in northern Denmark, and one of two major technical universities in the country, Aalborg University have been core to the Wave Dragon project since the earliest days. The first scale testing was conducted in their laboratories. In this project Aalborg University specialised in monitoring the prototype. This has led to many published research papers on all aspects of the prototype and countless students have been inspired from working on related projects.

Technical University Munich – The turbine group at this university joined the project with the aim of designing and testing the scaled turbines, and analysing their control strategies in cooperation with Veterankraft AB. As the project developed, they have also been crucial in many more practical matters, mainly with maintenance of the turbines.

Armstrong Technology

Armstrong Technology Associates – A structural engineering company from the UK. Initially in the consortium to provide naval engineering expertise to convert original concrete 1 : 1 construction drawings to 1 : 4.5 scale steel equivalents. Unfortunately after initial design work the company changed direction and withdrew, their responsibilities were taken on primarily by NIRAS AS.

Performance in storms

Wave Dragon has had survivability built into all systems from the start. Overtopping devices are naturally adapted to perform well in storm situations, where the wave will pass over and under the device with no potential end-stop problems. However as the prototype has been deployed for more than three years in an offshore situation it comes as no surprise that the platform has had to survive some severe weather. With the web cameras on board some dramatic moments have been caught, as in Figures 7.74 and 7.75.

The two incidents shown on camera did not cause any damage to the Wave Dragon. Unfortunately this has not always been the case. On one occasion damage was suffered to the main platform and a large fixed buoyancy tank was punctured. This was a reminder of the need for redundancy in the design, here the other fixed buoyancy tanks were sufficient to allow the Wave Dragon to continue operating. During the next calm period the breached tank was emptied, the puncture welded tight, and the tank separated into two smaller units to add extra redundancy.

Fig. 7.74. View from web camera mounted to control container of large wave surging down reflector wing of Wave Dragon

Fig. 7.75. View from web camera mounted to the device's shoulder of waves crashing into turbine area

In 2005 the largest storm for 100 years hit northern Denmark. Average wind speeds were in excess of 110 *km/h* with gusts above 150 *km/h*. In addition to widespread structural damage to buildings in the region the storm broke a force transducer mounted in the mooring system of the device. On the prototype the force transducer was selected to give accurate readings of mooring forces in even small waves. It therefore did not have the safety factors of the other sections of the mooring system. Small defects in the steel could be seen at the nucleus of the fracture shown in Fig. 7.76.

After loosing the mooring connection the Wave Dragon soon drifted onto a sandy shore, where it suffered little damage. The device was soon refloated and taken to harbour for some scheduled maintenance. Thus Wave Dragon became the first WEC to be successfully recovered and redeployed at sea.

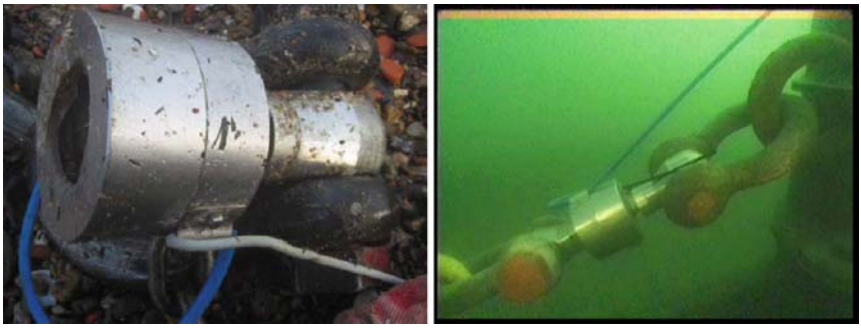

Fig. 7.76. Fractured force transducer after Force 11 storm and view of transducer in position taken by a diver

Control of the device

All of the control devices for the Wave Dragon prototype are housed in a container mounted to the back of the Wave Dragon platform. Clearly this is oversized on the 1 : 4.5 scale device as any operational staff will not scale.

The core of the control system is a Programmable Logic Controller (PLC). The PLC controls the blowers and valves to regulate the buoyancy of the device, aiming for a horizontal and stable platform. A series of regulation strategies have been implemented within the PLC with implementing aspects of PID control giving more stable behaviour. The regulation is able to change the floating height of the platform by around 20 *cm* every hour, allowing the crest freeboard to rise with increasing storms, and thus improve the power capture. The PLC is also responsible for controlling the action of the turbines, in order to extract the maximum energy from the water which has overtopped. The PLC controls a hydraulic pump and solenoid valves to allow the water hydraulic system to operate the turbine cylinder gates or evacuate the siphon. Again several strategies have been tested on board, with much improvement.

One of the PC's in the control room is running a System Control and Data Acquisition (SCADA) system allowing the primary human interface with the device. In Fig. 7.77 some screenshots from the system are shown. In addition to giving the current status of the device the system allows set points to be altered and records historic values for the power production system. In parallel with this a more typical data acquisition system is run recording the measurements not used in the active control of the device, but of interest for scientific and development uses, such as strain gauge readings and wind records.

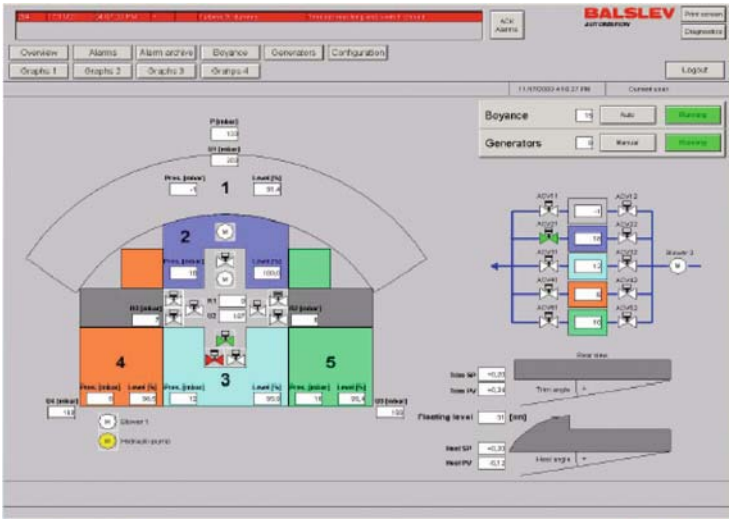

Fig. 7.77. Front page of the SCADA system showing stability of platform, buoyancy tank status, and turbine status

The SCADA PC is connected to the internet, and therefore allows control of the device remotely. This is aided by the use of five web cameras as a visual check on any abnormal behaviour. However on occasion this link has been lost; either due to grid power failures in the district, power failures on board, or simply issues with the internet provider. In these cases a backup system which uses the GSM network becomes operational. In the case of serious abnormalities the PLC will send SMS messages to two nominated people. These people are able to control the PLC in a basic way by sending coded messages to the device. If both of these lines of communication are all down then the PLC will continue to operate in a safe manner. If power is lost to the PLC, the structure of the Wave Dragon will stay afloat without any active control system.

Moorings

The design for a full sized Wave Dragon has the device moored to anchors by several catenary chains, a CALM buoy system. In Nissum Bredning the site is too shallow (at around $6\,m$) to allow this system. In the prototype the compliance of the mooring is provided by using elastic nylon and polyester ropes, a schematic of this is shown in Fig. 7.78. The anchor is provided by a steel bucket filled with local sediment. A pile is attached to this anchor which is of great use, for mounting wind measuring devices, a webcam, and a pressure transducer to measure the incoming waves. A second smaller back anchor is present in the prototype to prevent the device colliding with the mooring pile. This restricts the movement of the device to $\pm 60°$, which is acceptable close to a coast.

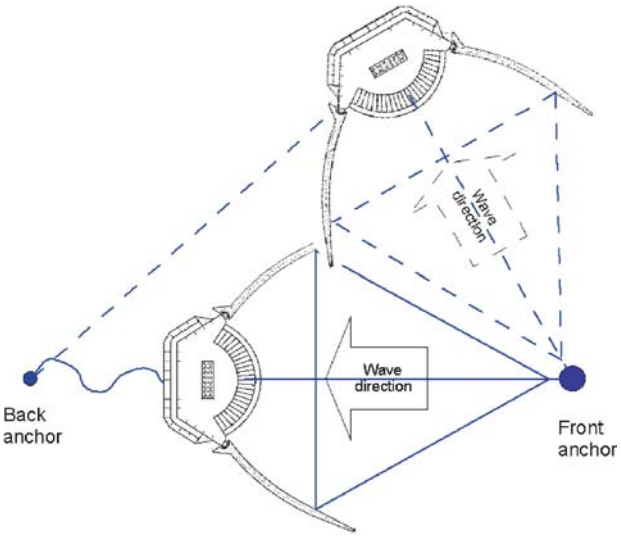

Fig. 7.78. Mooring Schematic

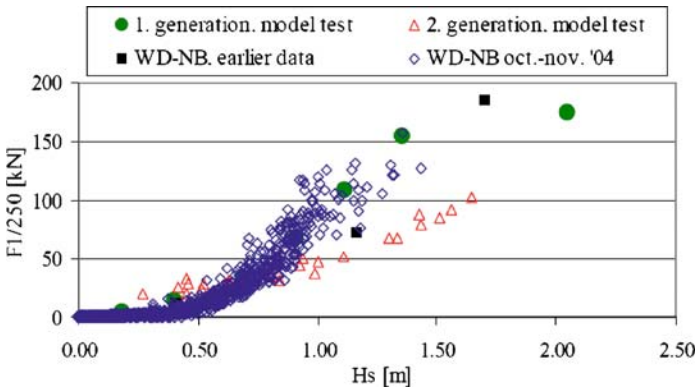

Fig. 7.79. Comparison of mooring forces in terms of F 1/250 (average of the 1/250 largest peaks) measured during 1 : 50 scale tests and prototype measurements (1 : 4.5). H_s is given in prototype scale

A lot of data has been recorded by the force transducers in the mooring system. As reported in Kofoed et al. (2006) and shown in Fig. 7.79, the mooring forces show good correlation to the scale testing in the laboratory. There was a noticeable increase in the stiffness of the mooring lines due to marine growth during the period. This will not be an effect on catenary chains in a full scale deployment.

Experience with hydro turbines

Power simulation investigations show that a power take-off system consisting of 16 to 20 variable speed on/off low-head turbines of the Kaplan type with fixed runners and guide vanes is optimal for a production Wave Dragon. For the prototype platform a choice was made to replicate these with a selection of turbines, 10 in all. Each generating turbine is directly connected (no gear box) to a permanent magnet generator (PMG). Each PMG is connected to a frequency converter, which is used for control of the speed of the turbine and for supplying the power from each turbine onto a common DC rail. The power is then via another frequency converter put onto the grid with grid frequency and voltage. The turbines used are shown in Fig. 7.80 and detailed below.

- A Kaplan turbine with siphon inlet. This is the original turbine which had been tested at the Technical University of Munich. The runner diameter of the siphon turbine is 0.34 m, rated flow is 0.22 m^3/s (at 0.5 m head) and rated power is 2.6 kW (at 1 m head) corresponding to 350 kW in a full scale North Sea Wave Dragon.
- Six Kaplan turbines with cylinder gates. These turbines have the same runner diameter and performance data as the siphon turbine. The turbines were fabricated in Austria by Kössler GmbH, their runners were made by TUM.

Fig. 7.80. Turbines in the reservoir of the prototype: The structure in the background is the siphon turbine, the grey towers are five of the six cylinder gate turbines, and the small devices in unpainted steel are two of the dummy turbines

- Three dummy turbines. These turbines are not able to produce power; they are merely calibrated valves which let the overtopped water run back into the sea. The diameter of the valves is 0.43 *m*, and discharge is about twice one of the real turbines. They permit accurate simulation of the discharge from a further six real cylinder gate turbines at a fraction of the cost.

In order to avoid debris in the turbines the turbine area was enclosed by a trash rack, see Fig. 7.81. There is also a powerful water pump on board to enable testing and calibration of the turbines in calm situations.

Fig. 7.81. Trash rack with 5×5 *cm* grid openings enclosing the turbine area

Fig. 7.82. The insides of two turbine draft tubes, on the left one painted with silicone paint, and on the right painting with conventional epoxy paint

Experience has shown that the aggressiveness of the salt water environment had been underestimated. A design proven in many river hydro power turbines has been used for the main turbine bearing, but the bearings failed after a few months of operation due to problems with the shaft seals.

The bearings of four out of the seven turbines have been modified and rebuilt during the 2004 summer, and the turbines have been operated without further problems from October to December 2004. The bearings of the remaining turbines have been modified and rebuilt during the 2005 summer. It was possible to conduct the majority of this work onboard the floating platform.

Dismantling the turbines during the above mentioned repairs has also shown that marine growth is a factor that may not been taken lightly. The draft tubes of the turbines had been made from different materials: uncoated stainless steel, black steel protected with conventional epoxy paint and black steel protected with a recently developed silicone-based anti-fouling paint. The draft tubes painted with the conventional paint system were found heavily overgrown (mainly by the acorn barnacle, *balanus crenatus*, and sea squirt, *ciona intestinalis*), which were almost impossible to remove. The stainless steel tubes as well as the ones coated with the silicone paint had only a few small barnacles on them which could be swept off very easily, as can be seen in Fig. 7.82.

Power Production

There are many ways to show the power production of a WEC, depending on where you measure the power. In several published papers (e.g. Tedd et al., 2006) some of these methods are explored. Figure 7.83 shows a typical time series for a record.

An enormous quantity of data has been collected during the testing period, which has not yet been fully analysed. However, the work done up to now has confirmed that the performance predicted on the basis of wave tank testing and turbine model tests will be achieved in a full scale prototype.

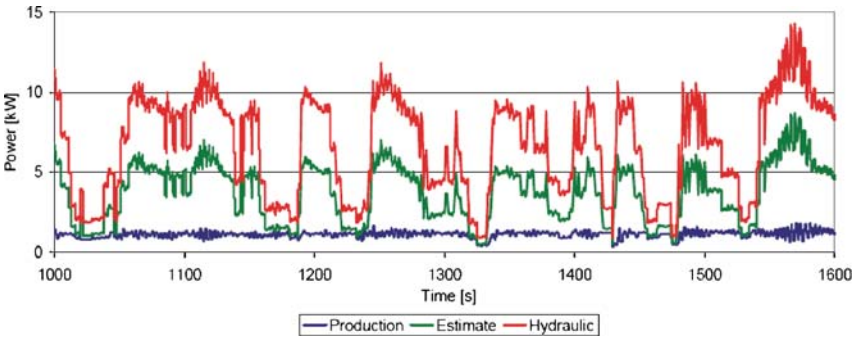

Fig. 7.83. Time series of a typical record, showing: Production, power delivered to the grid; Estimate power, which supposes the turbine set points were correct and the dummy turbines produced as real turbines; and Hydraulic power the power of the water passing through the turbines

Looking at the period May 2003 to December 2004 and scaling the energy production (1 : 4.5) to a typical 16 *kW/m* wave climate as found in the North Sea the prototype Wave Dragon would have produced from 50 to 500 M*Wh/month*. Taking into account down periods and testing periods the real production would have been approximately 3.2 *GWh/year*. The latest tests have shown that an optimal setting of the set points of the PM generators has increased the power production with a factor of two. Therefore it is assumed that the real production easily could have been 6.5 *GWh/year* or equal to an 18 % average wave-to-wire efficiency.

This result should be compared to the 16 % prototype goal and the 21 % long term goal for the Wave Dragon technology. Measurements of the hydraulic power indicate that it will be possible to reach this value of energy production. Some of the discrepancies are believed to be due to the scaling which will cause extra energy losses in bearings etc.

Summary

Since March 2003 a prototype of Wave Dragon has been tested in an inland sea in Denmark. This has been a great success with all subsystems tested and improved through working in the offshore environment. The project has proved the Wave Dragon device and has enabled the next stage, a production sized version.

7.6 Test Centres, Pilot Zones and European Cooperation

António Sarmento

Wave Energy Centre
Lisbon
Portugal

The design, construction, deployment and test of pilot plants and prototypes are of fundamental importance in the development of the technology as they provide an opportunity to assess design methods and criteria, to work out engineering solutions, to identify the real costs of building, deploy and operate the pilot plant or prototype and, most importantly, to learn from experience, given that no matter how much effort is put in theoretical, numerical and experimental models and in engineering considerations, there are aspects that are only properly addressed in this phase.

However, prototype construction and testing are just the first step in the industrial and commercial development of a given technology, which corresponds to the demonstration of the concept, i.e., of the technological possibility of producing energy with such technology. The other important phases are the demonstration of deliverance, proving that the risks involved in the costing, quality of fabrication and time required to supply the device. The following step is the demonstration of performance: showing that the risk related to energy production, maintenance and operation costs and the resulting cost of energy are controlled. Only then a project-finance can be set on the basis of which wave farms projects are financed due to their intrinsic economic value.

The first phase of development, the demonstration of concept, either via a 1 : 2 or 1 : 4 scale pilot plant or a full-scale prototype, requires a test centre, like the test site in Galway Bay in Ireland[3], EMEC in Scotland[4], or, up to a certain extent, the former AWS site in Northern Portugal, to be used now for the deployment of three Pelamis units. The demonstration phase is usually very limited in time, will involve very low power levels and small energy production and, as it concerns an experimental phase, will require easy access to the device and a significant monitoring program. The impact of a single demonstration device during a limited period of time will be very small and should allow simple and fast licensing procedures, in particular if the test site is chosen in a low environmental sensitivity area. The wave resource and other environmental data (wind and current climatology, bathymetry, seabed properties, etc.) should be known and, in the case of the wave resource, it should be appropriate for the scale of the pilot plant. The test site should have one or more offshore connection points, monitoring facilities related

[3] http://www.marine.ie/home/aboutus/organisationstaff/researchfacilities/Ocean+Energy+Test+Site.htm
[4] http://www.emec.org.uk/

to the device itself and the environment. Proximity to commercial harbours should be strongly encouraged for both O&M and safety.

The second phase, demonstration of deliverance, requires a small wave farm of three to five devices. The Wavehub[5] project in Southwest England is intended to facilitate the deployment of these first wave farms. With a total connection power of 20 *MW* it will allow up to four small wave farms to be deployed, again with a simplified licensing procedure. However the Wavehub initiative does not seem to provide the possibility of these wave farms to expand and it is not obvious if the demonstration of performance will be possible to achieve with such small wave farms.

The demonstration of performance is just the initial phase of pre-commercial development. If successful, the three to five devices wave farms will expand to medium size farms of around 20 units in a first phase and to commercial wave farms sizes of 50 or more devices in subsequent phases. If several wave energy technologies are able to attain this stage, we will get very easily to the level of several hundreds of *MW*. The development may then be frozen by the lack of available connection points or by the time required to obtain the required licenses. It thus seems important that pilot zones with simplified regulations and licensing procedures, with significant grid connection availability and subsidised tariffs for the produced energy are developed. Like in the case of the test sites, these pilot zones should be set in areas of low environmental sensitivity and conflict of use, easy access from nearby ports, well served by nearby shipyards and proximity to the electrical grid, small distance between the 50 *m* contour and the shoreline, etc.

The pilot zone recently announced in Portugal has been thought to provide the conditions indicated above for continuous experimentation and expansion of the technologies, from the demonstration to commercial phase. It is an area of around 400 km^2 in waters from 30 *m* to 90 *m* depth, with a connection point up to 80 *MW* to the distribution grid (medium voltage) and, at a later stage, 350 *MW* to the transport grid (high voltage). The area has low environmental sensitivity, low conflicts of uses, appropriate wave resources, no significant currents, good meteorological conditions, sandy bottom including along the route to the shoreline and is well served by the nearby electrical grid and several ports and shipyards. The pilot zone will be managed by a company that will be responsible for the licensing of the wave farms, the environmental characterisation of the area and the availability of environment data, and the development of the electrical infrastructure. It is desirable that other pilot zones are created in different countries to allow the development and testing of the technologies in different environments and legislations and to reduce the risk of shortage of connection points. The company will also be responsible for the monitoring of the wave farms. This will allow the identification of the resulting positive and negative environmental and socio-economic impacts of wave energy in order to foster the firsts and mitigate the lasts and to correct the regulations and legislation where necessary.

[5] http://www.wavehub.co.uk/

Wave energy will be still in a long term process before it reaches the degree of technological maturity and economic competitiveness that will in turn allow it to compete with other forms of well established technologies. The pilot zones may provide an easier route for this development, but do not avoid the need for international collaboration in many areas and through partnerships of different kinds.

The areas of collaboration include the identification and removal of technological and non-technological barriers, the development of best-practices and standards, the availability of adequate research and test facilities and the training of young technicians and researchers. The support of the European Commission (EC) to enhance this collaboration has been very important, either by funding R&D and demonstration projects, or by funding appropriate networks, such the Coordinated Action of Ocean Energy Systems (CA-OE)[6] or the Marie Curie Research Training Network Wavetrain (Sarmento et al., 2006). The Coordinated Action is a forum to coordinate the research and development of about 50 partners with its work scheduled along five areas: i) Modelling of Ocean Energy Systems; ii) Component technology and power take-off; iii) System design, construction & reliability; iv) Performance monitoring of ocean energy systems; v) Environmental, economics, development policy and promotion of opportunities. The Wavetrain RTN is a research and training network involving 11 European partners (9 R&D partners and 2 technology developers) intended to train 14 young and experienced researchers in the area of wave energy, covering about the same topics as the CA-OE.

The collaboration involves or should involve different types of partnership: companies providing different expertise, R&D institutes and universities and governments and public administration departments and should be developed both at national, European and international levels. Indeed, if Europe is the leading region in developing ocean energy, there is no doubt that the involvement of countries with ocean resources from other parts of the globe is fundamental to create the proper dynamics by providing extra funding, expertise and grid connection points. This last point may be a major factor affecting the development of ocean energy.

7.6.1 Case Study: Wave Dragon

James Tedd, Hans Christian Sørensen, Ian Russel

Wave Dragon ApS
Copenhagen
Denmark

Introduction

As one of the pioneers of the wave energy field, Wave Dragon has been instrumental in developing Denmark's test centre for wave energy in Nissum Bredning.

[6] www.ca-oe.net/home.htm

This has spurred development of Wave Energy in the area with more devices being tested in the vicinity. These later deployments have been much easier as Wave Dragon had already mapped the resource, performed environmental surveys, and liaised with local contractors to ensure reliable maintenance.

The next move for Wave Dragon is to build a device in Pembrokeshire, West Wales in the UK system. As a new technology deployed within a UK national park, Wave Dragon must provide a detailed Environmental Impact Assessment, before gaining consent for the deployment. This new pilot site is an early test case for the authorities of England and Wales, where it is only the second such application to be submitted.

Support from the European Commission together with the Danish and Welsh governments has been vital to the development of Wave Dragon. Support was forthcoming in the early tank testing stages, through the prototype development and now for development of a full sized pre-commercial demonstrator in Wales. Therefore Wave Dragon has operated a very open policy, publishing as much and as often as possible, supporting all Europe-wide initiatives, as well as hosting exchange students. This has proved to be of great value to the company.

Nissum Bredning Test Centre

Nissum Bredning (broads) is a sheltered sea in the Danish mainland separated from the Danish North Sea by two thin tongues of sand, see Fig. 7.84. The sea covers an area of approximately 200 km^2 with the longest continuous fetch in the area of 29 km. Therefore the waves in the area are solely driven by the local wind, with no long period swell waves. The water depth is mostly around 6 m, although there are shallower regions in the west.

Fig. 7.84. Satellite images of Nissum Bredning, from Google Earth. The detailed image shows shallower sandbanks to the West

In 1998 the Danish Energy Authority and the Danish Wave Power Association collaborated with the local Nordic Folkecentre for Renewable Energy to construct a pier for initial testing of Wave Energy devices. This has been used by several inventors to test small wave energy devices, by putting them in the water at the end of the pier.

In preparation for the Wave Dragon test deployment in Nissum Bredning several studies were undertaken. The most important was to analyse the wave resource within the broads. As the waves are fetch limited the Shore Protection Manual method (SPM) could be used to determine the waves. Wind speeds to be used were well defined from four weather stations in the vicinity and the bathymetry is also well known. The study of Svendsen and Frigaard (2001) produced maps showing the mean wave power per unit width.

The Wave Dragon deployed here was built in scale $1:4.5$ of a Wave Dragon for the North Sea. Wave power per meter of crest scales with a power of 2.5. The Northern site therefore has an equivalent power of $16\,kW/m$. The Wave Dragon was first tested here, as it is very accessible for early teething maintenance issues and a grid connection was available close to the test pier. The Southern site was chosen to test the device in the largest waves available within the broads; here there is an equivalent power of $24\,kW/m$. However it is less accessible, as a boat must travel from the harbours of Oddesund or Remmerstrand, both of which are around $5\,km$ from the site.

Before deploying, Wave Dragon sent a consent application – including a description of the device – to the Danish Energy Authority. They performed a consultation process with all possible authorities (environmental, H&S, regional, local and military), and with relevant associations (fishermen, environmental, etc.) and announced the project in local newspapers and called for public objections. The consent was granted with these objections converted into requirements. The authorities and others found that there would be no or close to no negative effects from the project given that it was temporary. All found that it was a good idea to test new technologies. The full process is described well by Hansen et al. (2003).

Fig. 7.85. The Nordic Centre for Renewable Energy's test pier, seen at sunset, with Wave Dragon floating to the right

Fig. 7.86. Bird life in Nissum Bredning. An Arctic Tern perches on the tip of the reflector wing, and a Herring Gull has made its nest in some spare cable on the roof of the control room

The broads area is designated an EU Bird Protection Area (due to three diving ducks species: Common Goldeneye, Red-Breasted Merganser and Goosander); the northern site is also protected by the Ramsar Convention (on wetlands and waterfowl habitat of international importance). In response Wave Dragon agreed to not perform intrusive on-site work during the spring breeding season. Only a small area of seabed is affected by the device, so it has only a small impact on mussel fishing. A non-toxic anti-fouling paint was applied to the turbine draft tubes to prevent poisoning of shellfish. The Wave Dragon has been grid connected at both the northern and southern locations.

In 2006 another Danish device, the Wave Star, a multi-point absorber was installed, mounted to the end of the test pier at the northern site. There are future plans for the southern site to be used for a prototype of a heaving buoy device. This would be using the offshore grid connection provided by Wave Dragon. Both of these devices have benefited from the Wave Dragon experience in the broads area, showing that wave energy can be environmentally benign.

Pembrokeshire Pilot Zone

Wave Dragon is progressing through the next stage of development: to build and deploy a device at a power production scale in order to show the technology to be commercially attractive. The project aims to deploy a 4–7 *MW* Wave Dragon, for 3–5 years in the Irish Sea, close to Milford Haven, Pembrokeshire, Wales. After the period of initial testing the device will be towed to a more energetic site, around 19 *km* offshore, to join a larger array. As this will be the first Wave energy device in Wales, and one of the earliest in the UK, a very stringent planning process must be observed.

Wave Dragon decided to make the pilot zone in Wales for practical and economic reasons. For a project to be economically feasible there must be possibilities to move the first pre-commercial demonstrator into a farm of devices. This

farm requires good wave conditions, a large port for construction and maintenance and good access to strong grid connection. Considering Fig. 7.87, the areas of good wave resource in the UK are the islands of Western Scotland and the South West of Wales and England. Unfortunately the Western Islands of Scotland have very weak grid connections. Pembrokeshire was chosen as the Welsh Development Agency (now the Welsh Assembly Government) has been very supportive of the project since 2001, and also all the facilities such as large deep harbours and skilled workforce exist within Milford Haven.

In Pembrokeshire there were several factors in choosing the precise site for the deployment. These varied from a desire to be close to shore and near a major port to reduce cabling and maintenance costs, to avoid major shipping lanes, and fishing areas, to avoid military training sites and munitions dumps, to minimise environmental impacts, and of course to choose a location with good wave climate. After initial considerations in the region, a 6 *km* square box was chosen with the intention to deploy the Wave Dragon within it. A scoping study (May and Bean,

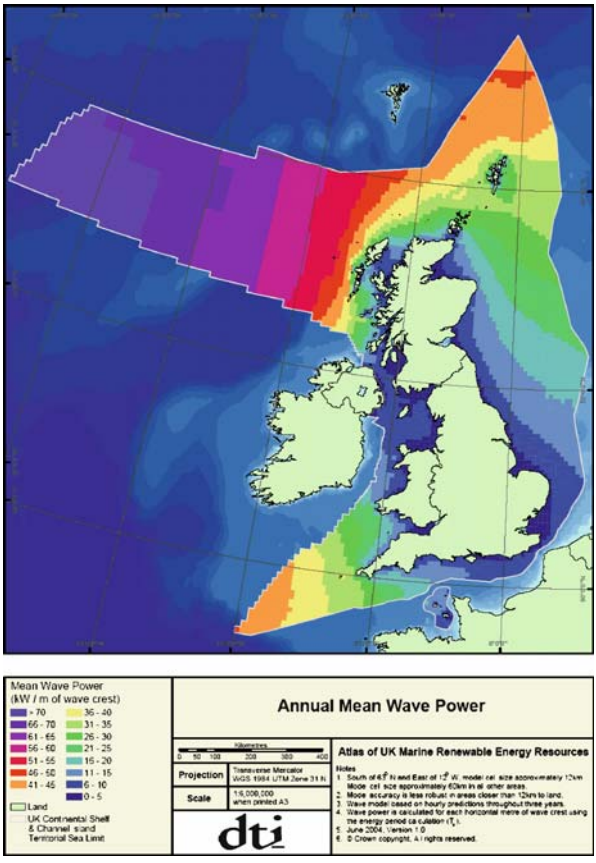

Fig. 7.87. Wave resource for the UK (Source: DTI)

2006) and consultation with all local, regional and national bodies and organisations enabled a full design for the Environmental Impact Assessment. This is required as the coast is a National Park, and the seabed itself is a Marine Reserve and a Site of Special Scientific Interest (SSSI).

Currently a wide variety of specialist consulting companies are working on the project, each looking at the impact within their own area of expertise. These vary from the wildlife including seabed, inter-tidal, marine mammals, birdlife, and more. The hydraulics of the device are studied for analyses of the effect on coastal processes such as erosion, sediment travel and surf waves. The human aspects are also covered including the effects on shipping, fisheries and navigation risk and any archaeology which may be disturbed. Some results from these studies are shown in Fig. 7.88 and 7.89. From the Geophysical survey, an area of coarse sediment could be seen to the north east of the survey zone. The pilot plant will be deployed here, with the best mooring option, the minimising of cabling costs, and limiting possible damage to some more sensitive rocky habitats.

This system of gaining consents in the UK is very rigorous; it must also be followed by other offshore projects, such as wind farm developments. This is advantageous as it clearly proscribes what needs to be done. However it is also a time

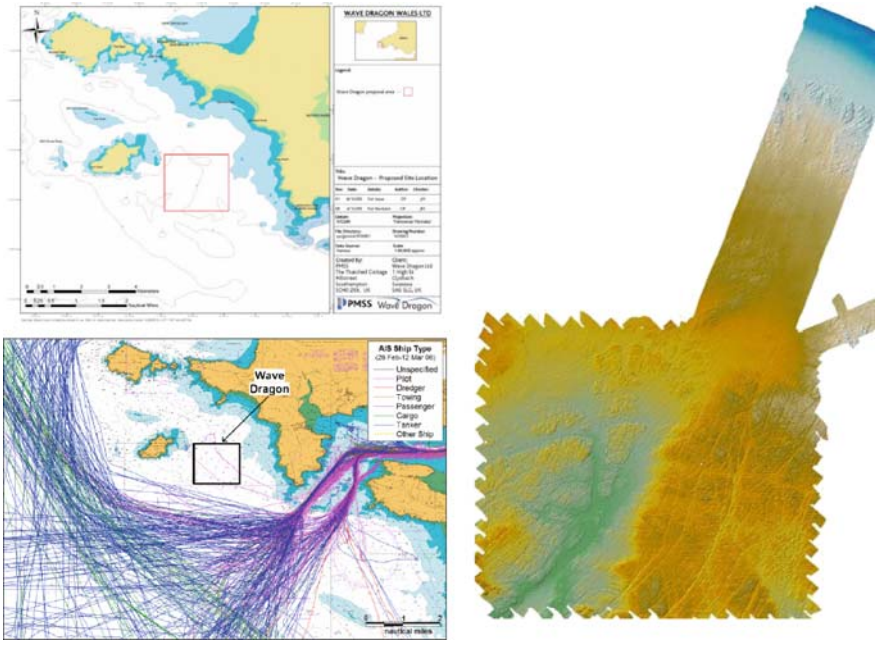

Fig. 7.88. Maps from the EIA, Clockwise from Top left, these show: Location of the surveyed 6 km^2; Bathymetry of the site and cable approaches taken during the Geophysical survey; Ship paths recorded by AIS during a 14 day period

Fig. 7.89. Visual impact: A 7 *MW* Wave Dragon seen from the Pembrokeshire Coast Path above Marloes Sands. Photomontage by Enviros

consuming and expensive process, two luxuries thinly spread in the field of wave energy. A full discussion of the UK system, and comparisons to other country procedures, can be found in Neumann et al. (2006).

In parallel with the consents procedure the engineering design work is being conducted. Wave Dragon has started a new European Research Project to produce a baseline design for a *MW* sized Wave Dragon, and to instrument and monitor its deployment. This partnership is very similar to the group involved in the last EU project, with additional academic partners from Warsaw and Swansea Universities who contribute their expertise on power electronics. To complete the concrete engineering Design, Dr. Tech. Olaf Olssen, a Norwegian engineering firm with extensive experience of construction and deployment in the North Sea, have joined. Finally Wave Dragon Wales Ltd, the UK subsidiary of Wave Dragon is the partner who will build, run and own the device.

European cooperation

Wave Dragon is currently actively involved in the following Europe Wide projects:

1. The EU funded WD-MW Research Project (contract number 019983). This three year project will provide a baseline design for a multi-*MW* sized Wave Dragon and develop the remaining subsystems. It will continue to monitor the deployment of the first multi-*MW* sized Wave Dragon. There are 10 partners involved from seven European countries.
2. The Co-ordinated Action on Ocean Energy (contract number 502701 (SES6) CA-OE), in which Wave Dragon ApS participates as developer. Wave Dragon partners SPOK ApS, the Technical University of Munich and Aalborg University participate as experts in their fields. This project enables a direct link to suppliers, utilities and other developers.

3. The Marie Curie Research Training Networks "WAVETRAIN" (Contract nr. MRTN-CT-2004-505166) in which SPOK is participating. This EC financed mobility network programme aims at knowledge transfer and training of researchers within the field of wave energy. The Wave Dragon Team already had a wealth of experience with this programme and have hosted a research fellow (James Tedd) for a period of three years. Further on Wave Dragon Team has recruited another fellow (Iain Russell) from the network to work permanently in the newly established UK company Wave Dragon Ltd, mainly dealing with the environmental development.
4. EU-OEA – Dr Hans Christian Sørensen is a founding member of the board of the European Ocean Energy Association. The association will act as the central network for its members on information exchange and EU financial resources, as well as promoting the ocean energy sector by acting as a single EU voice.
5. NEEDS – Dr. Hans Christian Sørensen is representing the ocean energy developers in the New Energy Externalities Developments for Sustainability project establishing the thorough picture of the full costs including externalities of future energy systems. A Life Cycle Analysis for Wave Dragon will be included.

Wave Dragon was previously involved in the following European projects:

1. EU Joule Craft project (phase 3a). This early project involved feasibility testing of the design, both by computer simulations in Denmark and Germany, as well as laboratory tests of a 1 : 50 scaled device in Denmark and Ireland, and tests of the low-head turbines in Germany.
2. WaveDragon 1 : 4.5 research project (contract number: ENK5-CT-2002-00603). This project supported the sea-testing and deployment of the 1 : 4.5 scale demonstrator of Wave Dragon. It is described in great detail in section 7.2. and in the final report to the Commission (Sørensen et al., 2006).

In addition to these formal projects that Wave Dragon has been involved with the company has been very active in promoting itself and wave energy in general to the academic and business world within Europe. This has involved giving many papers and presentations at conferences, and other workshops. Many students from France, the UK and Denmark have benefited from internships of several months with Wave Dragon, learning how a new technology can be brought forward.

Summary

Wave Dragon has been instrumental in developing the Danish Wave Energy test centre at Nissum Bredning. The company is now developing a pilot zone in Pembrokeshire to deploy a multi-*MW* device. This has been achieved with good support from national governments and European co-operation projects.

7.7 Discussion

Chapter 7 has provided a comprehensive review on the concepts that have reached the full-scale stage, including details regarding their development programmes. All concepts presented in sections 7.1 to 7.4, some *nearshore* some *offshore*, some *submerged* some *floating*, have generated and delivered electricity to national grids. There are hundreds of patented wave energy conversion machines, but at a time when wave energy is reaching a pre-commercial stage these concepts are the most likely to become immediately available and readily installed. However it is impossible to say with absolute certainty if any of these concepts will be selected for future large scale wave farms, or if alternative devices will emerge.

A section was also dedicated to the operation experience gathered with these technologies (7.5). It is essential that all existent or new technology developers incorporate these lessons in their own development programmes, ensuring that the same mistakes are not repeated. Although the industry is at its infancy, this considerable amount of experience is encouraging when predicting the future of wave energy conversion.

An account of the available (and planned) test centres was also given (see also Chapter 8). Finally it is encouraging to witness that there has been a great deal of cooperation between research centres and technology developers, which is particularly clear in the number of European collaboration networks that have been established. These networks are likely to be extended to other geographical areas in the near future.

References

Oscillating Water Column

Wave Energy Research and Development at JAMSTEC: Offshore Floating Wave Energy Device Mighty Whale (http://www.jamstec.go.jp/jamstec/MTD/Whale/)

Falcão de O AF (2000) The shoreline OWC wave power plant at the Azores. Proc 4th Eur Wave Power Conf, paper B1. University of Aalborg, Denmark

Neumann F, Brito e Melo A, Sarmento A (2006) Grid connected OWC wave power plant at the Azores, Portugal. Proc Int Conf Ocean Energy. From innovation to industry, OTTI, ISBN 3-934681-49-2, pp 53–60

Gato LM, Falcão AF (1990) Performance of Wells turbine with double row of guide vanes. Int J Japan Soc Mech Eng II 33:265–271

Archimedes Wave Swing

Cruz J, Sarmento A (2007) Sea state characterisation of the test site of an offshore wave energy plant. Ocean Eng 34(5–6):763–775

Leijon M, Bernhoff H, Agren O, Isberg J, Sundberg J, Berg M, Karlsson KE, Wolfbrandt A (2005) Multiphysics simulation of wave energy to electric energy conversion by permament magnet linear generator. IEEE Transactions on Energy conversion 20: 219–224

Prado M, Neumann F, Damen M, Gardner F (2005a) AWS results of pilot plant testing 2004. In: Proc 6th Eur Wave Tidal Energy Conf. Glasgow, United Kingdom

Prado M, Gardner F (2005b) Theoretical Analysis of the AWS Dynamics during Submersion Operation. In: Proc 6th Eur Wave Tidal Energy Conf. Glasgow, United Kingdom

Prado M, Gardner F, Damen M, Polinder H (2006) Modelling and test results of the Archimedes Wave Swing. Proc IMechE Part A. J Power Energy 220:855–868

Rademakers LWMM, Van Schie RG, Schitema R, Vriesema B, Gardner F (1998) Physical Model Testing for Characterising the AWS. In: Proc 3rd Eur Wave Energy Conf, Volume 1. Patras, Greece, pp 192–199

Sarmento AJNA, Luís AM, Lopes DBS (1998) Frequency-Domain Analysis of the AWS. In: Proc 3rd Eur Wave Energy Conf, Volume 1. Patras, Greece, pp 15–22

Pelamis

Cook S (1998) Investigation into Wave Loads on Catamarans. Dep Appl Phys. Curtin Univ Techonology, Perth, Australia

Falnes J (2002) Ocean Waves and Oscillating Systems. Cambridge University Press

Henderson R (2006) Design, simulation, and testing of a novel hydraulic power take-off system for the Pelamis wave energy converter. Renew Energy 31(2).271–283

Pizer D, Retzler C, Henderson R, Cowieson F, Shaw F, Dickens B, Hart R (2005) PELAMIS WEC – Recent Advances in the Numerical and Experimental Modelling Programme. Proc 6th Eur Wave Energy Conf. Glasgow, UK, pp 373–378

Retzler C, Pizer D, Henderson R, Ahlqvist J, Cowieson F, Shaw M (2003) PELAMIS: Advances in the Numerical and Experimental Modelling Programme. Proc 5th Eur Wave Energy Conf. Cork, Ireland, pp 59–66

Yemm R, Pizer D, Retzler C (1998) The WPT-375 – a near-shore wave energy converter submitted to Scottish Renewables Obligation 3. Proc 3rd Eur Wave Energy Conf, Vol. 2. Patras, Greece, pp 243–249

Yemm R, Henderson R, Taylor C (2000) The PWP Pelamis WEC: Current Status and Onward Programme. Proc 4th Eur Wave Energy Conf. Aalborg, Denmark

Wave Dragon

Corona L, Kofoed JP (2006) Wave induced stresses measured at the Wave Dragon Nissum Bredning Prototype. Co-ordinated Action on Ocean Energy. 3rd Workshop proceedings. Amsterdam

EMU et al. (2000) Publishable Final Report – Low Pressure Hydro Turbines and Control Equipment for Wave Energy Converters (Wave Dragon). Contract JOR3-CT98-7027. Copenhagen, Denmark

Franco L, de Gerloni M, Van der Meer JW (1995) Wave Overtopping on Vertical and Composite Breakwaters 1. Proc 24th Int Conf Coastal Eng. Kobe, Japan, pp 1030–1044

Hansen LK, Christensen L, Sørensen HC (2003) Experiences from the Approval Process of the Wave Dragon Project. Proc 5th Eur Wave Energy Conf. University College Cork, Ireland

Knapp W, Holmen E, Schilling R (2000) Considerations for Water Turbines to be used in Wave Energy Converters. Proc 4th Eur Wave Energy Conf. Aalborg

Knapp W (2005) Water Turbines for Overtopping Wave Energy Converters. Co-ordinated Action on Ocean Energy 2nd Workshop proceedings. Uppsala

Kofoed JP, Frigaard P, Soerensen HC, Friis-Madsen E (2000) Development of the Wave Energy Converter – Wave Dragon. Proc 10th ISOPE Conf, vol. 1, No 10, pp 405–412

Kofoed JP (2002) Wave Overtopping of Marine Structures – Utilization of Wave Energy. PhD thesis, Aalborg University

Kofoed JP, Frigaard P, Friis-Madsen E, Sørensen HC (2006) Prototype testing of the wave energy converter wave dragon. Renew Energy 31

Kramer M, Frigaard P (2002) Efficient Wave Energy Amplification with Wave Reflectors. Proc 9th ISOPE conference

May J, Bean D (2005) Wave Dragon Pre-Commercial Demonstrator – Environmental Impact Assessment Scoping Report, Prepared by PMSS, available at www.wavedragon.co.uk

Neumann F, Tedd J, Prado M, Russell I, Patrício S, La Regina V (2006) Licensing and Environmental Issues of Wave Energy Projects. Proc World Renew Energy Congr IX. Florence, Italy

Sørensen HC et. al. (2003) Development of the Wave Dragon from scale 1:50 to prototype. Proc 5th Eur Wave Energy Conf. Cork, Ireland

Sørensen HC et al. (2005) The Results of Two Years Testing in Real Sea of Wave Dragon. Proc 6th Eur Wave Tidal Energy Conf. Glasgow, September

Sørensen HC et al. (2006) Sea Testing and Optimisation of Power Production on a Scale 1:4.5. Test Rig of the Offshore Wave Energy Converter Wave Dragon. Final technical report, project NNE5-2001-00444

Svendsen R, Frigaard P (2001) Calculation of the Wave Conditions in Nissum Bredning, Report. Aalborg University Department of Civil Engineering

Tedd J, Knapp W, Frigaard P, Kofoed JP (2005) Turbine Control Strategy Including Wave Prediction for Overtopping Wave Energy Converters. Co-ordinated Action on Ocean Energy. 2nd Workshop proceedings. Uppsala

Tedd J, Kofoed JP Knapp W, Friis-Madsen E, Sørensen HC (2006). Wave Dragon, prototype wave power production. World Renew Energy Congr IX. Florence

Van der Meer JW, Janssen JPFM (1994) Wave Run-up and Wave Overtopping at Dikes. In: Kobayashi N, Demirbilek Z (eds) Wave Forces on inclined and vertical wall structures. ASCE, pp 1–27 [Also Delft hydraulics, Publ. No 487]

Additional References

Sarmento A, Whitaker T, Brito e Melo A, Clement A, Salter S, Pontes T, Neumann F (2006) The European Research Training Network For Competitive Wave Energy. Proc WREC IX [ISBN 008 44671 X]